ELECTRON TRANSFER IN CYTOCHROME *C* OXIDASE: CYTOCHROME *C* DOCKING & ELECTRON/PROTON COUPLING

By

Jun Yang

A THESIS

Submitted to
Michigan State University
in partial fulfillment of the requirements
for the degree of

MASTER OF SCIENCE

Department of Biochemistry and Molecular Biology

2002

Abstract

ELECTRON TRANSFER IN CYTOCHROME *C* OXIDASE:
CYTOCHROME *C* DOCKING & ELECTRON/PROTON COUPLING

By

Jun Yang

As the last complex in the respiratory chain, cytochrome *c* oxidase (C*c*O) reduces O_2 to water and is a key player in, and regulator of, the electron transfer process. Docking of its substrate, the electron donor cytochrome *c* (C*c*), involves a large protein-protein interface, but is a transient interaction. Certain positively charged lysine residues on C*c* and negatively charged carboxyl groups on C*c*O have been identified as critical to successful docking and electron transfer. A computer model has been generated for the C*c*/C*c*O complex. To test the model, we have conducted research with engineered disulfide bonds between C*c* and C*c*O. The results show evidence of a covalent C*c*/C*c*O complex in support of the data from computer modeling. Further studies to characterize the complex and use it to assist in crystallization are underway.

To determine where the products of the electron transfer reaction, protons and waters, exit from the protein, mutants of Asp271 in subunit I were made. This residue interacts with Arg234 from subunit II and is the first residue in a conserved sequence, D(/N)PxxY, found to be important for signal transduction in G-protein coupled receptors. The mutants show that the charge on Asp271 is important for holding the whole protein together; hence the disaggregation of mutant forms of the oxidase prevented us from analyzing the possible water/proton exit function of this residue.

To

My Family in China

ACKNOWLEDGMENTS

To say that this thesis is "by Jun Yang" overstates the case. Without the significant contribution from other people, this thesis would not exist.

At the top of the list are my advisor, Dr. Shelagh Fergson-Miller, my committee members, and members of my research lab. Shelagh not only has offered me her special scientific acumen, but also has tried her best to give me support and encouragement. Her professionalism and considerate efforts have made a remarkable impact in my professional and personal life. Also my committee members, Dr. Honggao Yan & Dr. Zachary Burton, have been very informative and supportive by offering me their scientific insights. I would like to extend a special thanks to Dr. Burton for reading through my thesis and providing valuable suggestions.

No word can express my gratitude to Dr. Carrie Hiser and Dr. Denise Mills. They showed extraordinary patience whenever I needed their help. I would like to thank Dr. Yuejun Zhen for helping me start my project, and continuously giving me advice even after he left the lab. I really enjoyed collaborating with Dr. Yasmin Hilmi on the cytochrome *c* docking project. Thanks to Bryan Schmidt for conducting EPR analyses for me and for improving my English and introducing me to American culture. I am sincerely thankful for the assistance from Ling Qin & Namjoon Kim. Many undergraduate students, including Erica Westley and Jamie Slater, have also helped accomplish the experiments in this thesis.

I would like to thank Dr. Frank Millett at the University of Arkansas for his help on having fast kinetics data acquired for the Y159 mutants and Dr. Jon Hosler for sharing his important research results.

Special thanks are to my family back in China for their unconditional support and understanding. Their love and sacrifice constitute an irreplaceable part of my achievement.

Last, to my friends, especially, Christine Mikkola, John Mikkola and Yuhui Wang, for helping me through the hardest moments of my life.

TABLE OF CONTENTS

LIST

CHA

Table

CHA

Table

CHA

Tabl

LIST OF TABLES

CHAPTER 1

CHAPTER 2

CHAPTER 3

CH

Figu

Figu

Figu

Figu

CH

Figu

Figu

Figu

Figu

Figu

Figu

Figu

Figu

Figu

LIST OF FIGURES

CHAPTER 1

CHAPTER 2

CH

Fig

Fig

Figu

Figu

Figu

Figu

Figu

Figu

Figu

Figu

Figu

Figu

Figu

Figu

CHAPTER 3

Ce
Ce
Ce
CeC
CeF
CqC
DE
ED
EPI
FPI
GP
LN
NF
PC
R.s
SD
TV
TV

LIST OF ABBREVIATIONS

C*c*	Cytochrome *c*
C*c*(H)	Cytochrome *c* from horse heart
C*c*(Y)	yeast Cytochrome *c*
C*c*O	Cytochrome *c* Oxidase
C*c*P	Cytochrome *c* Peroxidase
CqO	Quinol Oxidase
DEAE	diethylaminoethyl
EDTA	ethylenediaminetetraacetic acid
EPR	Electron Paramagnetic Resonance spectroscopy
FPLC	fast protein liquid chromatography
GPCR	G-Protein-Coupled Receptors
LM	lauryl maltoside
Ni^{2+}-NTA	Nickel-nitrilotriacetic acid
PCR	polymerase chain reaction
R.s.	*Rhodobacter sphaeroides*
SDS	sodium dodecyl sulfate
TMPD	N-N-N'N'-tetramethyl-p-phenylenediamine
TMS 7	TransMembrane Segment 7

Chapter 1

Literature Review

As most of the living organisms are not able to live photosynthetically, they acquire energy through metabolizing foodstuffs and storing the energy obtained in the form of fat and carbohydrate. The energy from foodstuffs is changed to ATP, the major energy form that living organisms can use directly. This process involves feeding electrons from NADH into a chain of membrane-bound complexes, the respiratory chain, where electrons are used to generate a transmembrane potential, which drives ATP synthesis (Figure 1.1) (Mitchell, 1976; Mitchell & Moyle, 1965).

Cytochrome *c* oxidase (C*c*O) is the last complex in the respiratory chain. It provides the sink for the electrons from NADH by reducing oxygen to water. It also contributes to the transmembrane potential that can drive the synthesis of ATP. The immediate electron donor to C*c*O is cytochrome *c*. It must react with a specific site on the oxidase to deliver electrons and then dissociate to pick up more because for every O_2, 4 electrons are required.

My thesis has involved the study of mutant forms of cytochrome *c* oxidase from *Rhodobacter sphaeroides* designed to address two questions: 1) Where does cytochrome *c* dock on cytochrome *c* oxidase to deliver electrons and 2) where do the protons and water, that are the products of the electron transfer reaction, exit from the protein? The studies were aimed at testing the accuracy of a computational prediction of the docking site, and the importance of a conserved sequence, D(N)PxxY, found in G-protein coupled receptors and oxidase, in controlling proton and/or water exit.

To provide background for this work, I will review the following issues:

1. The structure of C*c*O
2. Docking of cytochrome *c* on its redox partners

3. *C*-type cytochromes in *Rhodobacter sphaeroides*

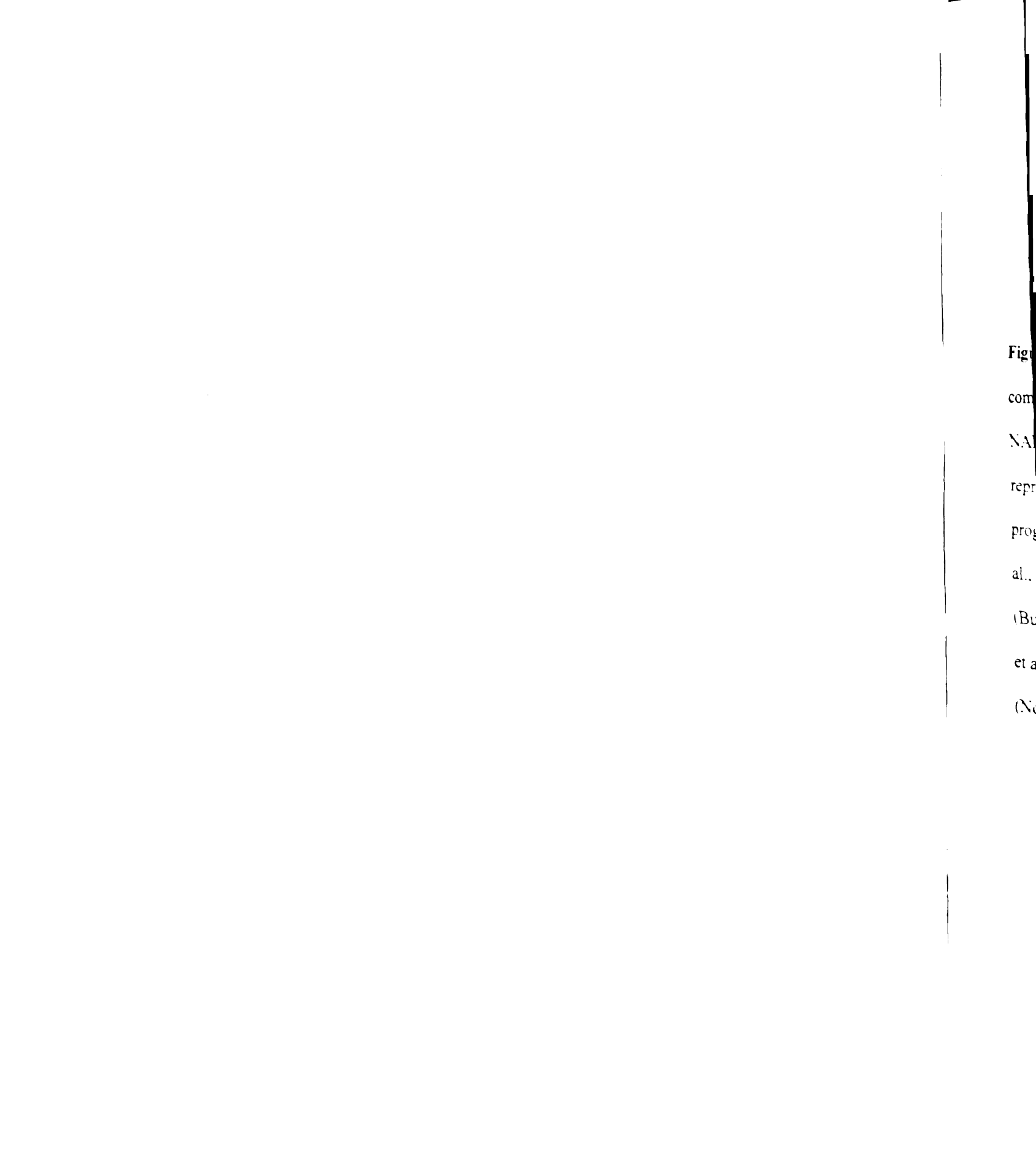

Figure 1.1 Respiratory Chain Complexes. The three-dimensional crystal structures of complexes II, III, IV, V and cytochrome *c* are shown. Because the crystal structure of NADH:ubiquinone oxidoreductase (complex I) is not available, green boxes are used to represent this complex. This figure was created by Dr. Denise Mills using the computer program Rasmol with the coordinates from fumarate reductase (Complex II) (Iverson et al., 1999), bovine *bc*1 complex (Complex III) (Iwata et al., 1998), horse cytochrome *c* (Bushnell et al., 1990), *R. sphaeroides* cytochrome *c* oxidase (Complex IV) (Svensson-Ek et al., 2002) and yeast ATP synthase (Complex V) (Stock et al., 1999).

(Note: Images in this thesis are presented in color.)

Respiratory Chain Complexes

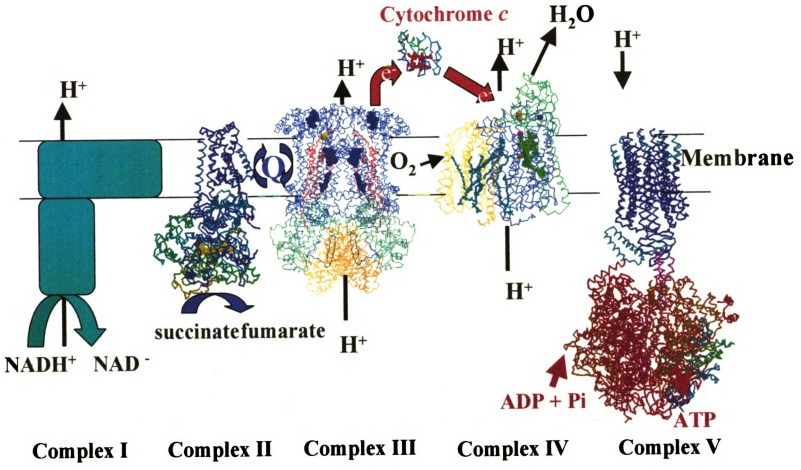

Part I The Structure of C*c*O

I. The Respiratory Chain

Of the three steps (glycolysis, citric acid cycle, oxidative phosphorylation) by which the organism converts foodstuffs to ATP, oxidative phosphorylation produces the most energy. In this step, electrons from NADH are first transferred to complex I (NADH:ubiquinone oxidoreductase or NADH dehydrogenase) and complex II (succinate:ubiquinone oxidoreductase or succinate dehydrogenase). Then electrons are further transferred to complex III (cytochrome bc_1 complex), from where C*c* shuttles electrons to complex IV (C*c*O) to reduce oxygen. In this process, a transmembrane potential is built up by pumping protons from the inside (matrix of mitochondria *or* cytoplasm of bacteria) to the outside (intermembrane space of mitochondria *or* periplasmic space in bacteria). The resulting electrochemical potential drives ATP synthesis.

The four complexes in the respiratory chain have been found in mitochondria (Hatefi, 1985) and many bacteria (Trumpower & Gennis, 1994) (Figure 1.1). As the complexes from prokaryotes are structurally and functionally homologous to their mitochondrial counterparts but with simpler structures, they are widely used to study the energy conservation in the respiratory chain. In our research, we use C*c*O from *R. sphaeroides* as a model system for the mitochondrial C*c*O, which has thirteen subunits, while the bacterial form has only four.

II.

oxy

For

are

III

oxi

bin

al..

hem

cyt

of w

oxid

oxid

rece

also

and

emb

II. Complex IV (C*c*O)

C*c*O takes four electrons sequentially from reduced C*c* and uses them to reduce oxygen to water. The overall reaction catalyzed by C*c*O follows equation I:

$$4\ Cc\ (\ Fe^{II+}\ ) + O_2 + 8H^{+}in \rightarrow 4\ Cc\ (\ Fe^{III+}\ ) + 2\ H_2O + 4\ H^{+}out \quad \text{(Eq. I)}$$

For each oxygen molecule reduced, four protons are used to form water and four others are pumped out of the bacterial cytoplasm (or the mitochondria matrix).

III. Heme-Copper Oxidase Family

The terminal oxidases found in eukaryotes and many prokaryotes are heme-copper oxidases. In these oxidases, all the subunits I are homologous and contain a heme-copper binuclear center, where the oxygen molecules are reduced to water (García-Horsman et al., 1994a). The heme in this center is a high spin heme. There is usually another low spin heme situated near to the high spin heme in subunit I as well.

Although mammalian mitochondria have only one type of oxidase, the aa_3-cytochrome *c* oxidase (C*c*O), bacteria normally have additional terminal oxidases, some of which use ubiquinol instead of cytochrome *c* as substrate. In *R. sphaeroides*, three oxidases have been found. They are aa_3- type oxidase (Hosler et al., 1992), cbb_3-type oxidase and bb_3-quinol oxidase (García-Horsman et al., 1994b; Yun et al., 1994). In the recently compeleted genome sequence for *R. s.*, genes, caa_3- and *bd*- type oxidases have also been located (JGI website).

All the heme-copper terminal oxidases catalyze the conversion of oxygen to water and build up an electrochemical gradient across the membrane in which they are embedded. While some oxidases, such as quinol oxidases (C*q*O) use membrane-bound

quinol as their electron donor, some use soluble or membrane-bound C*c*. Most heme copper oxidases of the C*c*O and C*q*O type have been shown to pump protons.

So far, four types of heme groups have been identified in the heme-copper oxidase family. They are A-, B-, C-, and O-type hemes. All of these heme groups have the same basic tetrapyrrole porphyrin rings in their structure with differences in the substituents on the ring. No C-type heme has been found in the binuclear center. However, it is found in caa_3- and cbb_3-type oxidases in which the covalently bound *c*-type hemes can transfer electrons to the binuclear center (García-Horsman et al., 1994b; Mather et al., 1993). Besides the heme differences, some heme-copper oxidases have a Cu_A site in their structures while some do not (Yun et al., 1994). This copper site, found in all C*c*O oxidases, aa_3-, caa_3- and ba_3-type C*c*O, is generally agreed to be the initial electron acceptor from C*c*.

IV. The structure of aa_3 oxidase

Before bacterial oxidases were discovered, the aa_3-type cytochrome *c* oxidase from bovine heart was the one that was studied most thoroughly. It has 13 subunits with the three largest ones highly homologous to the three largest ones from bacteria. Its crystal structure has been resolved, as well as the four-subunit oxidases from *P. denitrificans* and *R. sphaeroides*. The C*c*O from bacteria is also functionally similar to its counterpart from mitochondria. This makes the bacterial C*c*O an ideal system to study using molecular genetic techniques.

Although mammals and prokaryotes are evolutionarily distantly related, the largest three subunits of the oxidase structures are almost identical in their secondary

str

th

al

th

1. S

1.2

site

acti

two

resp

perp

dent

421

and

dista

sphd

ligan

structure and metal sites. The crystal structures confirm this similarity. I will discuss the three largest subunits and their similarities between three crystal structures (Ostermeier et al., 1997; Yoshikawa et al., 1998; Svensson-Ek et al., 2002). The residue numbering in this section is based on the *R. sphaeroides* C*c*O.

1. Subunit I

Subunit I has twelve transmembrane helices, with five metal centers in it (Figure 1.2). These metal centers are a low spin heme *a*, a high spin heme a_3, the Cu_B site, a Mg site and a Ca site.

Of the five metal centers in Subunit I, heme *a*, heme a_3 and Cu_B site are redox active. The two hemes are in close proximity, with an edge to edge distance between the two hemes of 4.7Å, 4.7Å and 5.6Å for *P. denitrificans*, bovine, and *R. sphaeroides*, respectively. The iron to iron distance is 13 to 14 Å. The heme planes are almost perpendicular to each other with the interplanar angles of 108° and 104° for *P. denitrificans* and bovine oxidases. The low spin heme *a* is ligated by His-102 and His-421 while the high spin heme a_3 is ligated by His-419. The Cu_B site is close to heme a_3 and they are strongly electronically coupled, usually making both of them EPR silent. The distance between the heme a_3 center and Cu_B is 4.5Å, 4.5 Å, 5.2 Å for bovine, *R. sphaeroides* and *P. denitrificans* respectively in the oxidized form of the enzymes. The ligands of Cu_B are His-284, -333 and –334.

Fig

Its

and

bla

sph

Figure 1.2 Crystal Structure of *Rhodobacter sphaeroides* Cytochrome *c* Oxidase and Its Metal Centers. Helices of subunit I, II, III and IV are shown in blue, magenta, cyan and orange respectively. Yellow balls represent Cu_A and Cu_B, orange for magnesium and black for Calcium. The figure was created using Insight II with coordinates for *R. sphaeroides* CcO from (Svensson-Ek *et al.*, 2002).

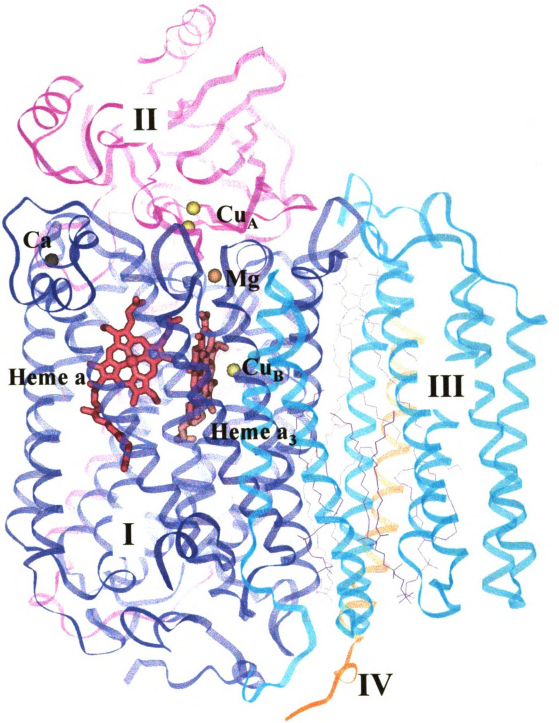
II
Cu_A
Ca
Mg
Heme a
Cu_B
III
Heme a_3
I
IV

The non-redox active Mg site is situated at the interface of subunit I and II. It is suggested to be important to stabilize the overall structure and modulate the redox potentials of the neighboring metal centers (Florens et al., 1998). A role in the proton/water exit channel is also proposed (Ferguson-Miller & Babcock, 1996). Mg has octahedral coordination in which it is ligated to His-411 and Asp-412 from subunit I and Glu254 from subunit II, along with three water molecules. The Ca site was not found until two to three years ago when the refined structures of *P. denitrificans* and bovine oxidases became available. It is situated at the periplasmic side of subunit I with five oxygen ligands from side chains and backbone. The metal to metal distances from this Ca site to Cu_A and the iron of heme *a* are about 18Å for the bacterial oxidases. A shift in the spectrum of heme *a* has been observed with binding of calcium in both *Paracoccus* and mitochondrial cytochrome aa_3 (Saari et al., 1980; Mkrtchyan et al., 1990; Riistama et al., 1999; Pfitzner et al., 1999).

2. Subunit II

The structure of subunit II is like a hammer with a big head (C-terminal domain) and a handle formed by two N-terminal transmembrane helices anchoring the subunit in the membrane. The soluble C-terminal domain forming a globular "head" consists of ten β-strands, similar to the blue copper protein structure (Figure 1.3). Many studies have suggested that part of the negatively charged surface of this domain, close to the Cu_A site, is where C*c* binds.

Figure 1.3 Crystal Structure of *Rhodobacter sphaeroides* Cytochrome *c* Oxidase and Its Subunits. Helices of subunit I, II, III and IV are shown in blue, magenta, cyan and orange respectively. Yellow balls represent Cu_A and Cu_B, orange for magnesium and black for calcium. The figure was created using Insight II with coordinates for *R. sphaeroides* CcO from (Svensson-Ek *et al.*, 2002).

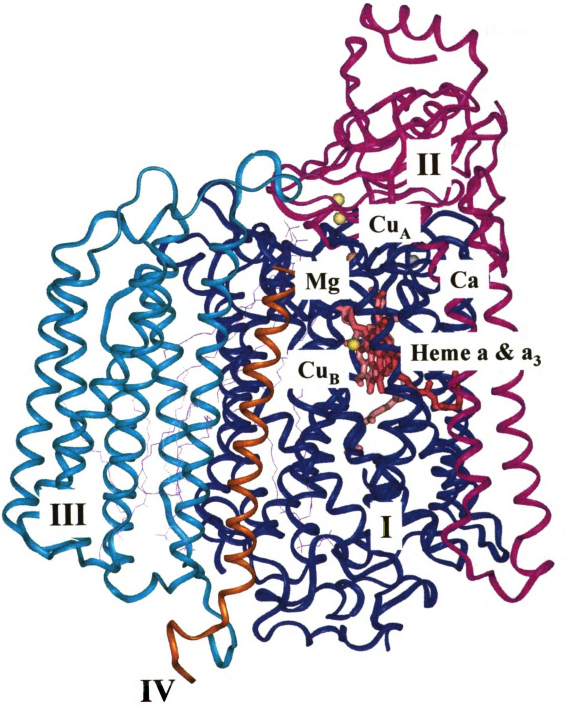
II
Cu_A
Mg
Ca
Heme a & a_3
Cu_B
III
I
IV

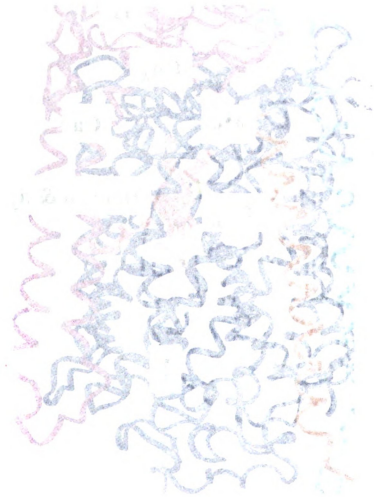

Cu_A is a binuclear center with the distances between the two copper atoms in the range of 2.5 to 2.8Å. This short distance implies strong electronic coupling. The two copper atoms have a mixed-valence state [Cu(1.5)-Cu(1.5)] ligated by two histidine residues (His-217 and -260), two shared cysteines (Cys-252 and -256), one methionine (Met-263), and one backbone carbonyl oxygen of Glu-254. The carboxyl side chain of Glu-254 is also ligated to the Mg site (Iwata et al., 1995; Tsukihara et al., 1995; Wilmanns et al., 1995). This binuclear site is the electron acceptor from C*c* heme.

Right around the Cu_A is a stretch of well-conserved aromatic residues (Tyr-141, Trp-143, Tyr-144, Trp-145, Tyr-147, and Tyr-149). In all the crystal structures, Trp143 is in van der Waals contact with one of the Cu_A ligands, Met-263, and is also hydrogen-bonded to His-217, which places it in a favorable position for possibly mediating electron transfer from C*c* to Cu_A. Mutations of other Cu_A ligands confirm the importance of the dinuclear copper in electron transfer but not the proton pumping function (Zhen et al., 2002). The detailed information about computational docking analysis is shown in Section IV of Part II.

The Cu_A site and accompanying aromatics are surrounded by several negatively-charged residues. These residues are suggested to be important for the binding of C*c* on the C*c*O from the mutagenesis, binding, and kinetics studies. The computational modeling also substantiates the idea that these carboxyl residues (Glu-148, Asp214, Glu195 and Glu157) interact electrostatically with corresponding lysine residues on the surface of C*c* to make the transient complex for electron transfer.

3.

4.

3. Subunit III

Subunit III forms a V shape with helices I and II forming one arm and helices III to VII forming the other, with space in the middle occupied by phospholipid. In the space-filling model of the oxidase, Glu-286, a conserved residue close to the Cu_B site, can be seen through a tunnel in the subunit I from the cleft of the two arms. If a bulky group blocks this channel, the oxygen diffusion is hindered (Riistama et al., 1996). This is consistent with the structural analysis suggesting that subunit III and its associated lipid may provide a reservoir for efficient oxygen diffusion from the membrane to the Cu_B site (Lappalainen et al., 1995). When the gene of subunit III is deleted from *R. sphaeroides*, the two-subunit oxidase is active and pumps protons (although with lowered stoichiometry, i.e. < 1 H^+/e^-), but undergoes rapid "suicide" inactivation during turnover, suggesting that subunit III may be important for the protein assembly and stability (Bratton et al., 1999).

4. Other subunits

The fourth subunit has been resolved in the crystal structure of *P. denitrificans* and *R. sphaeroides* C*c*O (Figure 1.3). This subunit is a one-transmembrane-helix subunit which contacts mainly with tightly bound lipids in *Rs* C*c*O (Svensson-Ek et al., 2002). It has no homology to the ten small subunits in the bovine oxidase but there is 56% homology between the *P. denitrificans* and *R. sphaeroides* version (personal communication with Dr. Carrie Hiser). Because deletion of this subunit from *P. denitrificans* has no obvious effect, it may not play a role in the catalytic function (Witt & Ludwig, 1997) but may be important for the assembly and stability for the whole enzyme.

The ten other small subunits of C*c*O from bovine heart surround the three core subunits. Some subunits may be important for the dimer structure of the protein. A zinc site has been found on the matrix side of the protein. Two possible ADP binding sites have also been located, occupied by cholic acid in the bovine structure, consistent with the result that ADP and ATP regulate allosterically the activity of the C*c*O (Arnold et al., 1999).

5. How C*c*O performs its function

5.1 Oxygen reactions

The overall reaction catalyzed by C*c*O is shown in Equation I in Section II of Part I. As oxygen has a high positive redox potential, reduction of oxygen is associated with a large negative free energy. The energy is efficiently stored as a transmembrane electrochemical proton gradient. The reduction of one O_2 molecule requires four electrons and four protons to generate two water molecules. Concomitantly, four protons are pumped across the membrane.

The process of oxygen reduction involves electron transfer, oxygen bond cleavage, and protonation. In C*c*O, proton transfer is the rate-limiting step (Ferguson-Miller & Babcock, 1996; Riistama et al., 1996, Karpefors et al., 1998). Protons are apparently loaded at certain sites before an electron transfer event takes place. There is still controversy about the oxygen reaction; however, a consensus of the reaction scheme has begun to emerge (Proshlyakov, et al., 2000; Babcock & Wikström, 1992). Oxygen first binds to Cu_B when the heme a_3 – Cu_B site of oxidase is in the reduced state. Then the oxygen binds to heme a_3 in an end-on configuration to form an initial oxy form, as in

oxygen binding to hemoglobin. Subsequently, the oxy form is reduced to the peroxy ("P") form which gives a characteristic absorbance at 608nm. The oxygen bond is already broken in the P form in a 4-electron transfer event of which one electron is believed to be from Tyr 280. An additional electron and one substrate proton are transferred to the binuclear center to make the "F" form (absorbance 580nm) and one or two protons are pumped across the membrane. Finally, an electron and proton is used to make the hydroxy form and the cycle is complete. This step pumps protons as well, but the stoichiometry of pumping at each step is still debated. In the cycle, two waters are produced at the active site and presumably go out into the bulk solvent.

5.2 Proton Pumping

The proton pumping activity of the oxidase is tightly coupled with the electron transfer activity. An electroneutrality principle has been advanced suggesting that the movement of negative electrons into a region of low dielectric must be compensated by proton movement to decrease the energy requirement (Rich, 1995). This theory is supported by the fact that many of the electron transfer steps are pH dependent and show a D/H isotope effect (Hállen & Nilsson, 1992; Oliveberg et al., 1991; Brzezinski & Malmstrom, 1987).

Two coupling mechanisms of proton pumping have been proposed, direct and indirect. The indirect mechanism proposes that electron transfer causes an overall conformational change that causes protons to be pumped at some sites at a distance from where the oxygen reduction occurs. On the other hand, direct coupling mechanisms postulate that one or more of the ligands of the redox active metal centers are protonated and deprotonated to transfer protons. Two proton uptake paths, D and K, have been well

defined but as yet it is uncertain where the proton exit paths are situated. One of the possibilities is that protons could exit with the product water. So far, there is no compelling evidence to support any of the models of the C*c*O proton pumping mechanism.

Part II Docking of Cytochrome *c* on Its Redox Partners

The role of cytochrome *c* in mitochondria is to transfer electrons from the bc_1 complex to cytochrome *c* oxidase in respiration. In bacteria, various cytochromes *c* transfer electrons to many different oxidases and to the reaction center in the photosynthesis system. Efficient electron transfer requires rapid complex formation but also rapid dissociation of oxidized cytochrome *c* to prevent inhibition of further electron transfer. However, the chemistry of the surface of cytochrome *c* that is used to interact with its redox partners, and whether different surfaces are used for different partners, is still not fully defined. Determination of the structure of the C*c*/C*c*O complex could reveal the types of interactions important for this transient interaction and also for efficient intermolecular electron transfer within the complex. A crystal structure of the docked complex with C*c* and C*c*O would be extremely useful. However, as C*c*O is a membrane protein and C*c* is soluble, it has proven difficult to obtain the crystal structure of the complex. Therefore, some indirect approaches such as chemical modification, crystallography for C*c*O, mutagenesis and computer modeling have been used to explain the interaction of the C*c*/C*c*O complex. This section gives a brief review of these approaches.

I. Chemical Modification

Decreased strength of interactions between C*c* and its partners by increasing ionic strength of the reaction medium is a proof that an electrostatic component is significant in

these interactions. Because conserved lysine residues in C*c* were thought to be important in these interactions, chemical modification studies were done with chemicals such as CNDP (Brautigan et al., 1978; Osheroff et al., 1980), TFA (Staudenmayer et al., 1976), and TFC (Smith et al., 1977) to define which specific residues were important for the interaction.

After these single-residue-modified cytochromes *c* were made and purified, spectroscopic analyses showed that these modifications had little effect on the overall conformation and redox properties of the protein. The steady-state kinetics were analyzed spectrophotometrically or polarographically (Smith et al., 1977; Ferguson-Miller et al., 1978; Osheroff et al., 1980). The results showed that Lysines-13, 86/87, 72, and 8 in horse C*c* had the most significant effect on the binding of C*c* to the oxidase. These results accompanied by the results that these five derivatives and Lys-27 also showed the biggest effects on their binding to the bc_1 complex (Smith et al., 1981), beef mitochondrial reductase (Speck et al., 1979) and C*c*P (Smith & Millett; Kang et al., 1977) suggesting that C*c* uses the same area of its surface to bind to its different redox partners. This area is where the heme edge is exposed. The other 13 lysine residues showed little effect on the binding.

A differential protection technique, in which modification was carried out in the presence of the complex, was also used to address the same issue (Rieder & Bosshard, 1980). The same residues suggested from chemical modification studies as important for binding also showed their significance with this technique. Now it is generally agreed that the area where these lysine residues are situated in C*c* is involved in the docking of C*c* to most of its redox partners.

II. Crystallographic approaches

A number of the physiological partners of C*c*, for example, the oxidases and the bc_1 complexes, are membrane-bound proteins. The insolubility of these proteins and the transient nature of the binding of C*c* make them hard to crystallize by themselves and even harder to crystallize with soluble C*c*. As an exception, C*c*P from yeast is a small soluble protein with a molecular weight of 34.2 kDa and a single heme group. The crystal structures of C*c*P itself (Poulos et al., 1980), horse C*c*/C*c*P complex [C*c*P:C*c*(H)] and yeast C*c*/C*c*P [C*c*P:C*c*(Y)] complex (Pelletier & Kraut) were all obtained. This makes the peroxidase system a good model for studying long-range electron transfer and the C*c* docking mechanism.

Even though the crystal of C*c*P:C*c*(Y) and C*c*P:C*c*(H) were obtained under different ionic strengths, 5mM and 150mM, the complex structures are similar, especially in that C*c*P and C*c* use similar domains to interact. The predominant interactions between these two complexes are hydrogen bonds and van der Waals interactions. Both of the complex structures showed that lysine residues 8, 13, 72, and 87 are important for the interaction between C*c* and its redox partner. These residues are the same residues that were suggested from chemical modification studies (Kang et al., 1978). They were also determined to be important for the interaction of C*c* and C*c*O by chemical modification(Smith et al., 1977; Ferguson-Miller et al., 1978; Osheroff et al., 1980). The heme methyl groups of both horse and yeast C*c* are all in van der Waals contact with Ala-193 and Ala-194 from C*c*P. An electron transfer pathway, which involves the backbone

chains of Trp-191, Gly-192, Ala-193, and Ala-194 has been identified. This pathway is actually the shortest straight line between the two heme groups (Pelletier & Kraut, 1992).

The most noticeable difference between the two complexes is the slight rotation-translation of C*c* as related to the C*c*P. This slight difference made a gap of 7Å between Ala-193 and194 and the methyl group of the heme from C*c* in C*c*P:C*c*(H) complex, suggesting a less efficient electron transfer. This low efficiency of electron transfer is confirmed by some kinetic studies (Geren et al., 1991; Hahm et al., 1992).

There is still a question about the extent to which the crystallographic studies faithfully represent the conformation of the protein when it is under normal physiological conditions. With the differences between the two complex structures, another question was whether differences arise from the crystal growth conditions or from intrinsic differences between the two cytochromes *c*. Mutagenesis approaches were used to help answer this question.

III. Mutagenesis approaches

1. Cytochrome *c* peroxidase

In the crystal structure of the complexes, a region on the surface of C*c*P is in close contact with C*c*, including Glu-32, Asp-33, Asp-34 and Glu-35, with Glu-35 forming a hydrogen-bond with Lys-87 of C*c*. Glu-290 in C*c*P hydrogen-bonds with Lys-72 from C*c*(H) or Lys-73 from C*c*(Y). Mutants have been made of these residues to convert the carboxyl groups to amide groups. These mutants include E32Q, D34N, E35Q, E290N and E291Q. Ala-193 has also been changed into phenylalanine and cysteine. The cysteine mutant was labeled with a bulky group of 3-(N-maleimidylpropionyl)biocytin (MPB) to

introduce a bulky group at the interface (Fishel et al., 1987; Miller et al., 1994; Miller et al., 1996). The electron transfer rates were measured with the ruthenium-C*c* photolysis technique. For D34N, E290N and A193F, the rate constants of k_{et} were found to decrease 2 to 4 fold. The binding constants (K_D) decreased 6 to 15 fold. Mutants E32Q and E291Q had no significant effect on the electron transfer and binding (Wang et al., 1996). These results are consistent with the results derived from the crystal structures. The A193C-MPB which introduced a bulky group into the interface had a ~150 fold decrease in the k_{et}. This is also consistent with the crystal structure of the interface. For both C*c*(H) and Cc(Y), the mutants had similar effects, indicating that they bind to the same region on C*c*P.

The controversy about whether the conformational differences in the two complex structures are due to the different crystal growth conditions or to the intrinsic difference between the two cytochromes *c* was addressed by using the mutant A193C-MPB(Miller et al., 1996). This bulky group caused 20 to 100 fold decrease in electron transfer rates for C*c*(Y) while only 2 to 3 decrease for C*c*(H). This result shows that the conformational difference in the crystal structure is present in solution too. So the interface resolved in the crystal structures represents the kinetically competent interaction in solution.

2. Cytochrome *c* oxidase

The mutagenesis analysis on the binding of C*c* and C*c*O has also been done. From chemical modification/protection (Millett et al., 1982; Millett et al., 1983), Asp-112 (Asp-151 in *R. sphaeroides*), Glu-114 (Glu-152 in *R. sphaeroides*), and Glu-198 (Glu-254 in *R. sphaeroides*) in subunit II of bovine C*c*O have been identified to be protected

from modification by Cc binding. Cross-linking studies also identified a cross-link between His-161 (His-217 in *R. sphaeroides*) and Lys-13 from horse Cc (Bisson et al., 1982). Time resolved electron transfer kinetic studies (Hill, 1991; Pan et al., 1993; Malatesta et al., 1998) and crystal structures of Cc from both bovine and *Paracoccus* (Iwata et al., 1995; Tsukihara et al., 1995; Tsukihara et al., 1996) show results consistent with the modification study with the exception of Glu-198 (Glu-254 in *R. sphaeroides*). These residues (Asp-112 & Glu-114) are all in a domain close to where Cu_A is situated (although not in the precise binding domain for Cc as determined by mutagenesis; see below) but Glu-198 (Glu-254 in *R. sphaeroides*) is a metal ligand shared by Cu_A and Mg and therefore unable to participate. Time resolved electron transfer kinetic studies have also shown that Cu_A is the initial electron receptor from Cc.

Using site-directed mutagenesis studies on *Paracoccus denitrificans* CcO, Glu-148, Glu-157, Asp-195, Asp-214, Asp-229, and Glu-254 (*R. sphaeroides* numbering) have been shown to be important for the binding of Cc (Lappalainen et al., 1995; Witt et al., 1995; Witt et al., 1998). Subsequently published crystal structures showed that Asp-229 and Glu-254 are buried inside the protein, and therefore do not interact with Cc. The mutational results must be attributed to general disruption of the CcO protein.

In parallel with the *P. denitrificans*, similar studies were done on the *R. sphaeroides* CcO; mutants E148Q, D151N/E152Q, E157Q, D188N/E189Q, D195N and D214N were made on the subunit II to test their importance in Cc binding (Zhen et al., 1999). The turnover numbers with both horse Cc and *R. sphaeroides* Cc_2 for these mutants vary from 20% to almost 100% of the wild type oxidase. To determine if these observed changes in activity reflected different contributions of these carboxyl residues to

the binding of C*c*, complete spectral analysis was carried out by UV-visible and EPR, showing no structural effects of mutations. In the ionic strength dependent activity studies with horse C*c*, the maximum activities are achieved at lower ionic strengths for the mutants, suggesting that Asp-214, Glu-148, Glu-157 and Asp-195 contribute to C*c* binding. Asp-151, Glu-152, Asp-188, and Glu-189 mutants have no significant effect on the ionic strength dependence activity, consistent with little or no involvement in the docking. These conclusions were confirmed by time-resolved kinetic assays that showed no change in the intrinsic electron transfer rate within the C*c*-C*c*O complex for the latter set of mutants, but significantly inhibited rates in the former. Direct binding assays further substantiated the conclusions (Wang et al., 1999).

The turnover number of wild-type C*c*O with horse C*c* is about 6-fold higher than with *R. sphaeroides* Cc_2; this was attributed to the different surface pattern of charge on the cytochromes. In particular, *R. sphaeroides* Cc_2 lacks Lys-13 and Lys-72. In the case of D214N and D195N, they were found to have different relative reactivities with the horse and *R.s.* cytochromes. D214N and D195N retain 24% and 71% of wide-type activity with horse C*c* respectively, whereas they retain 67% and 19% of wide-type activity with *R.s.* Cc_2. Further ionic strength assays showed Asp-214 did not contribute to the binding with *R.s.* Cc_2. This suggested that Asp-214 in C*c*O may interact with Lys-72 in horse C*c*. In contrast, Asp-195 contributes more to the formation and electron transfer capacity of the *R. sphaeroides* Cc_2:C*c*O complex. These results imply a specific complementarity of charge between C*c*O and C*c*.

There is a set of highly conserved aromatic residues Trp(143)-Tyr-Trp-X-Tyr-X-Tyr(149) in the C*c*O subunit II soluble domain which have been postulated to be involved

in the electron transfer from cytochrome *c* to Cu_A or Cu_A to heme a. The crystal structure shows Trp-143 in close proximity to Cu_A on the surface of the soluble domain. Mutants W143F and W143A were made to analyze the role of this tryptophan in electron transfer. The turnover rates for both mutants are 2% and 7% of wild type for W143A and W143F respectively when measured with both horse C*c* and *R. sphaeroides* Cc_2. This similar inhibition suggests that both horse C*c* and *R. sphaeroides* Cc_2 use the same residue, Trp-143, as the electron conduit to C*c*O, because the Cu_A center is spectrally unaltered and the mutants have the same binding strength as the wild-type. In the crystal structure, Trp-143 is about 5Å above the Cu_A center and in the center of the conserved carboxyl residues that appear to be involved in the binding. Indeed, the intrinsic electron transfer rates from C*c* to Cu_A are decreased up to 1000-fold in the rapid kinetic assay. This very large decrease strongly suggests that the pathway for electron transfer between heme *c* and Cu_A has been disrupted. With the report that the mutation W143Q in *P. denitrificans* C*c*O also leads to a large loss in steady-state electron transfer activity, Trp-143 is identified as the electron entry site to Cu_A. This also places the two cytochromes on approximately the same binding area on C*c*O but with slightly different orientation and guiding electrostatics.

The above analyses suggest a picture of the interface of the docking of cytochromes on the C*c*O. Lys-8, Lys-13, and Lys-86/87 interact with Asp195, Glu157, and Glu148, respectively. However, other interactions are possible and the exact interaction can only be guessed at from these data.

IV. Computational Modeling Approaches

com
kine
the b
bovi
Piqu
mole
six b
indic
cente
oxid
repre
analy

4A
143
elec
sph
Trp
com
exp
Phe

The transient binding of C*c* to C*c*O make this redox system amenable to computational modeling based on static crystallographic structures, because the fast kinetics of these interactions suggest that large conformational changes do not occur upon the binding of the electron transfer partner. The electron-transfer complex between bovine C*c*O and horse C*c* has been modeled with the docking program DOT (Roberts & Pique, 1999), which provides a complete search of all orientations between the two molecules by systematically rotating and translating one molecule about the other. Thirty-six billion configurations of the two molecules were calculated. The free-energy map indicates that the positively charged front face of C*c*, with the exposed heme edge in the center, is preferentially oriented toward the large negative region on the cytochrome *c* oxidase surface formed by the soluble domain of subunit II. In this interaction region, a representative configuration from the tight cluster of lowest energy solutions was further analyzed to determine the specific interface contacts.

In this most-probable model complex, the exposed heme edge of heme *c* is within 4Å of the indole ring of Trp-143*. This position and proximity imply involvement of Trp-143 in the electron transfer, as observed experimentally. A severe drop in intrinsic electron transfer rate is measured when Trp-143 is mutated to Phe and Ala in *R. sphaeroides* C*c*O (Zhen et al., 1999). A small, hydrophobic contact region surrounds the Trp-143 and the contacting heme-edge, which is in turn surrounded by electrostatically complementary hydrophilic interactions. The hydrophobic region of C*c* consists of the exposed heme edge, the adjacent Gln-16 and Cys-17 side chains, and residues Ile-81, Phe-82 and Ala-83, which form a β-strand paralleling one heme face. The corresponding

region on C*c*O consists of residues Tyr-141, Gln-142, Trp-143 and Tyr-144 forming a loop over the Cu_A site. Among the lysine residues from C*c* and the carboxyl groups from C*c*O, the interaction of Lys-13 with Glu-157 and Lys-72 with Gln-142 and Asp-214 are the most important hydrophilic interactions due to their proximity to the hydrophobic region and exclusion from bulk solvent. Glu-148 and Ala-213 (Glu-157 for bovine C*c*O) from C*c*O are slightly farther from the hydrophobic core of the interface. They are near C*c* Lys-86 and Lys-87. The OE1 of Asp-195 is about 8Å from NZ of Lys-8. The two residues might interact with each other through a water bridge.

The experimental and computational results agree that the soluble domain of C*c*O subunit II is involved in the interaction with C*c*. The main chains of subunit II of both bovine and *R. sphaeroides* are highly similar. Sequence identity is highest surrounding the Cu_A site and on the C*c*-binding surface. A one-to-one correspondence is present for most of the acidic residues surrounding the hydrophobic loop, even though bovine C*c*O has one additional carboxyl residue on subunit II, Asp-157(Ala-213 in *R. sphaeroides*). Mutagenesis studies in *Paracoccus denitrificans* C*c*O also implicates another carboxyl residue on *Paracoccus denitrificans* C*c*O subunit I, Asp-257 (Gln-265 in *R. sphaeroides*, Asp-221 in bovine) in C*c* binding (Roberts & Pique, 1999; Witt et al., 1998). The highly homologous crystal structures of both oxidases suggests that the docking studies with the bovine C*c*O should apply to its counterpart in *R. sphaeroides* C*c*O, and the mutagenesis, binding, and kinetic studies on *R. sphaeroides* C*c*O should apply to the bovine C*c*O.

The predicted structure is consistent with the mutagenesis, binding and time-resolved kinetics studies. The properties of the calculated interface strongly resemble

---

* All residue numbering in C*c*O is according to *R. sphaeroides* sequence.

those found in the crystallographic structure of the complex of yeast C*c*P with yeast Cc (Pelletier & Kraut, 1992).

Finally, the DOT calculation suggests that there may be a second binding site which is further from the membrane for C*c* in the large negative region. This is in agreement with the evidence that supports a second, weaker binding site of C*c*O in which a bound C*c* molecule could interact with a C*c* molecule in the primary binding site (Ferguson-Miller et al., 1976). This low-affinity binding could be more disordered than the high-affinity one and may need a bound C*c* at the high-affinity site to define its orientation.

Another computer modeling using program FTDOCK (Flöck & Helms, 2002) was conducted recently on complexes of cytochrome *c* oxidase from *Paracoccus denitrificans* with horse cytochrome *c*, and with its physiological counterpart cytochrome *c*552. The complex obtained from docking with horse heart cytochrome *c* has a very similar orientation to the complex found by DOT modeling, in which horse cytochrome *c* was docked against the bovine crystal structure of C*c*O. The position and orientation of these two complexes differ only by a few Angstroms and degrees, respectively. If one superimposes the corresponding amino acids of the two C*c*O structures in both C*c*/C*c*O complexes, the RMSD between the two cytochromes *c* coordinates is 3.8Å. The close outcomes of these two computational approaches add strength to both.

V. Summary

The results from chemical modification, crystallography for C*c*O, mutagenesis and computer modeling have provided consistent information about the docking of C*c* onto C*c*O. Of these methodologies, computer modeling offered a more detailed understanding of the docking. However, does the complex model truthfully reflect the physiological binding of C*c* onto C*c*O? In order to test the accuracy of the model, further work needs to be done.

chen

can

dive

grow

elec

sequ

bind

hem

puri

info

198

revi

whi

I. P

Dev

Part III *c*-type cytochromes in *Rhodobacter sphaeroides*

Rhodobacter sphaeroides, a purple nonsulfer bacterium, can grow chemoheterotrophically in the dark or photoheterotrophically in the light. Some variants can use N_2O as electron acceptor to grow anaerobically. To accommodate these diversified growing conditions, several electron transfer chains are used under different growth conditions and several *c*-type cytochromes play important roles in transferring electrons in these pathways.

Almost all the *c*-type cytochromes have a CXXCH heme binding motif in their sequences (Meyer & Kamen, 1982). These two cysteines of the apoprotein covalently bind to the vinyl side chain of the heme via two thioether bonds. So far, no other types of heme have been found to be covalently bound.

As cytochromes *c* are small, stable, mostly soluble and relatively easy to be purified, they are favorite proteins in many research areas. This has led to abundant information about these proteins (Margoliash, 1966; Bartsch, 1978; Meyer & Kamen, 1982; Pettigrew & Moore, 1987; Moore & Pettigrew, 1990; Scott & Mauk, 1996). This review will address cytochromes *c* in *Rhodobacter sphaeroides*. The question regarding which one is the physiological electron donor for the aa_3 oxidase is also discussed.

I. Properties of *c*-type cytochromes

Table 1.1 (Yu, Dong, & Yu, 1986; Trumpower, 1990; Overfield, Wraight & Devault, 1979; Chory, Donohue, Varga, Staehelin & Kaplan, 1984; Donohue, McEwan,

Van

Cusc

spha

cyto

oxid

spha

has t

al., 1

a sul

pred

mam

used

II. V

oxid

its p

und

cell

dark

grow

Van Doren, Crofts & Kaplan, 1984; Rott & Donohue, 1990; Cusanovich, 1971; Meyer & Cusanovich, 1985) shows the characteristics of most of the cytochromes *c* found in the *R. sphaeroides*.

Besides the cytochromes *c* covered in Table 1.1, there are three other *c*-type cytochromes that are part of the cytochrome cbb_3 oxidase complex. As a heme-copper oxidase, cytochrome cbb_3 oxidase has been found in many species, including *R. sphaeroides* (García-Horsman et al., 1994b). Instead of having a Cu_A site in the protein, it has two covalently bound *c*-type cytochromes (García-Horsman et al., 1994; de Gier, et al., 1996) at the C-terminus of subunit II and one covalently bound *c*-type cytochrome in a subunit basically homologous to subunit III of C*c*O. All of these cytochromes *c* have predominantly negatively charged residues with all the conserved lysine residues in mammalian C*c* missing. This suggests that other forces than electrostatic interaction are used to stabilize the cytochromes and the oxidase.

II. Which cytochrome *c* is the physiological substrate for aa_3-type oxidase in *R. sphaeroides?*

The aa_3-type C*c*O of *R. sphaeroides* has been crystallized and characterized, but its physiological substrate is still unknown. Knowing the real substrate can help to understand the electron flow in the respiratory chain and the regulatory mechanisms in cells. As aa_3-type C*c*O is at higher levels when the cells are grown aerobically in the dark, its physiological substrate should be present at relatively higher levels in the same growing situation. To transfer electrons efficiently, a reasonable amount of *c*-type

Table 1.1 Characters of the Cytochromes c in R. sphaeroides

Table 1.1 Characters of the Cytochromes *c* in *R. sphaeroides*

Name	Soluble / Insoluble	Molecular Weight (kDa)	Crystal Structure	Function	Redox Potential (mV)	α - Peak[a] (nm)	Soret (nm)	Comment
c_1	detergent soluble	30	N/A	Transfer electron from bc_1 complex to soluble C*c*	228	552.5	417	a subunit of the bc_1 complex
c_2[b]	H_2O soluble	14	1cxa.pdb	Transfer electron cyclically from the cytochrome bc_1 complex to the reaction center	356	550		Its deleted strains can not grow photosynthetically.
Iso - c_2	H_2O soluble	~14	N/A	May play the role of cytochrome c_2 in some c_2 deleted strains	294	552	415	highly homologous (44% identity) to cytochrome c_2
c'	H_2O soluble	28	N/A[c]	unknown	70 (at pH 7.0)	~552 (single, broad)	Split peaks around 425	homodimer. The heme iron is penta-coordinated.
c_{554}	H_2O soluble	~14	N/A	?	203 (at pH 7.0)	554	419	It is homologous (36% identity) to cytochrome *c'*.
$c_{551.5}$	?	16	N/A	unknown	-254	551.5	419	It has two *c*-type hemes.
c_y	Detergent soluble	24	N/A		N/A	N/A	N/A	
SHP			N/A			548	429	

a. In reduced optical spectrum.
b. Also known as c_{550}.
c. The crystal structure of cytochrome *c'* from *Rhodobacter capsulatus* – a strain closely related to *R. sphaeroides*, is available.

cyto

only

1. C

conc

char

cyto

aero

cssa

cyto

and

reas

anal

espe

occu

subs

2. C

thir

sph

cytochromes should be present in the cell, too. Of all the cytochromes *c*, until recently, only cytochrome c_2 and cytochrome c_{554} meet these criteria.

1. Cytochrome c_{554}

When *R. sphaeroides* is switched from photosynthetic to aerobic growth conditions, cytochrome c_{554} is five to eight fold more abundant than it was before the change of the growth condition. The level of the protein is also about three times that of cytochrome c_2 under aerobic growth. As the most abundant *c*-type cytochrome under aerobically growing condition (Bartsch et al., 1989; Flory & Donohue, 1995), cytochrome c_{554} is a prospective candidate as the substrate for C*c*O. Besides the sequence of cytochrome c_{554}, however, there is limited information about the protein so far.

As the oxidases from both *R. sphaeroides* and bovine are very similar structurally and functionally, and as the mammalian C*c* is a good substrate for both oxidases, it is reasonable to speculate that the physiological substrates should be similar. From sequence analysis, there is little similarity between cytochrome c_{554} from *R.s.* and mammalian C*c*, especially in the region around the exposed heme edge where interactions are known to occur. Given these observations, cytochrome c_{554} is an unlikely candidate for the real substrate of *R. sphaeroides* C*c*O.

2. Cytochrome c_2

Cytochrome c_2 can transfer electrons to aa_3-type oxidase with one-fourth to one-third the turnover rate of bovine C*c*. The binding constant Km of cytochrome c_2 and *R. sphaeroides* C*c*O is about 10 fold that for bovine C*c* (Zhen et al. , 1999; Kituchi et al.,

1965). When cytochrome c_2 is deleted from the strain, there is no significant effect on the cell's aerobic growth rate although there is an abolition of the strain's photosynthetic growth capability (Donohue et al., 1988; Rott & Donohue, 1990). Isocytochrome c_2 may take the role of cytochrome c_2 to transfer electrons to oxidase, but cells can still grow aerobically even when isocytochrome c_2 and cytochrome c_2 are deleted from the strain. When cytochrome c_2 is used to react with bovine C*c*O, the steady-state turn-over rate was only 1% of that of bovine C*c* with bovine C*c*O (Errede & Kamen, 1978). This difference of the reactivity suggests that the protein structures and heme electronic structures are different.

The low spin *R. sphaeroides* cytochrome c_2 (*R.s.* Cc_2) has a highly similar crystal structure to that of bovine C*c*. In their structures, the heme is surrounded by 5 helices and the N-terminal helix interacts with the one at the C-terminal in both structures. *R.s.* Cc_2 has all the residues that are conserved in bovine C*c* that are critical to maintain the overall structures (Figure 1.4). However, the low *pI* value of 5.5 for *R.s.* Cc_2 *versus* 10 for bovine Cc (Meyer & Cusanovich, 1985) tells us that they have different surface charges. Most importantly, the counterparts of Lys-13 and Lys-72 are absent in *R.s.* Cc_2 (Figure 1.4). Cytochrome c_2 does nevertheless have a dipole moment, with most of the positively charged residues located at the front face, where the heme edge is exposed. This front face is used to interact with electron transfer partners (Long et al., 1989).

On the other hand, *R.s.* Cc_2 has a longer sequence because of some insertions. Bovine C*c* has nine lysine residues (8, 13, 25, 27, 72, 73, 79, 86, 87), which are important for its interaction with its electron transfer partners (Smith et al., 1977; Ferguson-Miller

Figure 1.4 Crystal Structure Comparison for Horse Cytochrome *c* (A) and *R. sphaeroides* Cytochrome c_2 (B). The Lysine residues conserved for both cytochromes *c* are shown in green. The Lysine residues that are in horse C*c* but are missing in *R.s.* Cc_2 are shown in matching colors. The Nitrogen and Oxygen atoms are shown in blue and red respectively. The figure was created using Insight II with coordinates for horse C*c* (A) from (Bushnell et al., 1990), and for *R. sphaeroides* C*c*2 (B) from (Axelrod et al., 1994).

A. Horse Cytochrome *c*

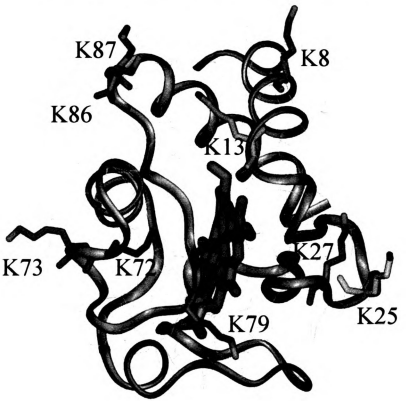

B. *R.s.* Cytochrome c_2

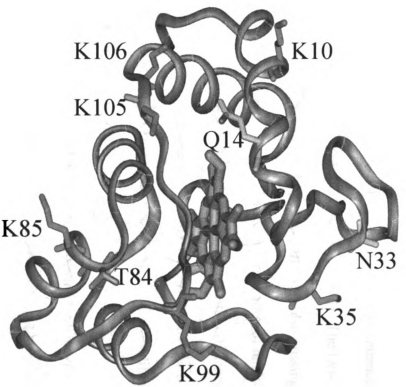

et

R

wi

id

lac

co

19

tha

co

fro

req

so

by t

ma

co

the

bou

3. N

et al., 1978; Rieder & Bosshard, 1980). The counterpart of Lys-13 is a glutamine residue in *R.s.* Cc_2. This Lys-13 is one of the most important charges for the interaction of bovine C*c* with its electron transfer partner (Ferguson-Miller et al., 1978). The Lys-72, which is also identified as very critical in horse C*c* binding to its partner, is also missing in *R.s.* Cc_2. The lack of Lys-13 and Lys-72 in *R.s.* Cc_2 may change the orientation of binding and, as a consequence, lower the binding affinity and the electron transfer efficiency (Zhen et al., 1999). *R.s.* Cc_2 has a high redox potential of 356mV (*versus* 260mV for bovine C*c*) meaning that it has a different heme environment than that of bovine Cc. This difference may contribute to the lower reactivity too.

Interestingly, *R.s.* Cc_2 has similar reactivity to bovine C*c* when it transfers electron from the bc_1 complex (Errede & Kamen, 1978). This evidence suggests that *R.s.* Cc_2 has the required characteristics for it to transfer electron from the bc_1 complex rapidly, whereas some characteristics are missing for it to transfer electrons to oxidase. This is also supported by the fact that cytochrome c_2 is crucial for photosynthesis but not for aerobic respiration. It may use different residues to interact with the bc_1 complex and the oxidase.

The above evidence suggests that *R.s.* Cc_2 may not transfer electrons from the bc_1 complex to oxidase physiologically. It is more likely to mediate the electron transfer from the bc_1 complex to the reaction center.

Besides these soluble cytochromes *c*, recent evidence suggests that some membrane bound cytochrome *c* may be the real substrate for aa_3-oxidase in *R.s.*

3. Membrane Bound Cytochromes *c*

Besides cytochrome c_1, which is a part of the bc_1 complex and an electron donor to cytochrome *c*, a membrane bound cytochrome c_{552} was found in *P. denitrificans* (Turba et al., 1995), and a homologous cytochrome c_y in *R. capsulatus* (Jenney Jr. & Daldal, 1993) and in *R. sphaeroides* (Myllykallio et al., 1999). *P. denitrificans* and *R. capsulatus* are closely related to *R. sphaeroides*.

3.1 Cytochrome c_{552} The genes for cytochrome c_{552} have been cloned from *P. denitrificans* (Turba et al., 1995), *R. capsulatus* (Jenney Jr. & Daldal, 1993) and *Bradyrhizobium japonicum* (Bott et al., 1991). Cytochrome c_{552} has been purified from *P. denitrificans* (Turba et al., 1995) and its soluble domain has been crystallized (Harrenga et al., 2000). The molecular weights of these homologous proteins are about 20 to 22 kDa. Analysis of the amino acid sequences show that there is a hydrophobic N-terminal domain and a globular C-terminal domain. The N-terminal domain (30 to 40 residues) is predicted to form a transmembrane helix in order to anchor the protein to the membrane. In general, the structure of the soluble C-terminal domain has the same features as that of known eukaryotic cytochrome *c*. Most of the important residues in the C-domain are conserved. This domain has the typical "cytochrome *c* fold" structure with the heme surrounded by five helices. Most of the lysine residues on the front face of the bovine C*c* are also present in a similar place in the structure of c_{552} from *P. denitrificans*, but with a larger negative surface charge overall, c_{552} has a smaller positively charged area around the solvent-exposed heme atoms. A neck region between the N-terminal domain and the C-terminal domain may have flexibility due to a high proportion of alanine and negatively charged residues. c_{552} may use this flexibility to transfer electrons between the bc_1 complex and the aa_3 oxidase(Bott et al., 1991).

The isolated complex of cytochrome c_{552}, bc_1 complex and aa_3 oxidase can oxidize ubiquinone rapidly without cytochrome c_2 and adding horse C*c* cannot increase the activity (Berry & Trumpower, 1985). An anti-c_{552} antibody inhibits the electron transfer in *P. denitrificans* (Turba et al., 1995; Smith & Davies, 1991; Steinrücke et al., 1991). The cytochrome *c* oxidase from *P. denitrificans* oxidizes horse heart cytochrome *c* and the cytochrome c_{552} with similar rates (Reincke et al., 1999). All of this evidence suggests that this membrane anchored cytochrome c_{552} shuttles electrons from the bc_1 complex to the aa_3 oxidase (Bakeret et al., 1998).

2.3.2 Cytochrome c_y Another membrane anchored *c*-type cytochrome, cytochrome c_y, has been found in *R.* capsulatus (Jenney Jr. & Daldal). It is found that either cytochrome c_2 or cytochrome c_y is essential for phototrophic growth only when the other is absent. Furthermore, the cytochrome c_2 deleted *R. sphaeroides* strain can be complemented to grow photosynthetically by the cytochrome c_y gene from *R. capsulatus*. This suggests that cytochrome c_y can mediate electron transfer between the bc_1 complex and the reaction center.

Until recently, *R. sphaeroides* was thought to have only soluble cytochrome c_2. Recent work on *R. sphaeroides* found a gene (Myllykallio et al., 1999), *cyc*Y^{Rs}, which is highly homologous to cytochrome c_y of *R. capsulatus* and c_{552} from *P. denitrificans*, too. Alignment of the amino acid sequences of cytochromes c_y from both *R. sphaeroides* and *R. capsulatus* shows that they have a conserved bipartite domain structure. Each of them contains a C-terminal cytochrome *c* subdomain and N-terminal stretch anchoring the protein to the membrane. Several lysine residues (Lys-8, 13, 72, and 87 in horse cytochrome *c* numbering) which are thought to be important for the interactions of cytochrome *c* with its

redox partners are well conserved, whereas several others (Lys-7, 25, 27, 73, 86, and 88) are not. The linker portion of cytochrome c_y from *R. capsulatus* is longer than those of *R. sphaeroides* and *P. denitrificans*.

It was found that cytochrome c_y cannot participate in photosynthetic electron transfer in *R. sphaeroides*, although it is active in respiratory electron transfer, unlike its *R. capsulatus* counterpart. Chimeric constructs showed that the inability to grow photosynthetically comes from, at least in part, its redox active subdomain, which carries the covalently bound heme. There is a big difference between the calculated *pI* of the different cytochromes c_y of 4.74 and 7.76 for *R. sphaeroides* and *R. capsulatus* respectively. It seems that the precise location of the charged residues determine whether cytochrome c_y can form a productive electron transfer complex with its partners. The photosynthetic inability of cytochrome c_y in *R. sphaeroides* suggests that its interactions with the reaction center and oxidase are different. Even though the question of whether this c_y is the real substrate for aa_3 oxidase is complicated by the presence of cbb_3 oxidase in *R. sphaeroides*, further studies will present more information to clarify this ambiguity.

Lately, *R. sphaeroides* mutants lacking either cytochrome c_2 or cytochrome c_y and either the aa_3-oxidase or the cbb_3-oxidase were obtained (Daldal et al., 2001). The data shows that both mobile cytochrome *c*2 and membrane-anchored cytochrome c_y can transfer electrons efficiently from the bc_1 complex to either the cbb_3-oxidase or aa_3-oxidase. The concurrent operation of multiple electron carriers and cytochrome *c* oxidases implies that the respiratory electron transfer pathways of *R. sphaeroides* are more complicated than those of *R. capsulatus*.

III. Summary

Several *c*-type cytochromes are involved in the branched electron transfer chains in *R. sphaeroides*. Cytochrome c_2 transfers electron from the bc_1 complex to the reaction center. It can also transfer electrons to the aa_3 oxidase at one-fourth the rate of bovine C*c*.

The finding of membrane bound cytochrome c_{552} and c_y in several bacteria and their properties suggest that c_y may be the physiological substrate for aa_3 oxidase in *R. sphaeroides*. If it is one of the substrates, it will anchor itself to the membrane and move between the bc_1 complex and the aa_3 substrate using its flexible neck region between the N-terminal transmembrane domain and the C-terminal soluble domain. This may require the bc_1 complex, the membrane bound cytochrome *c* and the aa_3 oxidase to be in proximity on the cytoplasmic membrane to guarantee efficient electron transfer(Berry & Trumpower, 1985). Using analysis of soluble cytochromes and modeling of cytochrome *c*, a good understanding of the important interactions has been obtained even in the absence of a verified, physiological electron donor to *R.s.* C*c*O.

Chapter 2

The Water and/or Proton Exit Pathway

and Its Relationship to Respiratory Control

Introduction

Cytochrome *c* oxidase (C*c*O) is the terminal oxidase in the mitochondrial electron transfer chain. In each reaction cycle, it takes four electrons from soluble cytochrome *c* (C*c*) and reduces one oxygen molecule into two water molecules. Using the energy available, four protons are translocated across the membrane (Wikström, 1977). This translocation results in an electrochemical gradient across the membrane, which can be used by ATP synthase to make ATP (Mitchell, 1966). ATP can be used as energy by organisms directly. A similar process using homologous enzymes is carried out in many prokaryotic as well as eukaryotic organisms.

With the availability of crystal structures of C*c*O from *P. denitrificans* (Iwata et al., 1995), *R. sphaeroides* (Svensson-Ek et al., 2002), and bovine heart (Tsukihara et al., 1995), several proton translocation pathways in the protein have been proposed. These pathways include two proton entry routes, the D and K channels, and a possible water and/or proton exit, immediately above the binuclear active site (Figure 2.1). This channel is at the interface of subunits I and II, with the non-redox-active Mg metal center right at the bottom of this channel (Figure 2.2). The octahedral coordination of this metal center has 3 amino acid residues and 3 waters as its ligands. With highly resolved crystal structures of oxidase, water molecules are seen in this region of the protein, which is consistent with the proposal that it could provide a proton and/or water exit channel.

Two residues, Arg-234 from subunit II and Asp-271 from subunit I are found to be at a possible external mouth of the channel. In the *R.s.* C*c*O structure, the distances from the closest N atom of Arg-234 to the carboxyl oxygen atoms of Asp271 are 3.46Å and 3.05Å, respectively. These distances are in the range of ionic strength interaction.

Figure 2.1 Crystal Structure of *Rhodobacter sphaeroides* Cytochrome *c* Oxidase and the Possible H_2O and/or H^+ Exit Pathway. Helices of subunit I, II, and III are shown in yellow, purple and cyan respectively. Yellow balls represent Cu_A and Cu_B, orange ball for magnesium and magenta ball for calcium. The green, blue and red arrows represent the suggested K- and D- proton uptake pathways and H_2O and/or H^+ Exit Pathway. The figure was created using the Insight II program with coordinates from Svensson-Ek et al., 2002.

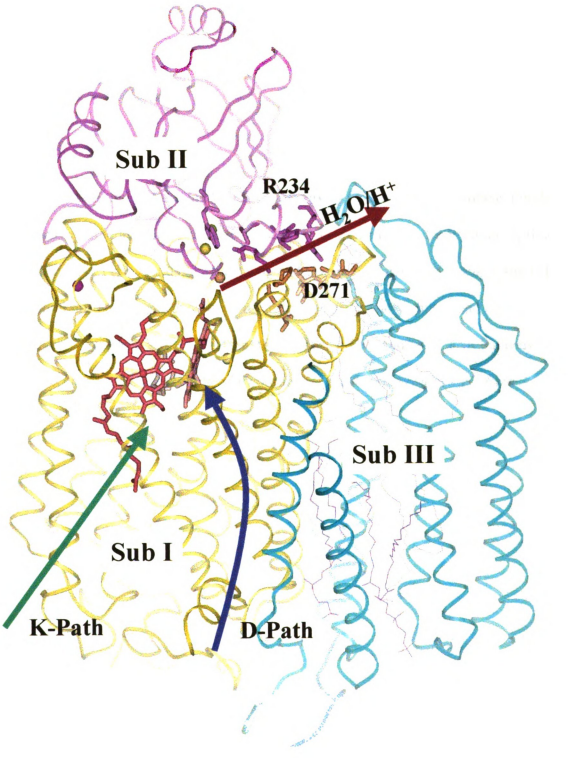
Sub II
R234
H_2O/H^+
D271
Sub III
Sub I
K-Path
D-Path

Figure 2.2 Possible H_2O and/or H^+ Exit Pathway of Cytochrome *c* Oxidase. Purple, orange and cyan represent residues involved with the exit pathway from subunit I, II, and III respectively. Yellow balls represent Cu_A and Cu_B and orange ball for magnesium. The oxygen and nitrogen atoms involved with the pathway are shown in red and blue respectively. The green arrows represent the suggested H_2O and/or H^+ Exit Pathway. The figure was created using Insight II with coordinates for *R. sphaeroides* C*c*O from Svensson-Ek et al., 2002.

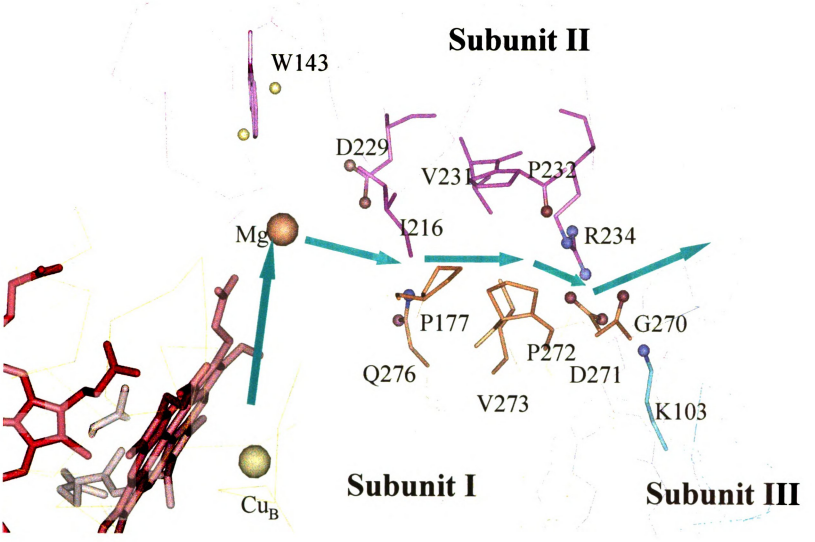
Subunit II
W143
D229
V231
P232
I216
R234
Mg
P177
G270
P272
Q276
D271
V273
K103
Subunit I
Subunit III
Cu_B

Further, Asp-271 is the first residue in a conserved DPxxY region, which is part of a loop, situated at the periplasmic end of the helix VI. This (N/D)PxxY motif is also highly conserved in the transmembrane segment 7(TMS 7) of G-protein-coupled receptors (GPCRs) (Wess et al., 1993; Zhang & Ewinstein, 1993; Lou, Zhang & Weinstein, 1994; Van Rhee & Jacobson, 1996). TMS 7 has been shown to play an important role in the signal transduction function of GPCRs. Instead of being an alpha-helix, as most of the transmembrane segments are, the sequence of TMS 7 is inconsistent with it being an ideal alpha-helix and (N/D)PxxY motif has been identified as the major determinant for deviation of TMS 7 from ideal helicity (Konvicka et al., 1998). The deviation includes an Asn/Asp turn and a flexible "hinge" region. The flexibility introduced by the specific structural perturbation produced by the (NP/DP) motif in TMS 7 is proposed to have a significant role in transmitting the signal from ligand binding to the receptor, across the membrane.

In C*c*O, the DPxxY motif is situated at the periplasmic end of helix VI of subunit I. Helix VI contains a number of essential, highly conserved residues (H284, Y288, E286, and S299), which are important for the oxygen reduction at the heme a_3 – Cu_B site, and for proton pumping (Figure 2.3). His-284 is a ligand of Cu_B (Shapleigh et al., 1992; Hosler et al., 1993); Tyr-288 is covalently bound to His-284 (Ostermeier et al., 1997; Yoshikawa et al., 1998); Glu-286 is a buried charge that is part of a proton uptake pathway, the D-path (Konstantinov et al., 1997; Junemann et al., 1999); and Ser-299 is part of another proton uptake path, the K-path. Also close to this loop region are the heme propionates or nearby protonatable groups that are also proposed to trap protons during

Figure 2.3 The Overall Structure of Helix IV and Possible Proton Pathways. Purple and yellow represent residues involved with the exit pathway from subunit I and II respectively. Yellow balls represent Cu_A and Cu_B and the orange ball represents magnesium. The oxygen and nitrogen atoms involved with the pathway are shown in red and blue respectively. K-path and residues involved with it are shown in purple, D-path and residues involved with it are shown in green and red represents the possible H_2O and/or H^+ Exit Pathway. The figure was created using Insight II with coordinates for *R. sphaeroides* C*c*O from Svensson-Ek *et al.*, 2002.

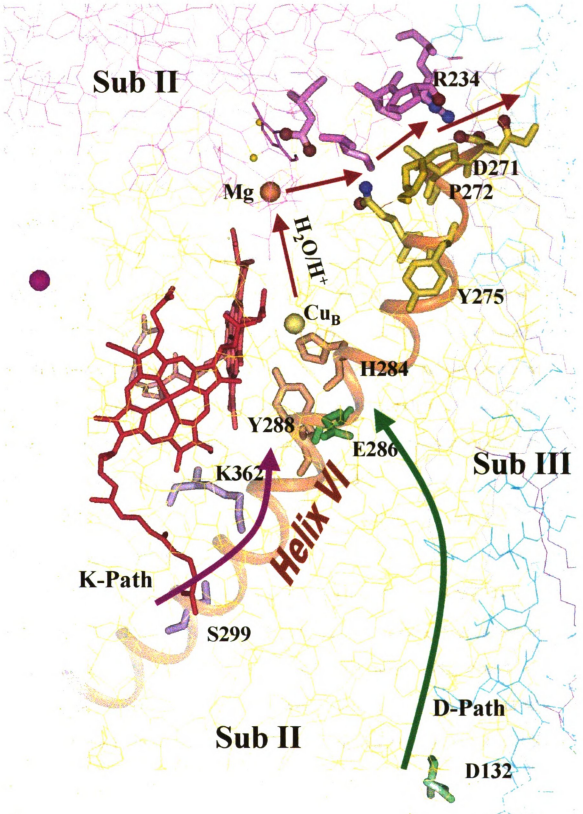
Sub II
R234
D271
P272
Mg
H_2O/H^+
Y275
Cu_B
H284
Y288
E286
Sub III
K362
Helix VI
K-Path
S299
D-Path
Sub II
D132

coupled electron transfer (Michel, 1999). Due to its relationship to all these critical groups, it is proposed (Ferguson-Miller, S., NIH proposal) that the DPxxY motif may undergo conformational changes during the catalytic cycle and mediate the interaction between subunits I and II, possibly controlling the release of the pumped protons. This externally situated, charged region may also respond to the pH or electrical gradient to mediate respiratory control, the inhibition of oxidase activity in the presence of a membrane potential.

Arg-234 in subunit I has been converted to His and Cys mutants. These mutants had ~100% and 50% of the wild type activity. The Cys mutant shows perturbed proton pumping behavior and low respiratory control (Florens et al., unpublished data; personal communication, Bryan Schmidt). As Asp-271 from subunit I strongly interacts with Arg234 and has the proposed role in proton pumping as stated above, Asn and His mutants were made to test the nature of the interaction and its importance in the function of the protein. The data of these two mutants is reported.

Materials and Methods

Materials All restriction endonucleases were from Boehringer Mannheim (Indianapolis, IN); Plasmid pRK415 and *E. coli* strain S-17-1 were obtained from the sources indicated in Shapleigh and Gennis (Shapleigh & Gennis, 1992). Plasmid pYJ100 containing the sequence of *cox*II and *cox*III was originally prepared by Cao et al. (Cao et al., 1992). The gel purification kit and Ni^{2+}-NTA resin were from Qiagen (Santa Clarita, CA). Ultrafree-15 centrifugal filters were from Millipore (Bedford, MA), lauryl maltoside from Anatrace Inc. (Maumee, OH). Horse heart Cc (Sigma type VI) was

purchased from Sigma and was purified on a carboxymethyl cellulose column before use (Brautigan et al., 1978).

Construction of the D271 mutants Site-directed mutagenesis at residue Asp-271 was performed by the overlap extension PCR method (Ho et al., 1989). In the PCR reactions, the high fidelity *Pfu* polymerase (Stratagene, La Jolla, CA) was used, and all PCR products were sequenced to make sure that no secondary mutations were introduced.

The PCR products were digested with Kpn I and Bgl II restriction enzymes. These digested products were cloned into the pSL1180 vector. Then the fragments were inserted into pJS3-X6H2 vector, which has the whole COX I gene. At this step, the sequences were checked to make sure that the mutations were introduced. After cutting out the mutated COX I, the fragments were inserted into pUC19 vector to get rid of the unknown fragment in pJS3-X6H2. This plasmid is called pJS3-SH. Then COX II and III were inserted into pJS3-SH to make mutated plasmid pYJ123H. At this step, the genes for all three subunits were together into one plasmid. The whole genes were then inserted into pRK415 so that the protein could be overexpressed in *R. sphaeroides*. This was followed by transformation into the *E.coli* host strain S17-1, then the plasmid was conjugated into *Rhodobacter sphaeroides* strain JS100, a COX I – deleted strain.

Conjugation Plasmid pRK415 and its derivatives were conjugated into *R. sphaeroides* strain JS100 with *E. coli* strain S-17-1 as the donor. Basically, JS100 cells in late exponential phase were mixed with S-17-1 cells in early exponential phase before the mixture was spun for 1min. The pellet was resuspended in 100μl LB medium and spotted onto a nitrocellulose filter on a LB plate. After incubation at 30°C for 6 hours, the filter

was washed with 5ml Sistrom's media. The cells were spun down and resuspended in 1ml Sistrom's medium. Then the cells were plated on Sistrom's agar plates containing Streptomycin/Spectinomycin antibiotics and were grown at 30°C for 2-3 days. A single colony was picked and restreaked on a new Sistrom's plate with the same antibiotics. Cells were grown at 30°C for 3 days, then inoculated into two 100 mL volumes of Sistrom's media with the same antibiotics and grown at 30°C for about 2 days.

Cell growth *E. coli* strains S-17-1 were grown in LB medium at 37°C. Plasmids pUC19, pRK415 and their derivatives were maintained in the presence of the following antibiotics: ampicillin (Ap) (50μg/ml), streptomycin (Sm) (50μg/ml), spectinomycin (Sp) (50μg/ml) and tetracycline (Tc) (15μg/ml).

R. sphaeroides strain JS100 and its conjugated derivatives were grown aerobically at 30°C in 2.8 liter Fernbach flasks containing 800ml of Sistrom's minimal medium A (Cohen-Bazire et al., 1957) with rapid swirling. All the strains used here were maintained in the presence of Sm (50μg/ml) and Sp (50μg/ml). For the conjugated strains, Tc of 1μg/ml was added.

Preparation of cytoplasmic membranes Membranes were prepared as described in Zhen et al. (1999). Approximately 40g of wet weight cells were resuspended in 200ml of 50mM KH_2PO_4, 1mM EDTA, 50mg/ml DNaseI and RNase. The resuspended cells were broken by two passages through a French pressure cell at 20,000psi. Unbroken cells and debris were removed by centrifugation at 30,000g for 30 minutes. The supernatant was centrifuged at 200,000g for 1.5 hours at 4°C to get the pellets of the membranes. The membrane pellets were resuspended in 10mM Tris-HCl, 40mM KCl at pH8.0. Lauryl maltoside (LM) was added to a final concentration of 2% for solubilization. The

membranes were stirred at 4 °C for 30 min and then centrifuged at 200,000g for 30 min to remove unsolubilized material.

Ni^{2+}-NTA purification of C*c*O The solubilized membranes were mixed with Ni^{2+}-NTA resin after washing the resin with water in a ratio of 1ml of packed resin for every 2.5mg of oxidase. Ten mM imidazole was added to prevent nonspecific binding. The mixture was stirred at 4 °C for 1h and then poured into a gravity column. The column was washed with 10mM Tris-HCl, pH8.0, 40mM KCl, 10mM imidazole, 0.1% LM until the flow-through was clear of color and turbidity. The column was further washed with 5 bed volumes of 10mM Tris-HCl, pH8.0, 40mM KCl, 0.1% LM to wash off the imidazole. The enzyme was eluted slowly with 100mM histidine, 10mM Tris-HCl, pH8.0, 40mM KCl, 0.1% LM. The green colored fractions containing oxidase were pooled together and washed 3 times with 10mM Tris-HCl, pH8.0, 40mM KCl, 0.1% LM, by centrifugal filtration in Ultrafree-15 centrifugal filters with molecular weight cutoff of 50kD to reduce the histidine level to less than 1mM.

FPLC-DEAE chromatography The tandem DEAE-5PW Fast Performance Liquid Chromatography (FPLC) columns (8mm × 7.5cm, TosoHaas) were attached to an FPLC system (Pharmacia LKB Biotechnology Inc.). The columns were preequilibrated with 10mM KH_2PO_4, pH7.6, 1mM EDTA, 0.2% lauryl maltoside. The Ni^{2+}-NTA purified C*c*O was applied to the columns. The samples were eluted with the same buffer but having gradient of 0.01-0.35M KCl at a flow rate of 0.5 ml/min. The fractions containing oxidase were concentrated and stored at -80°C.

Activity assay The maximum turnover number (molecular activity) of C*c*O from *R. sphaeroides* was measured polarographically using a Gilson model 5/6H oxygraph at

25°C in a reaction medium containing 50mM KH_2PO_4, pH6.5, in the presence of 0.05% LM, 2.8mM ascorbate, 0.55mM TMPD and 30μM of horse C*c*. The oxidase concentrations were in the range of 5 to 50nM.

SpectroPhotometric analysis The solubilized membrane or oxidase was diluted in 50mM KH_2PO_4, pH6.5, 2% LM and the spectra were taken on a UV/visible spectrometer (Perkin Elmer, Lamda 40P). Dithionite and ferricyanide were used to fully reduce or oxidize the samples, respectively. The extinction coefficients used were $\Delta\varepsilon_{606\text{-}640}=37cm^{-1}mM^{-1}$ for absolute spectra of the purified dithionite-reduced enzyme, and $\Delta\varepsilon_{606\text{-}630}=28.9cm^{-1}mM^{-1}$ for difference spectra of the dithionite-reduced minus ferricyanide-oxidized enzyme or membranes(Callahan & Babcock, 1983).

Results

Design of Mutants

From the crystal structure of *Rhodobacter sphaeroides* oxidase, we can see that Asp271 in subunit I is in close proximity to Arg234 from subunit II and Lys103 from subunit III. Arg234 has been mutated to histidine, cysteine and serine (Florens et al., unpublished data). Even though all of these mutants have lower activity than wild type, R234H mutant shows behavior close to wild type oxidase. There is evidence that all the mutants have a tendency to dissociate and lose subunit II and III during purification of the protein and possibly during assay procedures. This indicates that the salt bridge between Arg234 and Asp271 may be important for holding subunit I together with II and III. Mutation of Lys103 also caused subunit III to be lost, but does not result in

significant loss of activity when the fraction still containing subunit III is purified by a his-tag-III version of C*c*O (personal communication with Dr. John Hosler).

Because Asp-271 is also in the motif (N/D)PxxY, which has been shown to play an important role in the signal transduction function of GPCR (Wess et al., 1993; Zhang & Ewinstein, 1993; Lou, Zhang & Weinstein, 1994; Van Rhee & Jacobson, 1996), changing Asp-271 to Asn should show us whether Asn can substitute for Asp at this position for the function of signaling. Also, changing the carboxyl group to amide removes the negative charge. This might demonstrate the significance of the charge on Asp-271.

Histidine has a normal pKa of 6.0 so that under physiological conditions of pH 7.2 for *R. sphaeroides*, histidine should be neutral. However, the pKa of an amino acid depends on its microenvironment in the protein. Also, histidine is a good metal ligand. Changing Asp to His can give us further options to put a metal site at this exit of the presumed water channel to reversibly block it.

The substitution of cysteine for Asp 271 was chosen because it can form a disulfide bond with another cysteine residue if the two residues are close enough in space. By changing both Arg234 from subunit I and Asp 271 from subunit II to cysteines, they could form a disulfide bond , assuming some flexibility in the region, to shut down the suspected water channel in a way different from the metal ligand method. We can also attach a bulky and/or fluorescent group onto the cysteine residue.

Construction of Mutants

The mutants D271N and D271H were successfully made. However, the mutant for D271C could not be made when constructing the pYJ123H plasmid. Therefore, only two mutants were expressed and characterized.

Optical spectral characteristics of mutants

In the reduced form, wild-type C*c*O from *R. sphaeroides* has a characteristic absorbance at 445nm and 606nm for the Soret and α-peaks, respectively, with a Soret to α-peak ratio ($A_{445\text{-}490}/A_{606\text{-}630}$) of 5.6. Both mutants, D271H/N, have shown shifted α-peaks in the visible spectrum. Specifically, both α-peaks shifted to about 605nm in the solubilized membranes before the Ni^{2+}-NTA column. After Ni^{2+}-NTA purification, the α-peaks shifted to 600nm and 597nm for D271N and D271H, respectively (Figure 2.4 & 2.5). This indicates structural alteration at the heme centers in the proteins. Asp271 was revealed by X-ray structures to be at the interface of subunits I, II and III, not internally located to ligate with the metal centers (Ostermeier et al., 1997; Yoshikawa et al., 1998; Svensson-Ek et al., 2002). The observation of severely disrupted heme centers might indicate the disaggregation of the subunits and exposure of the heme centers to a more aqueous environment. It is also possible that the environment of the heme centers has been changed with the introduction of the mutants because of the movement of helix VI. Because the α-peak shifted from 605nm to 600nm during Ni^{2+}-NTA purification for D271N, the mutant could have gone through further dissociation during the purification process.

The Activities of mutant enzymes

C*c*O from *R. sphaeroides* shows high activity with horse C*c*; as a result, horse C*c* is used routinely in kinetics assays. The maximum turnover numbers of mutated C*c*O have been measured using horse C*c* as the substrate in polarographic assays. Normally, wild-type oxidase shows a maximum turnover rate of 1700 s^{-1} in 50mM KH_2PO_4, pH6.5, in the presence of detergent. Under the same condition, the turnover rates for D271N and D271H mutants are 5.9% and 4.5% of the rate for wild-type oxidase. These are shown in Table 2.1. With the spectral data observed, the low activity might be the result of the disaggregation or metal center disruption.

SDS-Page Analysis

During SDS-page, the protein is denatured with detergent and urea so that the subunits are dissociated and the peptides are in an extended conformation. Then the subunits can be separated dependent on their different molecular weights. Under this analysis, C*c*O of *R. sphaeroides* mainly shows 3 bands, 49kD for subunit I, 37kD for subunit II and 22kD for subunit III. The real molecular weights for the three subunits are 62.6kD, 32.9kD and 30.1kD for subunit I, subunit II and subunit III respectively. The observation of lower molecular weight bands of two of the subunits after the SDS-page indicates that the hydrophobic peptides of oxidase bind more of the negatively charged SDS and thus migrate faster during electrophoresis. Subunit IV at ~ 6 kD (Sevensson-Ek et al., 2002), is only clearly seen in a higher resolving gel (18% acrylamide).

Table 2.1 The Activity Comparison of D271 Mutants of Cytochrome *c* Oxidase from *R. sphaeroides*

Enzymes	α-peak (nm)	Turnover* (s^{-1})
Wild-type	606	1700
D271N	599	100
D271H	597	77

*The turnover rate is measured with 30 μM horse C*c* in 50mM KH_2PO_4, pH 6.5.

Figure 2.4 Visible Spectra for Ni^{2+}-NTA Purified D271N and D271H Mutants. The proteins (purified with Ni^{2+}-NTA column) are reduced with dithionite and measured in a Perkin-Elmer Lambda 4.0 UV/VIS Spectrophotometer. These measurements were conducted in 100mM KH_2PO_4, 0.1% LM with pH 7.2.

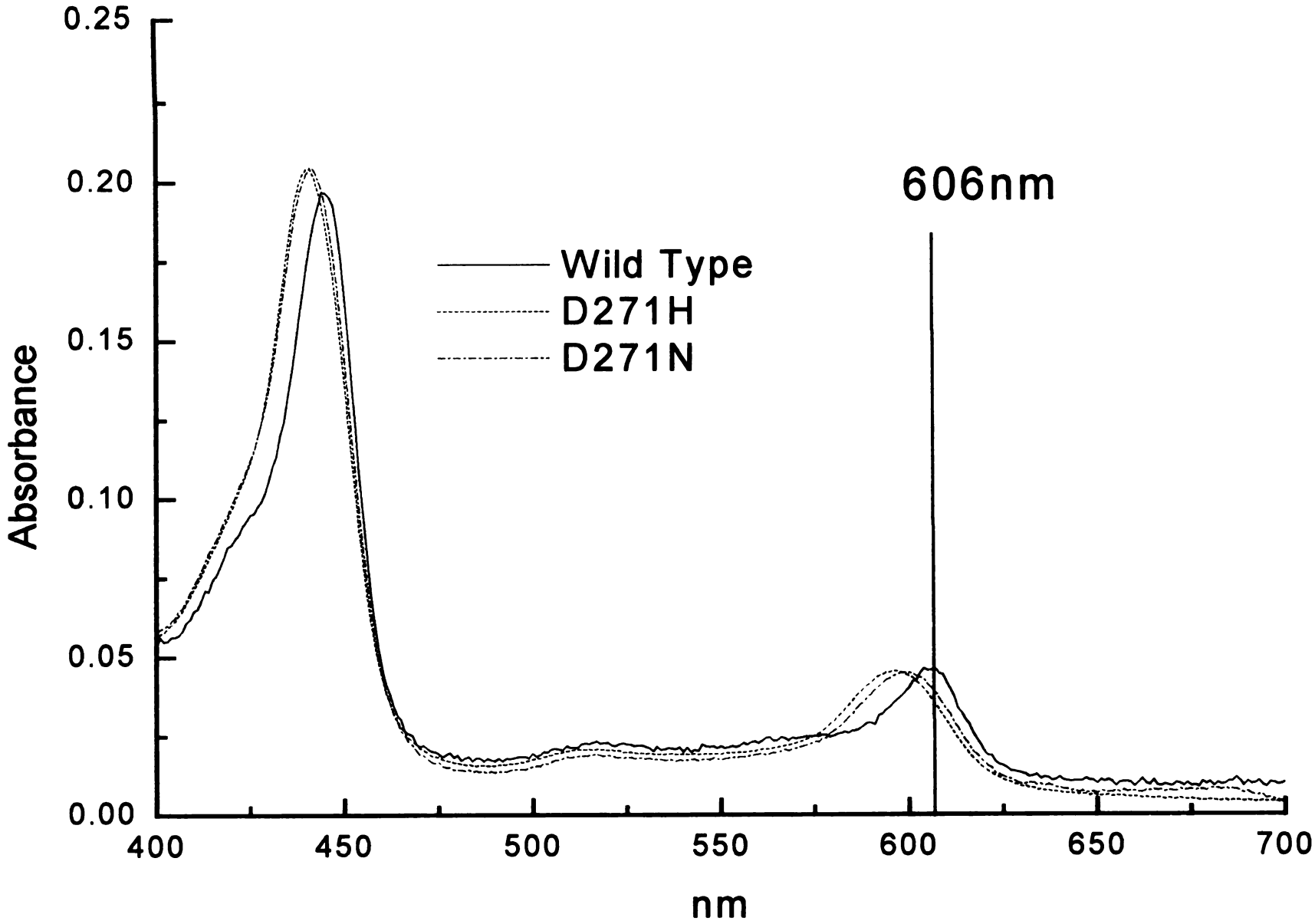
0.25
0.20
0.15
0.10
0.05
0.00
Absorbance
606nm
Wild Type
D271H
D271N
400
450
500
550
600
650
700
nm

Figure 2.5 Comparison Between Visible Spectra for Solubilized Membrane and Ni^{2+}-NTA Purified D271N Mutant. The membranes are reduced with dithionite and measured with membranes oxidized with ferricyanide as a reference in order to obtain the difference spectra in a Perkin-Elmer Lambda 4.0 UV/VIS Spectrophotometer. The Ni^{2+}-NTA purified proteins are reduced with dithionite. These measurements were conducted in 100mM KH_2PO_4, 0.1% LM with pH 7.2. The absorbance for solubilized membrane was magnified by 5 fold.

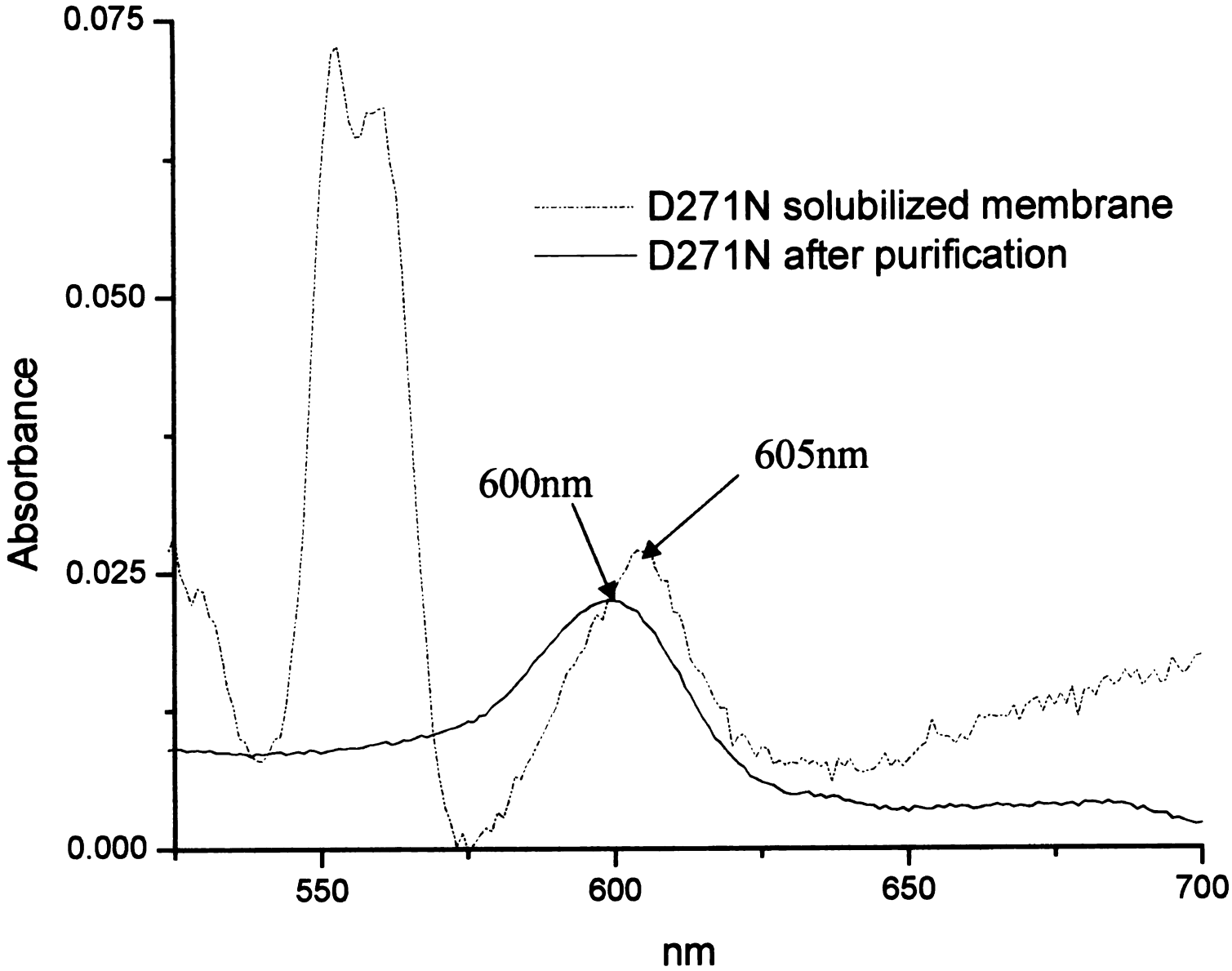
0.075
0.050
0.025
0.000
Absorbance
D271N solubilized membrane
D271N after purification
600nm
605nm
550
600
650
700
nm

Figure 2.6 shows the SDS-page gel analysis for D271 mutants after the Ni^{2+}-NTA purification. From the gel we can see that the purified mutant proteins have a greater than stoichiometric ratio of subunit I compared to wild type. Ni^{2+}-NTA column binds oxidase by interacting with the His-tag, which is constructed on subunit I. If the mutated oxidase cannot hold all the subunits together, Ni^{2+}-NTA purification could result in extra subunit I in the purified mixture.

To avoid getting extra subunit I after the Ni^{2+}-NTA purification, FPLC-DEAE chromatography was conducted for the D271N mutant without prior Ni^{2+}-NTA purification. The tandem DEAE-5PW column separates proteins by their negative amino acid charges on the surface of the 3-D structure and also somewhat by their molecular weights. Figure 2.7 shows the FPLC profile. Figure 2.8 shows the SDS-page analysis for the FPLC results. Because subunit II has a lot more negative amino acids on its surface, it is responsible for much of the binding to the column. The whole oxidase that is attached to subunit II is separated from other impurities, but will co-purify with subunit II alone. From the SDS gel, we can see that the purified mutant has a lot of extra subunit II. This further demonstrates that the protein is dissociating.

Due to the overall disruption of the structure of the mutant forms, further functional characterization was not attempted because it would be difficult to interpret.

Figure 2.6 SDS-Page (14% Separation and 8% stacking) Analysis of Ni^{2+}-NTA Purified D271N and D271H Mutants. ~20 μg of proteins were added in each lane.

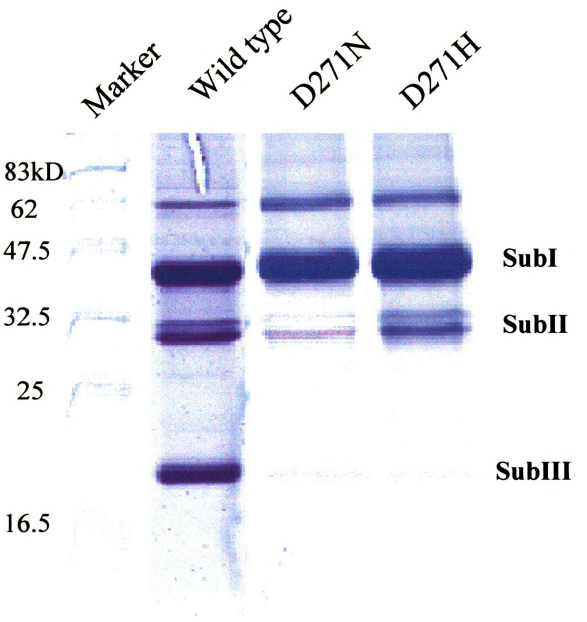
Marker
Wild type
D271N
D271H
83kD
62
47.5
32.5
25
16.5
SubI
SubII
SubIII

Figure 2.7 FPLC Profile for D271N Purification with Tandem DEAE-5PW Column.

The blue line shows the 280nm spectrum for the fractions eluted from the column. Fractions are labeled I-VII. The SDS-page analysis of some of the fractions is shown in Fig. 2.8.

D271N0006091_UV
D271N0006091_Pressure
D271N0006091_Cond
D271N0006091_Fractions
D271N0006091_Conc
mAU
mS/cm
ml
Waste
I
II
III
IV
V
VI
VII
VIII

Figure 2.8 SDS-Page Analysis of FPLC Purified D271N Fractions. The Roman numbering refers the fractions in Figure 2.7.

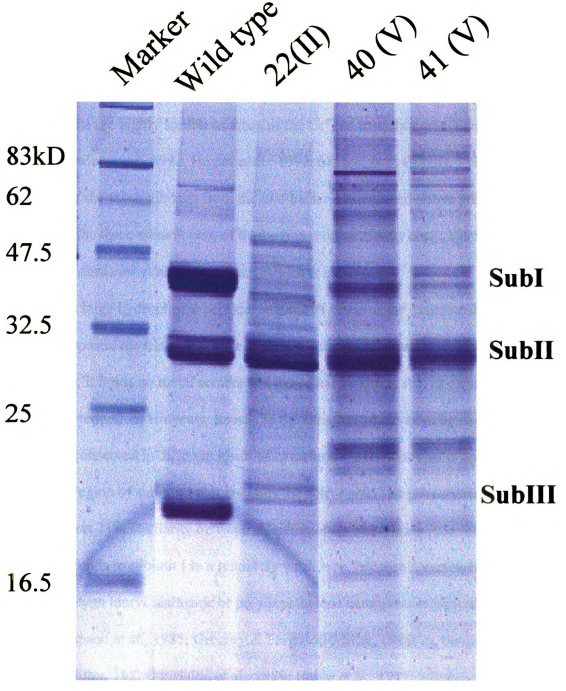
Marker
Wild type
22(II)
40 (V)
41 (V)
83kD
62
47.5
32.5
25
16.5
SubI
SubII
SubIII

Discussion

Subunit III

The catalytic core of CcO of the non-sulfur purple bacteria *Paracoccus denitrificans* and *Rhodobacter sphaeroides* is made up of three subunits: I, II and III. The three subunits are highly similar to those of the CcO of mitochondria (Saraste, 1990; Cao et al., 1991; Cao et al., 1992; Hosler et al., 1992; Shapleigh & Gennis, 1992). Indeed, the structures of the three subunits from the two bacteria mentioned above are almost identical to the three-subunit core of the bovine oxidase (Iwata et al., 1995; Tsukihara et al., 1996; Ostermeier et al., 1996; Svensson-Ek et al., 2002).

As a large hydrophobic peptide, subunit III binds to the transmembrane face of subunit I opposite the transmembrane helices of subunit II (Iwata et al., 1995; Tsukihara et al., 1996). It holds no metal centers and hence has no direct role in electron transfer and oxygen reduction. However, its role in the catalytic core cannot be neglected because it is highly conserved in different kinds of cytochrome *c* oxidase and is situated right against the region of subunit I that contains the active site. The primary structure of subunit III has 71% similarity between *R. sphaeroides* and human (Cao et al.; 1991). Subunit III binds to subunit I in a relatively weak way, because it can be removed from the enzyme with lauryl maltoside or polyoxyethylene detergents at high pH (Solioz et al., 1982; Thompson et al., 1985; Gregory & Ferguson-Miller, 1988(1); Gregory & Ferguson-Miller, 1988(2); Haltia et al., 1989; Haltia et al., 1991; Nicoletti et al., 1998;). How subunit III functions still needs to be determined.

The Lys103 in subunit III

Lys-103 from subunit III sits right next to D271 from subunit I and Arg 234 from subunit II, making a charged triad (Figure 2.2). The mutation of Lys103 to Ala results in loss of subunit III (Personal communication with Dr. Jon Hosler). However, the fraction of the mutated protein containing stoichiometric amounts of subunit III (isolated by a his-tag on subunit III) is as active as wild type in terms of oxygen reduction and proton pumping. Nor does the mutated protein suicide inactivate. Comparing Arg234 mutants of subunit II and D271 mutants of subunit I to the Lys103A, the latter has a less dramatic effect on activity although all of these residues appear to play a role in protein stability (Personal communication, Bryan Schmidt, Dr. Jon Hosler). From subunit III sequence alignments, we found that Lysine at 103 is not highly conserved. In some other C*c*Os such as in bovine and human, this residue is substituted by a histidine. This substitute could be positively charged and play a similar role but it suggests that Lys103 has less significance in the function of C*c*O, compared to Asp271 and Arg234, which are very highly conserved. The importance of these residues in holding the protein together can be assigned as Asp271(I) > Arg234(II) > Lys103(III).

What Forces Are Important in Holding the Protein Together?

In the *R. sphaeroides* crystal structure, the distances from the closest 2 nitrogens of Arg234(II) to the 2 carboxyl oxygen atoms of Asp271(I) are 3.05Å and 3.03Å respectively (Figure 2.2 & 2.9). The two residues are not facing each other head-to-head; the side-on arrangement allows for a stronger interaction. The distance from the closest

Figure 2.9 Conformation Comparison of Possible H_2O and/or H^+ Exit for *R. sphaeroides* (A) and Bovine (B) Cytochrome *c* Oxidase. Purple, orange and cyan represent residues involved with the exit pathway from subunit I, II, and III respectively. The figure was created using Insight II with coordinates for *R. sphaeroides* C*c*O (A) from Svensson-Ek et al., 2002 and for bovine C*c*O (B) from Tsukihara et al., 1995.

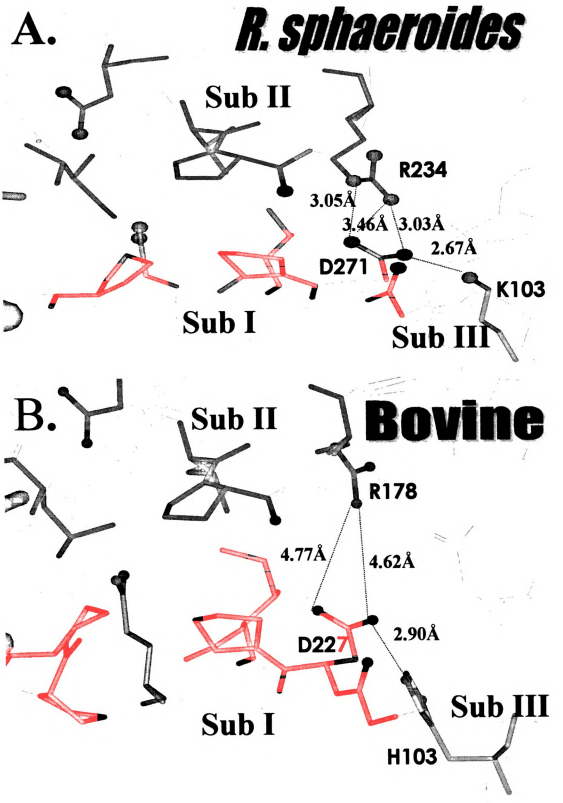
A.
R. sphaeroides
Sub II
R234
3.05Å
3.46Å
3.03Å
2.67Å
D271
K103
Sub I
Sub III
B.
Sub II
Bovine
R178
4.77Å
4.62Å
2.90Å
D227
Sub I
Sub III
H103

oxygen atom of Asp271(I) and ε-nitrogen of Lys103(III) is 2.67Å. These latter two residues are oriented in a way that is favorable for hydrogen bonding, by aligning the O-atom of Asp271 and the N-atom of Lys103 in a head-to-head conformation. Because of relatively strong opposite charges and the short distance among them, the ionic interaction can be very strong and may be the dominant force to hold the subunits together. This does not exclude the existence of water molecules connecting the residues together, although they are not resolved in the 2.3 Å resolution X-ray structure (Svensson-EK et al., 2002).

From the crystal structure of bovine C*c*O (Tsukihara et al., 1996), we can see that Arg234(II) (*R. sphaeroides* numbering) is in a conformation to form a hydrogen bond with Asp271(*R. sphaeroides* numbering) (Figure 2.9). However, the distances from the closest N-atom of Arg234(II) to the carboxyl oxygen atoms of Asp271(I) are 4.77Å and 4.62Å respectively, too far for a direct hydrogen bond. Even though the crystal structure does not reveal water molecules, we can assume that either a water molecule or ionic interactions are playing an important role at this position.

In both structures, the interaction between Lys103 and Asp271 should be stronger than the interaction between Asp271(II) and Arg234(I) because of the shorter distance. From the data shown above, we know that changing the charge on any of the three residues to neutral, by site-directed mutagenesis, leads to dissociation of the protein. Thus, this charged triad is clearly important in the stability of the subunit I, II, III association.

Signaling Motif

As previously discussed, Asp271 is the first residue in the conserved DPxxY motif, which is also highly conserved in the transmembrane segment 7 of G-protein-coupled receptors. (Wess et al., 1993; Zhang & Ewinstein, 1993; Lou, Zhang & Weinstein, 1994; Van Rhee & Jacobson, 1996). This motif has been shown to play an important role in the signal transduction function of G-protein coupled receptors.

In C*c*O, the DPxxY motif is located at the periplasmic end of helix VI of subunit I. This helix is critical in the function of C*c*O, containing several important residues for oxygen reduction and proton pumping (Figure 2.3). These residues include His-284, Tyr-288, Glu-286 & Ser-299. Mutagenesis studies and crystal structures have shown that His-284 is one of the Cu_B center ligands in the active site (Shapleigh et al., 1992; Iwata et al., 1995; Tsukihara et al., 1995). This is involved in an unusual covalent linkage with Tyr-288 whose hydroxyl side chain is located within hydrogen-bonding distance of the hydroxyl group of the farnesyl side chain of heme a_3. The tyrosine residue is highly conserved among the heme-copper oxidases and has been postulated to participate in the oxygen reduction process by donating an electron and proton to form a neutral tyrosine radical (Konstantinov et al., 1997; Proshlyakov et al., 2000). Reprotonation of the tyrosine is thought to occur via the K-channel, which is postulated to be a proton intake channel. Glu-286 is situated in the interior of the protein, the likely end point of the D-channel for protons. It has been mutated to aspartate and glutamine (Junemann et al., 1999). E286D retained 50% of wild-type catalytic activity, while E286Q retained less than 0.01%. The observation implies a "glutamate trap" model for proton translocation. Ser-299, toward the inside end of helix VI, is near the entry point of K-channel. Mutants

at this residue inhibit activity and help explain the function of Lys-362 and oxygen reduction (Brändén M., 2001; Sigurdson H., 2002). Therefore, because of the importance of residues on helix VI in the function of the oxidase, both in proton movement and at the heme a_3 – Cu_B binuclear site, it is reasonable that slight conformational movements of helix VI could cause drastic changes in the function of oxidase.

Because the crystal structures of both bovine and *R. sphaeroides* reveal different conformations for Arg-234(II) and Asp-271(I) (Figure 2.9), this could show the flexibility of the interaction between the two residues. This flexibility could be essential for them to act as the gate of the water channel and/or possible proton exit. A signal from the chemical changes at the active site could be transmitted through helix VI to induce a conformational change at the external loop region, opening or closing the channel. Unfortunately, the instability of the mutants produced at Asp271 do not allow us to test this model.

Disulfide Bonds

Because changing Asp-271 causes dissociation of the subunits of the protein, further research can be conducted by making a double mutant in which Asp-271 and Arg-234 are both made into cysteines. This might allow a disulfide bond to form between them. If the interaction between them is important in the structural stability of wild-type oxidase, binding them together should help hold the protein together, but the loss of flexibility might lead to inhibition of the protein. By connecting this interface of subunit I and subunit II, the function of the area in both regulation and the water exit channel may be elucidated.

Conclusion

Even though the dissociation of the protein after neutralizing the charge on Asp 271 prevents us from further analysis of the functionality of the residue, the experimental results still helped us to understand the following:

Because the protein disaggregates with the removal of any one of the charges on Asp 271 from subunit I, Arg 234 from subunit II and Lys 103 from subunit III, these charges are of critical importance in holding the protein together. Because these charges are relatively strong, ionic interactions could be the major force to hold the protein together. This is an unexpected result, given the large hydrophobic interfaces between the three subunits that would be expected to be more significant.

As the first residue of the highly conserved motif D(/N)PxxY, Asp 271 could play a role in conformational transmission along helix VI of subunit I to regulate the events in the protein, but the mutants examined so far do not provide any information on this question.

Chapter 3

The Cross-Linking Analysis of Cytochrome *c*

and Cytochrome *c* Oxidase

Introduction

The electron transfer process between *c*-type cytochrome and C*c*O in the respiratory chain is generally understood to require the transient formation of a C*c*/C*c*O complex. There is considerable evidence that the formation of the complex is guided by electrostatic interactions among some positively-charged residues on C*c* and some negatively-charged residues on subunit II of C*c*O, facing the periplasmic side of the membrane (Figure 3.1 & 3.2). This is discussed in detail in chapter 1.

Most of the *c*-type cytochromes are small (12kD), stable, soluble and easy to handle. For mitochondria of higher eukaryotes, a single soluble and highly conserved C*c* operates as the electron carrier between complex III (cytochrome bc_1 complex) and complex IV (cytochrome *c* oxidase). This is not the case in the bacterial system. Under different growth conditions, bacteria normally use several aerobic and anaerobic electron transfer chains. This requires variety and specificity of the electron transfer carriers under different circumstances. Therefore, there is more than one cytochrome *c* which function in almost the same way but with different electron transfer partners.

R. sphaeroides, our major research organism, has mainly two growth conditions. Under photosynthetic growth conditions, cytochrome c_2 or isocytochrome *c* transfers electrons between the photochemical reaction center and bc_1 complex. Under respiratory growth, a membrane bound cytochrome c_y has been found to function as the electron carrier between the bc_1 complex and cytochrome *c* oxidase. This cytochrome c_y, unlike that of *R. capsulatus*, cannot function effectively as an electron carrier between the photochemical reaction center and the bc_1 complex. (Myllykallio et al., 1999). A recent

Figure 3.1 The Interacting Lysine Residues from Horse C*c* and Carboxyl Residues from *R. sphaeroides* C*c*O in Proposed C*c*/C*c*O complex. C*c* and C*c*O are shown in purple and yellow respectively. The oxygen and nitrogen atoms involved with the docking are shown in red and blue respectively. The figure was created using the Insight II program with coordinates from (Dr. Brandon Hespenheide, personal communication).

Cc
CcO
K8
D195
E157
K13
K87
K86
E148
CuA
W143
D214
K72

Figure 3.2 Space-Filling Models of Subunit II Soluble Domain of C*c*O (A), Horse C*c* (B), and *R. sphaeroides* Cc_2 (C). All of the C*c*O residues that are proposed in complex formation are highlighted in *color*. The residues in C*c*O and C*c* that are proposed to interact with each other are highlighted in the *same color*. The structure of C*c*O is from *P. denitrificans* (1ar1.pdb) with *R. sphaeroides* numbering, horse C*c* from 1hrc.pdb, and *R. sphaeroides* Cc_2 from 1cxa.pdb. This figure was made by Dr. Yuejun Zhen.

A. Soluble Domain of Sub II of C*c*O **B. Horse C*c*** **C. *R. Sphaeroides* Cc_2**

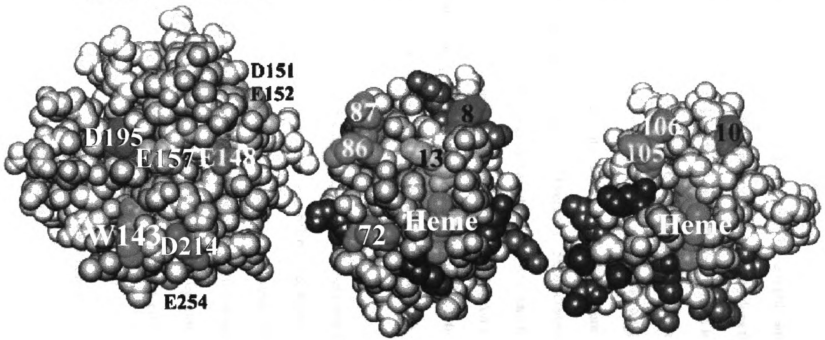

study indicated that cytochrome c_2 also participate in the electron transfer process under respiratory growth as well (Daldal et al., 2001).

The low spin *R. sphaeroides* cytochrome c_2 has a highly similar crystal structure to that of bovine C*c*. Even though it has almost all of the residues that are conserved in bovine C*c* which are critical to keep the overall structure, it has a lower p*I* value of 5.5 compared to 10 for bovine C*c* (Meyer & Cusanovich, 1985), and residues Lys-13 and Lys-72 (bovine C*c* numbering), which have been shown to be important charges for bovine C*c* to bind to C*c*O, are absent in the c_2 cytochrome (Figure 3.2). Also, *R. sphaeroides* cytochrome c_2 is larger, 14kD versus 12.5kD, because of some insertions. The absence of the two lysine residues may change the orientation of binding and likely, as a consequence, have lowered the binding affinity and electron transfer efficiency (Zhen et al., 1999). Its high redox potential of 356mV, versus 260mV for bovine C*c*, may also contribute to the lower reactivity toward *R. sphaeroides* C*c*O, about one third the turnover rate of horse heart C*c*.

Although there is evidence that *R. spheroides* cytochrome c_2 is the electron carrier between the bc_1 complex and the reaction center (Errede & Kamen, 1978), cytochrome c_2 may not be the physiological electron donor for C*c*O. However, because cytochrome c_2 is soluble and can be overexpressed, while the possible physiological electron donor, cytochrome c_y, is membrane-bound and not available yet, our research is based on the use of *R. sphaeroides* cytochrome c_2. As horse heart C*c* is a very efficient electron donor to both bovine and *R. sphaeroides* C*c*O, it has also been used.

With its 3 core subunits highly similar to the 3 core subunits of its mitochondria counterpart, bacterial C*c*O from *R. sphaeroides* has been used to observe the chemical

and biological function of C*c*O because of its smaller size, 4 subunits compared to 13 subunits in bovine C*c*O, and accessibility to mutational analysis.

As C*c*O is a membrane protein and C*c* is soluble, it has proven difficult to obtain the crystal structure of the complex for C*c*O and C*c* (Yoshikawa, personal communication). Therefore some indirect approaches have been taken to understand its nature. Here, using a prediction from the computational modeling for docking horse C*c* onto bovine C*c*O (Roberts & Pique, 1999), research was conducted to bind the electron donor-acceptor partners together using engineered disulfide bonds. This could confirm the computational model of the docking of C*c* on C*c*O, and possibly assist the crystallization process.

Materials and Methods

Materials Refer to **Materials** section in chapter 2.

Polymerase Chain Reaction (PCR) In this method, double-stranded DNA from plasmid pYJ006 for Y159 mutants or pYJ302 for A213 mutants was used as the template for the reaction. For each mutant, four primers were made, two of which were complementary to the flanking pUC19 sequences located at the end of the plugged-in C*c*O sequence, equivalent to the "M13 universal and reverse" primers. The other two primers are partially complementary to each other and to the template since they carry mutations. High fidelity *Pfu* polymerase was used to extend the primers in the presence of nucleotides and templates. The PCR product was cloned into pUC19 and sequenced before cloning back to the *cox*II/III operon. The following primers were used to generate the corresponding mutants, with the mutated codons underlined:

Y159C: TCGTTCGAGAGCTGCATGATC

Y159L: TCGTTCGAGAGCCTGATGATC

Y159T: TCGTTCGAGAGCACCATGATC

A213C: GGTGACCGGTTGCGACGTGATCC

A213E: GGTGACCGGTGAAGACGTGATCC

A213Y: GGTGACCGGTTACGACGTGATCC

A213T: GGTGACCGGTACAGACGTGATCC

A213S: GGTGACCGGTTCCGACGTGATCC

Construction of the Y159 and A213 mutants All the mutated oxidases were constructed using the overlapping extension PCR method (Ho, et al., 1989) addressed above. After the sequencing confirms the insertion of the mutant, a procedure is followed to put the mutated gene into overexpression plasmid pRK-pYJ123H. The mutated oxidases were overexpressed and purified using Ni^{2+}-NTA affinity column chromatography as described in chapter II.

Purification of *R. sphaeroides* cytochrome c_2 The his-tagged *R. sphaeroides* cytochrome c_2 was isolated from a cytochrome c_2 overexpression strain, pC2P404.1 (Brandner, et al., 1989). The cells were grown photosynthetically to maximize cytochrome c_2 expression, and harvested at late exponential phase. The harvested cells were resuspended in 50mM KH_2PO_4, 1mM EDTA, 50mg/ml DNaseI and 50mg/ml RNase. The resuspended cells were broken by two passages through a French pressure cell at 20,000psi. Unbroken cells and debris were removed by centrifugation at 30,000g for 30 minutes. The supernatant was centrifuged at 200,000g for 1.5 hours to remove the pellets of the membranes. The supernatant was mixed with Ni^{2+}-NTA resin in a ratio of

1ml of packed resin for every 2.5mg of C*c*. Ten mM imidazole was added to prevent nonspecific binding. The mixture was stirred at 4°C for 1h and then poured into a column. The column was washed with 10mM Tris-HCl, pH8.0, 40mM KCl, 10mM imidazole, until the flow-through was clear of color and turbidity. The enzyme was eluted slowly with 50mM histidine, 10mM Tris-HCl, pH8.0, 40mM KCl. The pink colored fractions containing Cc_{552} were pooled together and washed 3 times with 10mM Tris-HCl, pH8.0, 40mM KCl by centrifugal filtration in Ultrafree-15 centrifugal filters to reduce the imidazole level to less than 1mM.

Activity Assay Refer to the **Activity assay** section of chapter 2.

Fast Electron Transfer Measurements by Flash Photolysis These experiments were conducted by Dr. Frank Millett's lab at University of Arkansas. In order to measure the rate of electron transfer with a 1:1 complex between C*c* and C*c*O, the transient absorbance measurements were conducted in a 1 cm glass microcuvette by flash photolysis of 300 µl solutions containing about 10µM C*c*O and equal amounts of ruthenium labeled C*c* (Millett & Durham, 1991). Ten mM of aniline and 1mM of 3-carboxyl-2,2,5,5-tetramethyl-1-pyrrolidinyloxy free radical (3-CP) were used. Ru-39-C*c*, a horse C*c* derivative labeled with the inorganic complex ruthenium trisbipyridine ($Ru(bpy)_3$) at position 39, was used in the experiments. Once the laser is flashed on the sample, electron transfer from C*c* to the Cu_A center of C*c*O was measured by tracking the decrease of absorbance at 550nm for Ru-39-C*c*, as well as 830nm for Cu_A reduction, and the increase of absorbance at 605 nm for the heme *a* reduction. By varying the ionic strength of the solution from 5mM to 300mM, the ionic strength dependencies for electron transfer were determined.

Electron paramagnetic resonance (EPR) spectroscopy These experiments were done as described in Hosler et al., 1992. The exception is that the solutions of the samples were 50mM KH_2PO_4, 1mM EDTA, 0.1% LM, pH 7.2. The high Mg/low Mn sample was made by growing *R. sphaeroides* cells in a high Mg/low Mn Sistrom's media (Hosler et al., 1995). The EPR spectra were taken with a Bruker ESP-300E spectrometer. This experiment was conducted by Bryan Schmidt.

Reconstitution of Cytochrome *c* Oxidase All glassware was rinsed with ethanol and de-ionized water to remove any residues of detergent. Asolectin was suspended to 40mg/ml by sonicating in 1% cholate, 75mM Hepes, pH 7.4 at 0°C under the protection of argon. The suspension was centrifuged at 10,000 rpm for 15 min at 4°C to remove titanium particles. After 4% cholate was added to the purified C*c*O, the enzyme was added to the above resuspension buffer to a final concentration of 0.65nmol/mL and dialyzed at 4°C with rapid stirring in 100 volumes of 75mM Hepes, 14mM KCl, 0.1% cholate, pH 7.4 for 6 hours; 100 volumes of 75mM Hepes, 14mM KCl, pH7.4 for 12 hours; 100 volumes of 50mM Hepes, 24mM KCl, 15mM sucrose, pH7.4 for 12 hours; and 500 volumes of 50μM Hepes, 44.6mM KCL, 45 mM sucrose for 12 hours. Measurement of oxygen consumption was determined for the reconstituted enzymes in order to determine the respiratory control ratio (RCR), which is a test of whether the vesicles are intact and the enzymes are inserted correctly (Qian et al., 1997; Fetter et al., 1995)

Proton Pumping Assay This assay was conducted on an Olis Rapid-Scanning Monochromator (RSM). Horse C*c* was fully reduced by adding dithionite, and purified with Sephadex G-75 column in 1mM Hepes, and 44.6mM KCl, pH 7.4. C*c*O vesicles

were diluted to about 200nM. Five μM of horse C*c* (final concentration) was used for each assay (about 10 turnovers). Two hundred μM phenol red was added to detect the proton pumping at 557nm. Measurements were taken at 1000 scans/sec. Cytochrome *c* oxidation was followed at 550nm and the reduced minus oxidized spectra were fit by Global analysis to obtain the first-order rate. The reaction between C*c* and C*c*O were carried out under three conditions:

1) Without ionophore (controlled)

2) With 2 μM valinomycin

3) With 2 μM valinomycin and 10 μM CCCP (uncontrolled)

The isosbestic point of the reduced and oxidized spectra of cytochrome *c* was determined for each reaction. This wavelength is used for the proton pumping assay. The acidification and alkalinization rates were analyzed with a non-linear curve fitting in Microcal Origin program. The small mixing artifact was subtracted and the backleak in the kinetic trace with valinomycin (proton pumping) was fitted and subtracted from the individual scan to eliminate the contribution of proton leakage through the membranes which competes with the proton release.

Cross-Linking Assay Wild-type and cysteine mutants of cytochrome c_2 and C*c*O of *R. sphaeroides* were purified as mentioned above. After combining C*c* and C*c*O, the mixture (final concentration of 20μM each with total volume of 50μl) was passed through a Sephadex G-75 0.5cm by 20cm column. The flow-through fractions were scanned with visible spectrometry to detect the elution volumes for C*c*, C*c*O and possible C*c*/C*c*O complex. With individual cysteine mutants, 1mM dithiothreitol was present to keep a disulfide bond from forming. After mixing C*c* & C*c*O, the mixture went through either

dialysis or a G10 spin column to get rid of the DTT before being loaded on the G-75 column.

Results

Design of Mutants

The analysis of the model complex of C*c*:C*c*O to predict where a disulfide might be inserted was conducted by Brandon Hespenheide. Using the original computationally modeled complex for horse C*c* and bovine C*c*O (Roberts & Pique, 1999), the *R. sphaeroides* C*c*O was superimposed onto the crystal structure of bovine C*c*O in the complex. The 3-D structural superposition of subunit I and II from *R. sphaeroides* and bovine C*c*O were conducted independently using the DALI server (www2.ebi.ac.uk/dali). Combining the alignment information from the server, superposition was performed again using InsightII's superposition command. The RMSD for all backbone atoms in this superposition was 1.246Å (Figure 3.3).

With this superimposed complex model, search for any pair of C_α atoms between the *R. sphaeroides* C*c*O and the docked C*c* whose distance is between 4.0Å and 7.5Å was conducted. By inspecting visually for potential appropriate C_α–C_β vector direction, C*c*:12-C*c*O:159(subunit II) has been identified. Even though other sites do not have the proper geometry, disulfide bond formation is still considered possible for the following 3 pairs: C*c*:77-C*c*O:183(subunit I), C*c*:83-C*c*O:213(subunit II), C*c*:83-C*c*O:214(subunit II) (Figure 3.4). As Asp214 is highly conserved and observed to be a significant charge for docking of C*c*, the pair C*c*:83-C*c*O:214(subunit II) was not considered a good candidate

Figure 3.3 Overall Structure of Proposed Horse C*c* / *R. sphaeroides* C*c*O Complex.

Cyan, yellow, blue and orange represent subunit I, II, III and IV of C*c*O respectively. C*c* is shown in magenta. The figure was created using the Insight II program with coordinates from (Dr. Brandon Hespenheide, personal communication).

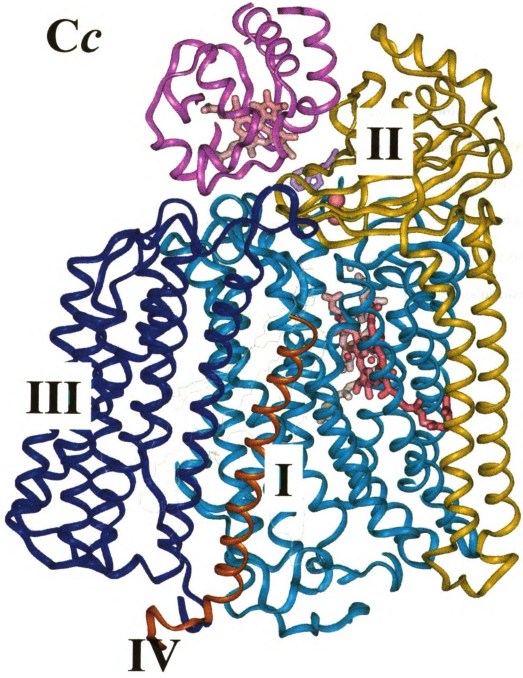
Cc
II
III
I
IV

Figure 3.4 Interaction Interface of a Possible Complex of Horse C*c* and *R. sphaeroides* C*c*O and the Residues that Could Possibly Form a Covalent Bond between Them. C*c* and Subunit I & II of C*c*O are shown in magenta, cyan and yellow respectively. The residues in C*c*O and C*c* that are proposed to be sufficiently proximal if changed to cysteine to link covalently are highlighted in the *same color*. The figure was created using the Insight II program with coordinates from (Dr. Brandon Hespenheide, personal communication).

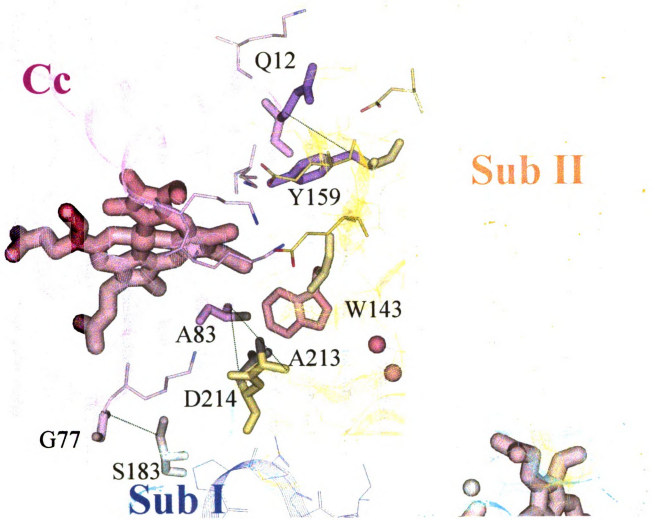
Cc
Q12
Y159
Sub II
W143
A83
A213
D214
G77
S183
Sub I

for cross-linking. Because the pair C*c*:77-C*c*O:183(subunit I) of C*c*O is at the edge of the speculated docking site, the possibility of the cross-link might not be as high as the pairs closer to the center of the docking site. Therefore, 2 pairs, C*c*:12-C*c*O:159(subunit II) and C*c*:83-C*c*O:213(subunit II) was chosen to perform the cross-linking experiment.

This research is a cooperative project with another graduate student in Dr. Shelagh Ferguson-Miller's lab, Yasmin Hilmi. My focus was to make mutants in *R. sphaeroides* C*c*O and Yasmin made mutants in cytochrome c_2 of *R. sphaeroides*. Therefore, this thesis concentrates on mutagenesis on the C*c*O and characterization of these mutants. Further cross-linking experiments are also reported.

Because Tyr159 is in a region where a stack of aromatic residues, including Tyr144 & Tyr141 was found (Figure 3.5), threonine and leucine mutants were also made in addition to the cysteine mutant. If this aromatic alignment is important functionally, the Thr and Leu mutants will help us to understand whether the aromaticity of the benzene ring or the hydroxy group are important.

Pro83 (Pro71 in horse C*c*) in Cc_2 is a highly conserved residue and it is next to Thr84 (Lys72 in horse C*c*). In horse C*c*, Lys72 plays a significant role for the docking of C*c* onto C*c*O. Because of these observations, a glutamate mutant was made along with the cysteine mutant to change the charge distribution in this region. This might give us more information about the docking mechanism.

Several mutants, including the cysteine mutant, were also designed at the Ala213 position to test the functional significance of this residue.

Optical characteristics of mutants

Figure 3.5 Tyrosine Alignment at the Possible Interface of C*c*O with Its Redox Partner C*c*. The highly conserved Tyr-141, 144, and 159 in C*c*O are shown in blue. Other highly conserved aromatic residues are shown in purple. Trp 143 is shown in red. Yellow balls are Cu_A atoms. The figure was created using Insight II with coordinates for *R. sphaeroides* C*c*O from Svensson-Ek *et al.*, 2002.

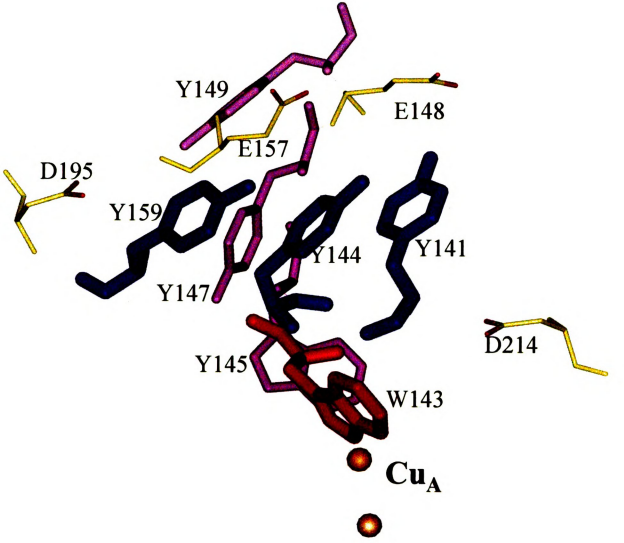
Y149
E148
E157
D195
Y159
Y144
Y141
Y147
D214
Y145
W143
Cu$_A$

All of the mutants have been successfully expressed and their spectra in the *R. sphaeroides* membranes are shown in Figure 3.6 & 3.7. From the height and position of the α-peak, we can tell that all mutants are well expressed and similar to wild-type spectrally. Because of time constraints, we focused our research on the Y159C and Y159T mutants. More data is presented below.

Cu_A/heme EPR analysis

For the X-band EPR spectrum of *R. sphaeroides* C*c*O, the signals at g = 2.83, 2.31 and 1.62 arise from the low spin heme *a*, the signal at g = 6.0 from heme *a* and the signals at g = 2.0 and 2.19 from Cu_A (Figure 3.8) (Hosler et al., 1992). The EPR spectra of Y159C and Y159T mutants are similar to that of wild-type, except that both mutants have a peak at g = 2.35. This could be some other type of heme *a* than the type in wild-type C*c*O or due to some impurities in the sample. The sample is only Ni^{2+}-NTA column purified. As the His-tag used to purify C*c*O is in subunit I, the purified oxidase could contain some extra subunit I due to its binding to the Ni^{2+}-NTA. This subunit I could have lost its heme a_3 as sometimes observed (Jon Hosler, personal communication), making the signal for heme *a* different. The EPR spectra indicate that the metal centers in these mutants are mainly intact. This is consistent with the result from the visible spectra.

The activities of mutant enzymes

It is important that the mutants used for cross-linking should not affect the conformational state of C*c*O. Additionally, in order to see if the cross-linked C*c*O:C*c*

Figure 3.6 Absolute Visible Spectra for Reduced Y159 Mutants. The proteins (purified with Ni^{2+}-NTA column) are reduced with dithionite and measured in a Perkin-Elmer Lambda 4.0 UV/VIS Spectrophotometer. These measurements were conducted in 100mM KH_2PO_4, 0.1% LM with pH 7.2.

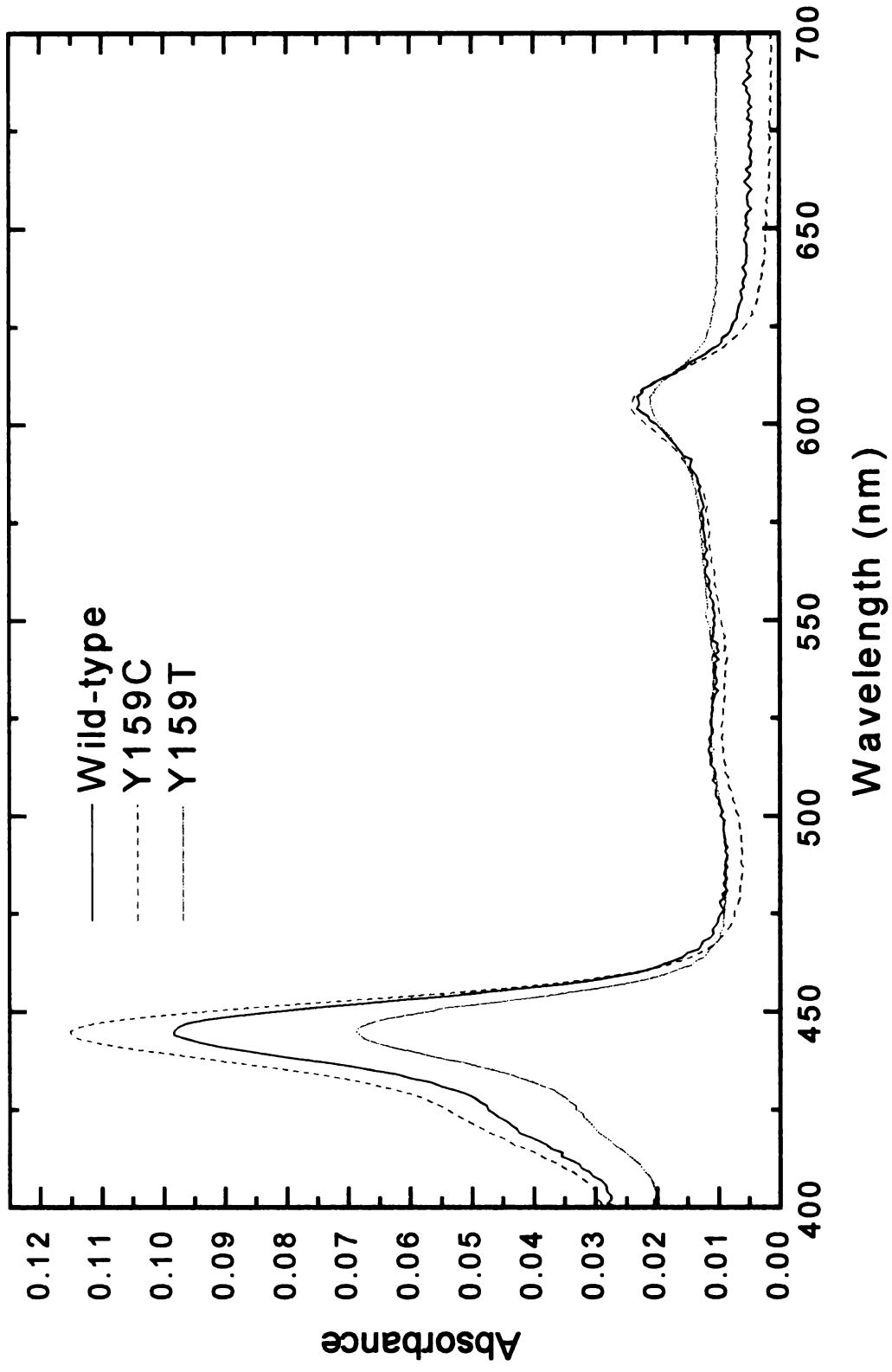
Wild-type
Y159C
Y159T
Absorbance
Wavelength (nm)
0.00
0.01
0.02
0.03
0.04
0.05
0.06
0.07
0.08
0.09
0.10
0.11
0.12
400
450
500
550
600
650
700

Figure 3.7 Visible Spectra for A213 Mutants in Solubilized Membrane. These are reduced-minus-oxidized *R. sphaeroides* membrane spectra. The membranes are reduced with dithionite and measured with membranes oxidized with ferricyanide as a reference in order to obtain the difference spectra in a Perkin-Elmer Lambda 4.0 UV/VIS Spectrophotometer. These measurements were conducted in 100mM KH_2PO_4, 0.1% LM with pH 7.2.

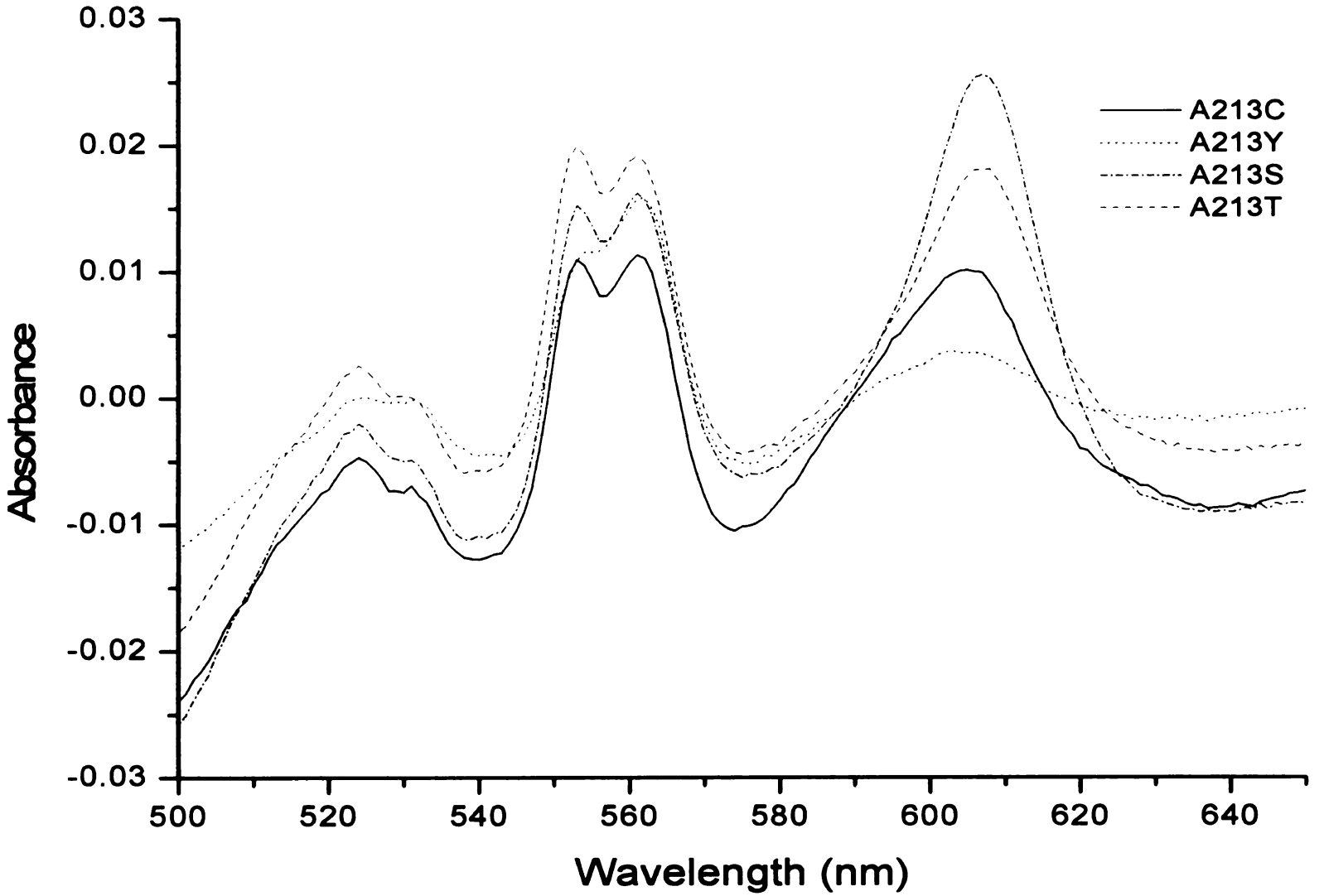
0.03
0.02
0.01
0.00
-0.01
-0.02
-0.03
Absorbance
500
520
540
560
580
600
620
640
Wavelength (nm)
A213C
A213Y
A213S
A213T

Figure 3.8 Cu_A EPR Spectra of Y159 Mutants. EPR spectra of 30 μM oxidases in 50mM KH_2PO_4, 1mM EDTA, 0.1% LM, pH 7,2 were recorded at X-band using a Bruker EP=3000E spectrometer. The related g values are indicated in the plots. The EPR spectra were recorded at 10K with the following settings: microwave frequency 9.4831GHz for Y159T and 9.4809 GHz for Y159C; microwave power 2mW; modulation amplitude 12.5G; sweep time 40s; The cells were grown in high Mg / low Mn media. The data shown is the average of three scans.

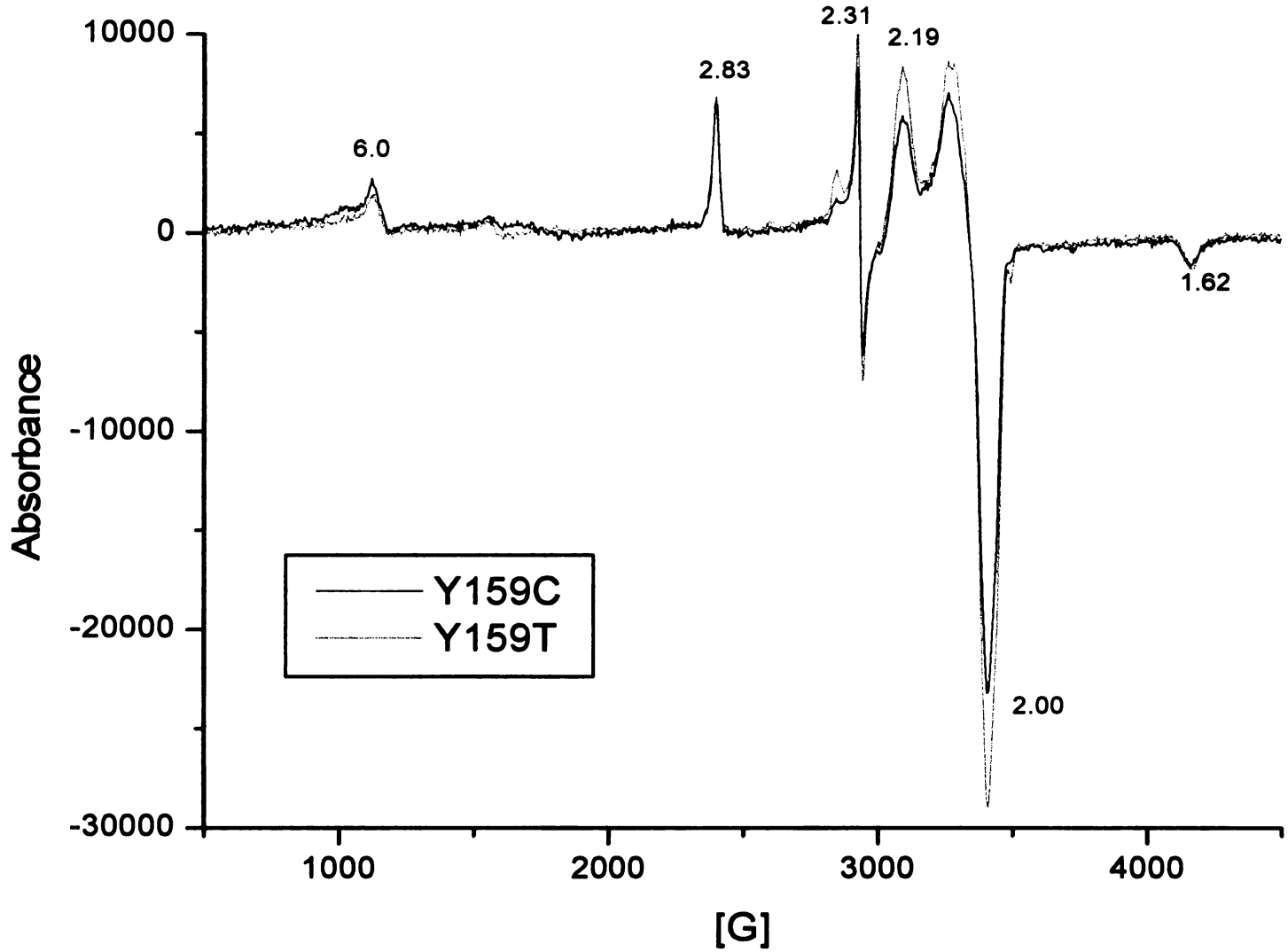
10000
0
-10000
-20000
-30000
Absorbance
1000
2000
3000
4000
[G]
6.0
2.83
2.31
2.19
2.00
1.62
Y159C
Y159T

complex is correct, it is important to assess the activity of the mutant under normal C*c* binding conditions. Since *R. sphaeroides* C*c*O shows high activity with horse C*c*, horse C*c* has been used in this part of the experiment. The maximum turnover numbers of wild-type and Y159 mutants have been measured using an excess of horse C*c* as the substrate in polarographic assays (Table 3.1). With the turnover rate of 1,700e^-/sec/aa_3 for wild-type C*c*O, Y159C and Y159T have rates of only about 396 and 520 e^-/sec/aa_3. These slower turnover rates may be the result of subtle changes in the docking of C*c* on C*c*O, or to the presence of some interfering contaminant forms.

Laser flash photoreduction study of kinetics of Y159C mutant

The flash-induced photoreduction technique measures the electron transfer activity from C*c* to Cu_A of C*c*O within the complex, as well as the second order reaction between C*c* and C*c*O from solution. Of the intracomplex and 2nd order reaction phases, the latter phase normally shows a bell-shaped dependency on the ionic strength of the solution. From the result shown in Figure 3.9, the two mutants show similar ionic strength dependence as the wild type C*c*O but with lower activity, with Y159T and Y159C showing about 1/6 and 1/8 of the wild type activity for the fast phase electron transfer, respectively. This is consistent with, and may account for, the activity measurement and steady-state kinetics result.

Proton-pumping assay

A normally functioning C*c*O is capable of pumping one proton per electron transferred. The stopped-flow analysis gives the proton pumping results for both Y159T

Table 3.1 Activity Characteristics of Y159 Mutants

	Turnover rate (e-/sec/aa3)
Wild Type	1,700
Y159C	396
Y159T	525

Figure 3.9 Ionic Strength Dependent Electron Transfer from Ru-39-C*c* to Cytochrome *c* Oxidase. The rates (k_{obs}) are measured from the ruthenium-kinetics assays, with rates for both the fast and slow phases plotted together.

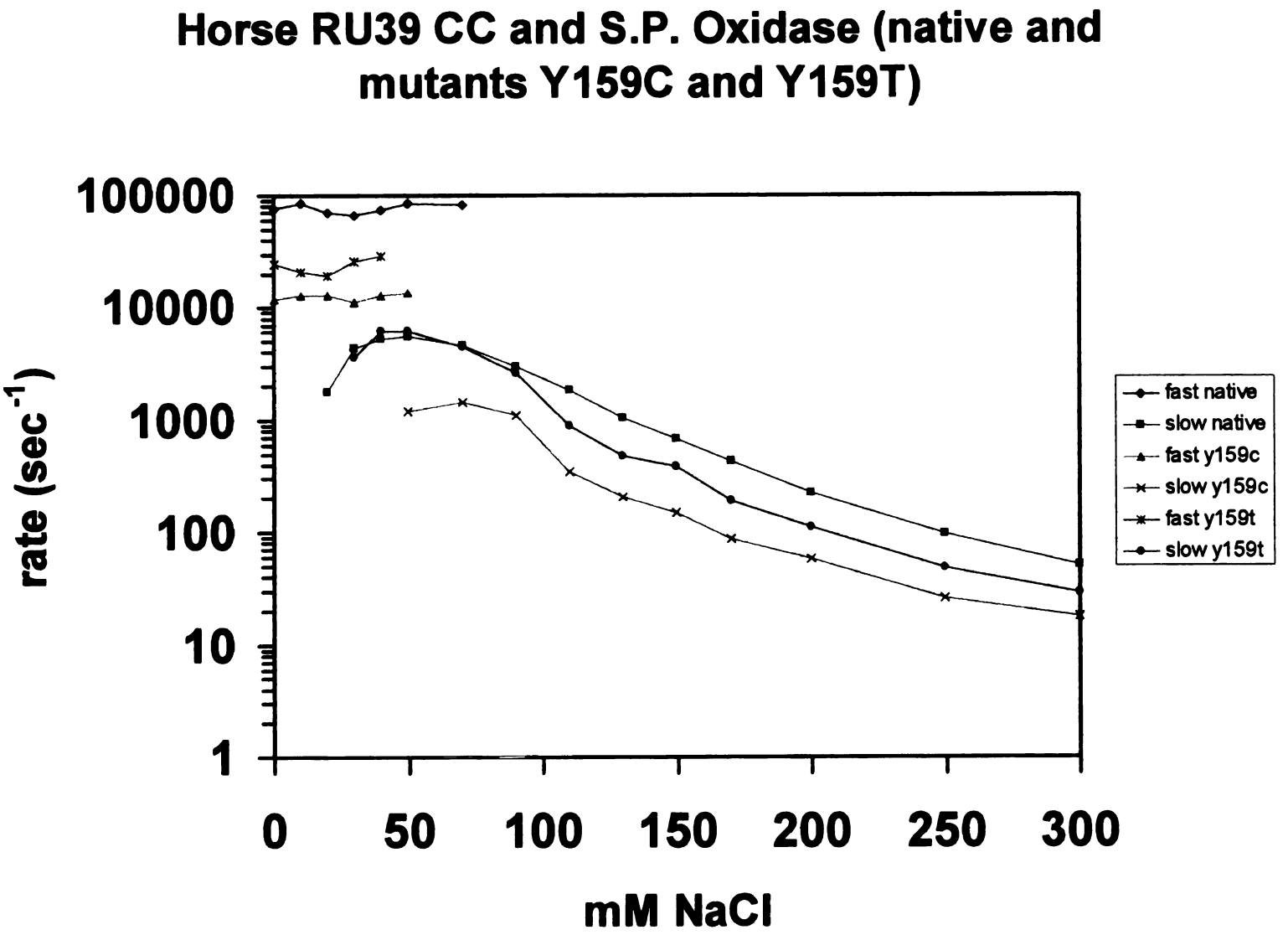
Horse RU39 CC and S.P. Oxidase (native and mutants Y159C and Y159T)
rate (sec-1)
100000
10000
1000
100
10
1
0
50
100
150
200
250
300
mM NaCl
fast native
slow native
fast y159c
slow y159c
fast y159t
slow y159t

and Y159C mutants. (Figure 3.10 & 3.11) The results show that both mutants pump protons in a similar way to that wild-type oxidase, with the normal 1:1 stoichiometry 1 H^+:e^- when valinomycin is added. The usual increase in rates of cytochrome *c* oxidation are also seen as the membrane potential is removed with valinomycin and the pH gradient is relieved with CCCP as an uncoupler.

Complex Formation

The C*c*O mutant was designed to test the accuracy of the predicted C*c*/C*c*O complex by formation of a covalent bond between the C12 mutant of *R. sphaeroides* cytochrome c_2 (C*c*12) and the Y159C mutant of *R. sphaeroides* cytochrome *c* oxidase (C*c*O159). The experiment was conducted as described in the **Materials and Methods** section. Both dialysis and spin column techniques were used to remove DTT from the samples. Four other experiments were done with (1) CcO159 and C*c*12; (2) C*c*O159 and wild-type cytochrome c_2; (3) wild-type C*c*O and C*c*12; and (4) C*c*O159 and C*c*12 with DTT in the sample throughout the experiment.

Sephadex G-75 column retains molecules of 3 – 80kD. This works well when separating C*c*2 (14kDal) from C*c*O (126kDal) as shown in Figure 3.12. If a complex (140kDal) of C*c* and C*c*O was formed, it would be expected to be resolved on the column from C*c* but not from C*c*O.

The results show no evidence for formation of complexes in any of these samples, including the case where the two Cys mutants are mixed in the absence of DTT (Figure 3.12).

Figure 3.10 Proton Pumping Analysis For Y159C Mutant. Kinetic traces for cytochrome *c* oxidation at 550nm (A) and phenol red changes at 557nm (isosbestic point of cytochrome *c*) (B) were collected. The measurement is conducted according to Hiser et al., 2001.

A.

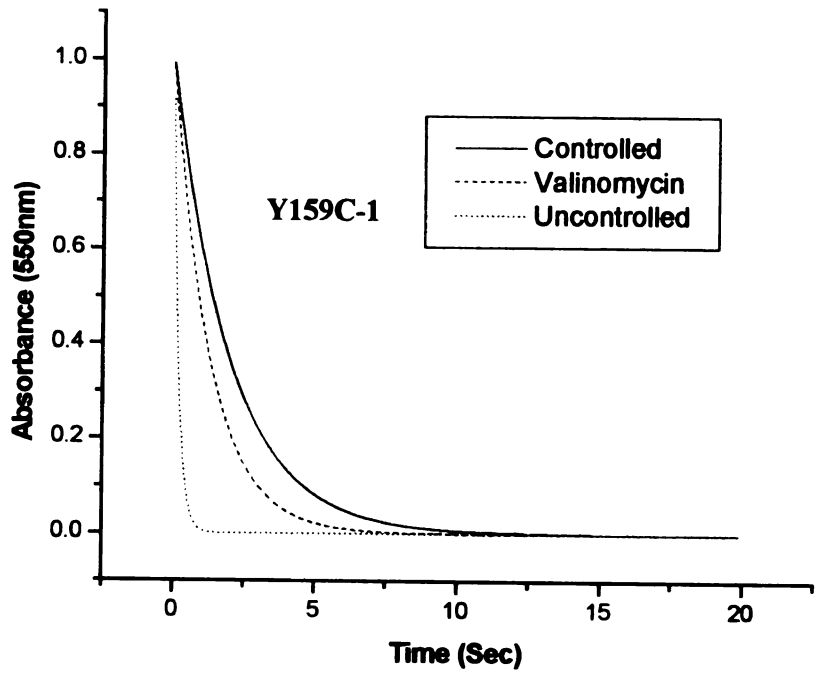
Absorbance (550nm)
1.0
0.8
0.6
0.4
0.2
0.0
0
5
10
15
20
Time (Sec)
Y159C-1
Controlled
Valinomycin
Uncontrolled

B.

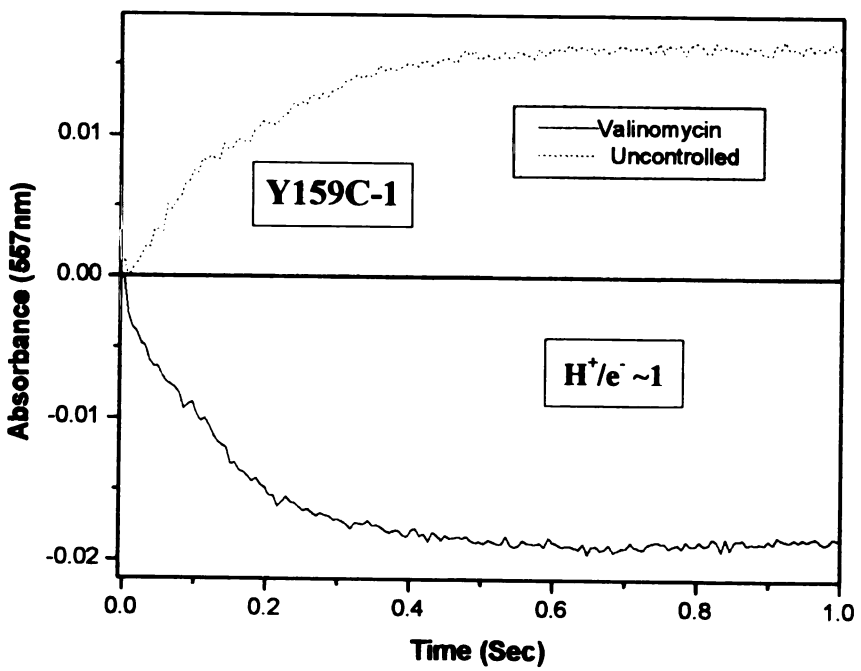
Absorbance (557nm)
0.01
0.00
-0.01
-0.02
0.0
0.2
0.4
0.6
0.8
1.0
Time (Sec)
Y159C-1
Valinomycin
Uncontrolled
H+/e- ~1

Figure 3.11 Proton Pumping Analysis For Y159T Mutant. See Figure 3.10 legend.

A.

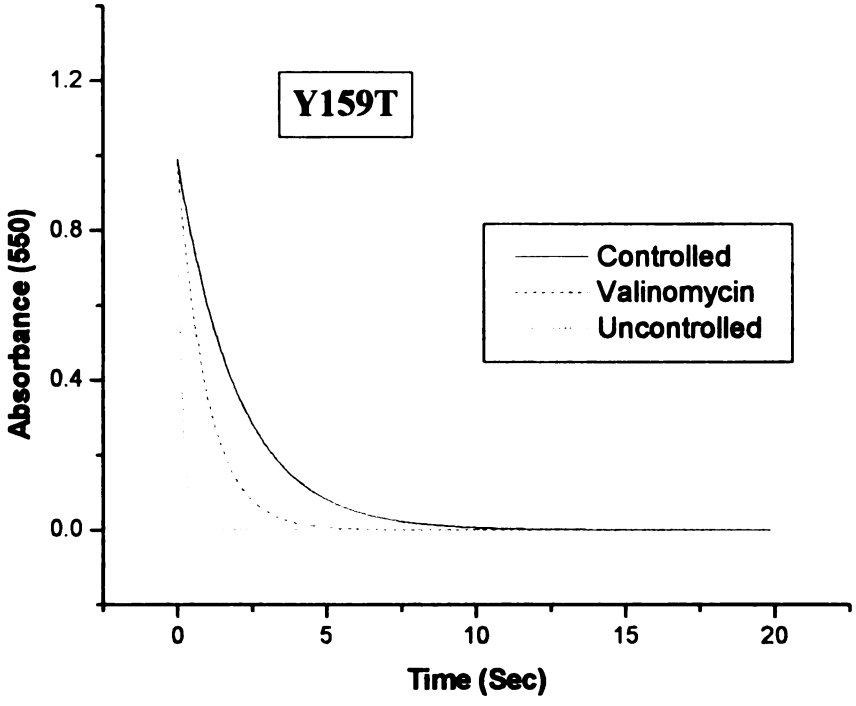
Y159T
Controlled
Valinomycin
Uncontrolled
Absorbance (550)
1.2
0.8
0.4
0.0
0
5
10
15
20
Time (Sec)

B.

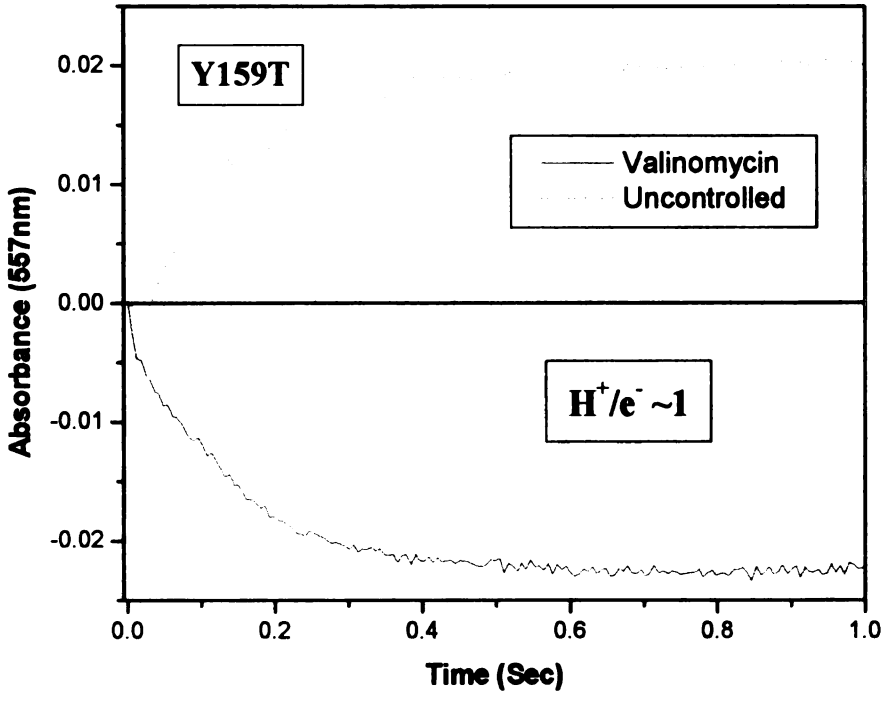
Y159T
Valinomycin
Uncontrolled
H+/e- ~1
Absorbance (557nm)
0.02
0.01
0.00
-0.01
-0.02
0.0
0.2
0.4
0.6
0.8
1.0
Time (Sec)

Figure 3.12 Gel-filtration for Cytochrome *c* Oxidase Cysteine Mutant (Y159C) with Cytochrome *c* Cysteine Mutant (N12C). The absorbances for cytochrome *c* and cytochrome *c* oxidase were plotted against elution volume (μl). Each point on the plot represents the actual absorbance at 550nm for cytochrome *c* and 606 nm for cytochrome *c* oxidase of the specific elution fraction (50 μl).

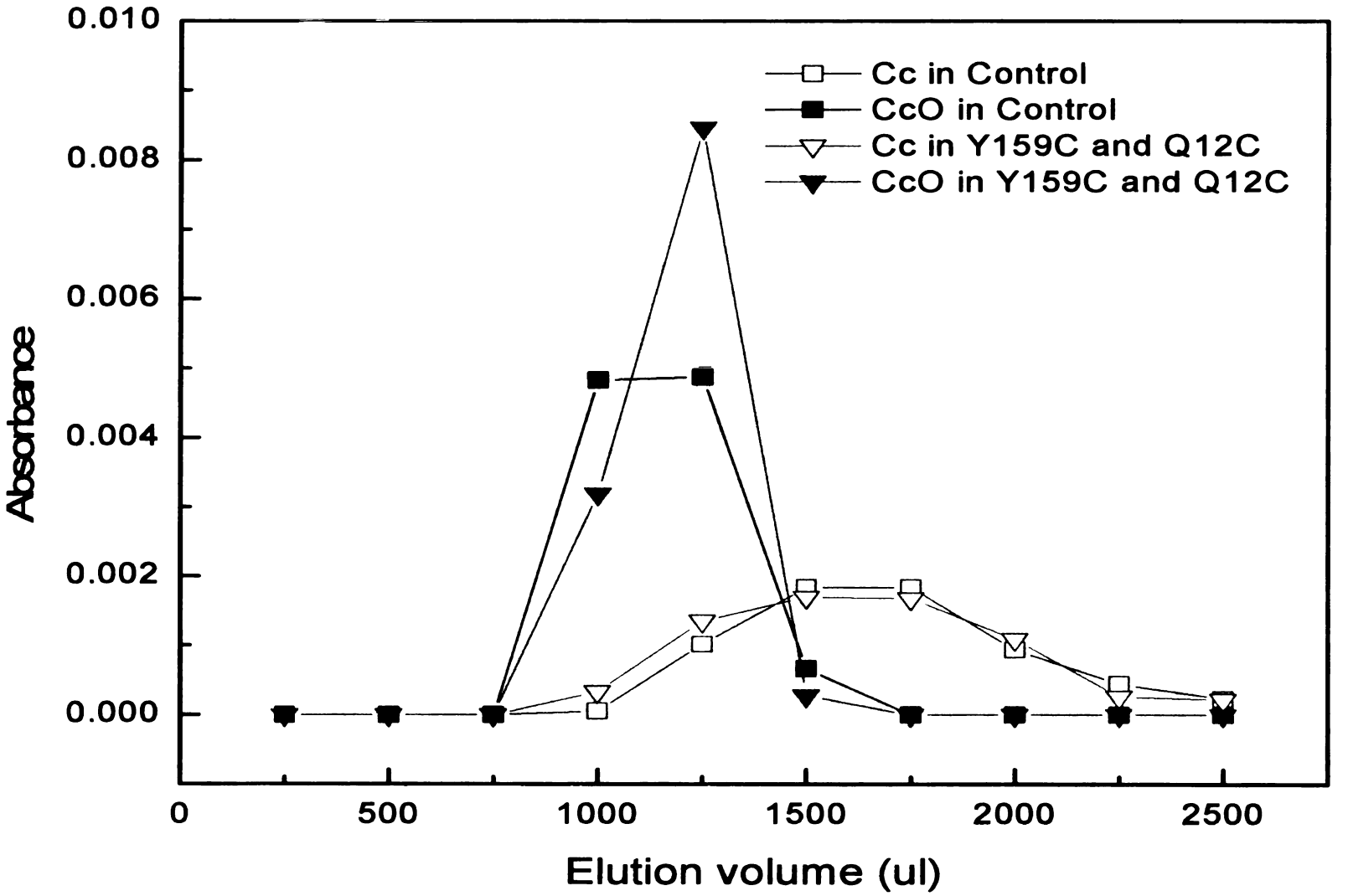
0.010
0.008
0.006
0.004
0.002
0.000
Absorbance
0
500
1000
1500
2000
2500
Elution volume (ul)
Cc in Control
CcO in Control
Cc in Y159C and Q12C
CcO in Y159C and Q12C

However, in all these cases the Cc_2 mutant forms did not have the missing key Lys13 residue put into the Cc_2 to make it resemble the horse C*c* upon which the model was based. Yasmin Hilmi has made the double mutant of N12C/Q13K of *R. sphaeroides* Cc_2 and conducted a similar crosslinking experiments. The result is shown in Figure 3.13. From this result we can see that there is a significant amount of C*c* eluting from the column with C*c*O. Compared to the result in Figure 3.12, it suggests that covalent complex was formed when the Lys13 positive charge was present to properly orient the complex.

Discussion

Are the Changes Introduced by the Mutation at Position Y-159 Disruptive to the Structure and/or Function of C*c*O?

The data acquired from visible spectra, EPR, activity, flash photolysis and proton-pumping assay have shown that except for the lowered activity compared with that for wild type C*c*O, the Y159C and Y159T mutants are not significantly different from wild type in their metal and heme sites, proton pumping mechanism and binding behavior to their redox partner, Cc_2.

Because Y159 is the third tyrosine residue in the highly conserved Tyr141-Tyr144-Tyr159 triad (Figure 3.5), which is part of the hydrophobic stretch surrounding the Cu_A entry site, it could be important for electron transfer from C*c* to the Cu_A within the complex. This is consistent with the slower electron transfer rate observed from the flash photolysis assay. Y144 in this triad has also been mutated into more conservative

Figure 3.13 Gel-filtration for Cytochrome *c* Oxidase Cysteine Mutant (Y159C) with Cytochrome *c* Cysteine Mutant (N12C/Q13K). The absorbances for cytochrome *c* and cytochrome *c* oxidase were plotted against elution volume (μl). Each point on the oxidase plot represents the absorbance at 444 nm for cytochrome *c* oxidase of the specific elution fraction (50 μl). For the cytochrome *c* plot, data were corrected and the absorbance of the oxidase at 416 nm was subtracted using this formula:

Cytochrome *c* absorbance at 416 = absorbance at 416 – (absorbance at 444 nm X 0.32)

where 0.32 = absorbance at 416nm / Absorbance at 444 nm for oxidase alone.

This Figure was made by Dr. Yasmin Hilmi.

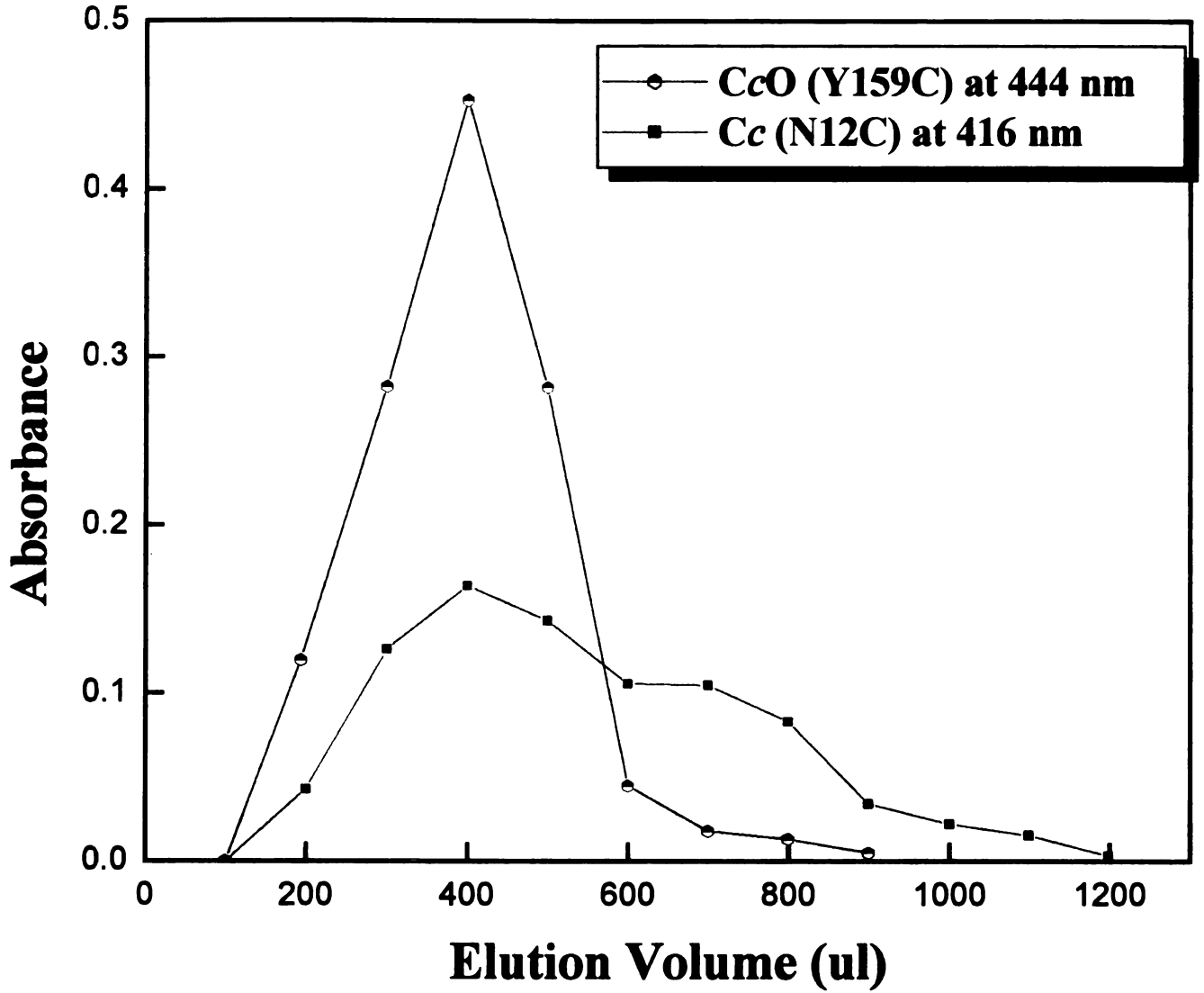
0.5
0.4
0.3
0.2
0.1
0.0
Absorbance
0
200
400
600
800
1000
1200
Elution Volume (ul)
CcO (Y159C) at 444 nm
Cc (N12C) at 416 nm

residues such as phenylalanine, histidine and serine. These mutants also show lower electron transfer rates from C*c* to Cu_A (Personal communication with Dr. Yuejun Zhen). These data suggest that this triad could be more important in controlling the electron transfer than in the actual docking of C*c* (For a detailed discussion, please refer to chapter 1). Since the Y159C mutant has a cysteine residue externally exposed, self-dimerization could also contribute to the slow turnover rate of the protein.

Because the mutants do not show a significant change in C*c* binding, as indicated by the ionic strength dependence of the second order reaction, the potential formation of a disulfide bond between C*c* and C*c*O should reflect the true docking conformation of wild-type C*c*O:C*c*. If a covalently-bound complex can be obtained and even crystallized, it would support the conclusion based on computational modeling and further reveal the binding behavior of both redox partners.

Cation-Pi Interaction

Contrary to the fact that electrostatic interactions play a major role in the complex of cytochrome *c* and cytochrome *c* oxidase, binding of C*c* and bc_1 is mainly stabilized by hydrophobic interactions between amino acid residues around the heme crevices. These residues form a trapezoid-shaped contact area (Lange & Hunte, 2002; Hunte et al., 2002). In the center of the binding site a planar stacking cation-π interaction has been found important to stabilize the complex of the redox partners. This interaction is between Arg18 of C*c* and Phe230 of cytochrome c_1 of bc_1 complex, with the guanidine group oriented parallel to the aromatic plane. This kind of stacking pattern has been found at

molecular surfaces of proteins (e.g. Tyr 39 of C*c*P with Arg 19 of C*c*) (Pelletier & Kraut, 1992) in formation of enzyme substrate complexes.

Remarkably, at position 19 (position of Lys13 in bovine C*c*) of C*c* a positive charge is highly conserved. Lys13 in horse C*c* has been shown to be important for binding of C*c*O (Rieder & Bosshard, 1980; Ferguson-Miller et al., 1978; Smith et al., 1977) and bc_1 complex (Yu et al., 1973). From the computational modeling of the complex of horse C*c* and bovine C*c*O (Roberts & Pique, 1999), we found that Lys13 of C*c* is only 3.933Å away fromTyr144 of C*c*O. Tyr144 mutants were made and further analysis can be done to explore the importance of this cation-π interaction. With the results from these future experiments, we can achieve a better understanding of the role of Lys-13 in the docking mechanism.

Covalently Bound Complex and Anion Exchange Chromotography

From the cross-linking experiments, we have evidence that only when a mutation is carried out in Cc_2 to put a lysine at position 13 (bovine numbering), is a significant amount of complex detected (Yasmin Hilmi, personal communication). This helps to validate the computational docking model and it further supports the important role of Lys-13 in the binding of C*c* onto C*c*O.

Even though we have proved that a complex can be formed between C*c* and C*c*O, separation of this complex from the two proteins, C*c* and C*c*O has not been satisfactorily achieved. Further experiments can be conducted with FPLC-DEAE chromatography. Because the presumed complex would have a different charge distribution on the surface

of C*c*O, we should be able to get a better separation of the combined complex from the other proteins in the sample.

Conclusion:

Introduction of Lys-13 into *R. sphaeroides* cytochrome c_2 improves the inter-molecule disulfide bond formation and thus confirms the computer model results as well as experimental data, that emphasizes the significant role of Lys-13 in docking of C*c* onto C*c*O. If the formation of the inter-molecule disulfide bond between the two molecules can be made more efficient and gives an active complex, the covalent complex could assist in crystallization efforts.

BIBLIOGRAPHY

BIBLIOGRAPHY

Arnold, S, Goglia, F, & Kadenbach, B. (1998) 3,5-Diiodothyronine binds to subunit Va of cytochrome-c oxidase and abolishes the allosteric inhibition of respiration by ATP. *Eur J Biochem.* 252:325-30.

Axelrod, H. L., Feher, G., Allen, J. P., Chirino, A. J., Day, M. W., Hsu, B. T. & Rees, D. C. (1994) Crystallization and X-ray structure determination of cytochrome-*c*(2) from *Rhodobacter-sphaeroides* in 3 crystal froms. *Acta Crystallogr. D. Biol. Crystallogr.* 50:596-602.

Babcock, G. T. & Wikström, M. (1992) Oxygen activation and the conservation of energy in cell respiration. *Nature* 356:301-9.

Baker, S. C., Ferguson, S. J., Ludwig, B., Page, M. D., Richter, O.-M. H. & van Spanning, R. J. M. (1998). Molecular genetics of the genus Paracoccus: metabolically versatile bacteria with bioenergetic flexibility. *Microbiol. Mol. Biol. Rev.* 62:1046-1078.

Bartsch, R. G., Ambler, R. P., Meyer, T. E. & Cusanovich, M. A. (1989) Effect of aerobic growth conditions on the soluble cytochrome content of the purple phototrophic bacterium *Rhodobacter sphaeroides*: induction of cytochrome c_{554}. *Arch. Biochem. Biophys.* 271:433-440.

Bartsch, R. G. in *The Photosynthetic Bacteria.* Clayton, R. K. & Sistrom, W.R., Eds. (Phenum Press, New York, 1978) pp. 249-280.

Berry, E. A. & Trumpower, B. L. (1985) Isolation of ubiquinol oxidase from *Paracoccus denitrificans* and resolution into cytochrome bc_1 and cytochrome c-aa_3 complexes. *J. Biol. Chem.* 260:2458-2467.

Bisson, R., Steffens, G.C.M., Capaldi, R. A. & Buse, G. (1982) Mapping of the cytochrome *c* binding site on cytochrome *c* oxidase. *FEBS Lett.* 144:359-63.

Bott, M., Ritz, D. & Hennecke, H. (1991) The *Bradyrhizobium japonicum cyc*M gene encodes a membrane-anchored homolog of mitochondrial cytochrome *c*. *J. Bacteriol.* 173:6766-6772.

Bradford, M. M. (1976) A rapid and sensitive method for the quantitation of microgram quantities of protein utilizing the principle of protein-dry binding. *Anal. Biochem.* 72:248-254.

Brändén, M., Sigurdson, H., Namslauer, A., Gennis, R.B., Ädelroth, P. & Brzezinski, P. (2001) On the role of the K-proton transfer pathway in cytochrome *c* oxidase. *Proc. Natl. Acad. Sci. USA* 98:5013-18.

Brandner, J. P., McEwan, A. G., Kaplan, S. & Donohue, T. J. (1989) Expression of the *Rhodobacter sphaeroides* cytochrome c_2 structure gene. *J. Bact.* 171:360-368.

Bratton, M.R., Pressler, M.A., & Hosler J.P. (1999) Suicide Inactivation of Cytochrome *c* Oxidase: Catalytic Turnover in the Absence of Subunit III Alters the Active Site. *Biochemistry* 38:16236-45.

Brautigan, D. L., Ferguson-Miller, S. & Margoliash, E. (1978) Mitochondrial cytochrome *c*: Preparation and activity of native and chemically modified cytochromes *c*. *Methods Enzymol.* 53:128-164.

Brzezinski, P. & Malmstrom, B. G. (1987) The mechanism of electron gating in proton pumping cytochrome *c* oxidase: the effect of pH and temperature on internal electron transfer. *Biochim. Biophys. Acta* 894:29-38.

Bushnell, G., W., Louie, G. V., Brayer, G. D. (1990) High-resolution three-dimensional structure of horse heart cytochrome c. J. Mol. Biol. 214: 585-95.

Callahan, P.M. & Babcock, G.T. (1983) Origin of the Cytochrome *a* Absorption Red Shift: A pH-Dependent Interaction between Its Heme *a* Formyl and Protein in Cytochrome Oxidase. *Biochemistry* 22:452-61.

Cao, J., Hosler, J., Shapleigh, J., Gennis, R., Revzin, A. & Ferguson-Miller, S. (1992) Cytochrome aa3 of *Rhodobacter sphaeroides* as a model for mitochondrial cytochrome c oxidase. *J. Biol. Chem.* 267:24273-8.

Cao, J., Shapleigh, J., Gennis, R., Revzin, A., & Ferguson-Miller, S. (1991) The gene encoding cytochrome c oxidase subunit II from *Rhodobacter sphaeroides*; comparison of the deduced amino acid sequence with sequences of corresponding peptides from other species. *Gene* 101:133-137.

Chory, J., Donohue, T. J., Varga, A. R., Staehelin, L. A. & Kaplan, S. (1984) Induction of the photosynthetic membranes of *Rhodopseudomonas sphaeroides*: biological and morphological studies. *J. Bacteriol.* 159:540-554.

Cohen-Bazire, G., Sistrom, W. R. & Stanier, R. Y. (1957) Kinetic studies of pigment synthesis by non-sulfur purple bacteria. *J. Cell Comp. Physiol.* 49:25-68.

Cusanovich, M. A. (1971) Molecular weight of some cytochrome *c*'. *Biochim. Biophys. Acta* 236:238-241.

de Gier, J. L., Schepper, M., Reijinders, W. N. M., van Dyck, S. J., Slotboom, D. J., Warner, A., Saraste, M., Krab, K., Finel, M., Stouthamer, A. H., van Spanning, R. J. M. & van der Oost, J. (1996) Structural and functional analysis of aa_3-type and cbb_3-type cytochrome *c* oxidases of *Paracoccus denitrificans* reveals significant differences in proton-pumping design. *Mol. Microbiol.* 20:1247-1260.

Donohue, T. J., McEwan, A. G., Van Doren, S., Crofts, A. R. & Kaplan, S. (1988) phenotypic and genetic characterization of cytochrome c_2 deficient mutants of *Rhodobacter sphaeroides. Biochemistry* 27:1918-1925.

Daldal, F., Mandaci, S., Winterstein, C., Myllykallio, H., Duyck, K. & Zannoni, D. (2001) Mobile cytochrome c_2 and Membrane-Anchored cytochrome c_y are both efficient electron donors to the cbb_3- and aa_3-type cytochrome *c* oxidase during respiratory growth of *Rhodobacter sphaeroides. J. Bacteriol.* 183:2013-24.

Das, T.K., Pecoraro, C., Tomson, F.L., Gennis, R.B. & Rousseau D.L. (1998) The post-translational modification cytochrome c oxidase is required to establish a functional environment of the catalytic site. *Biochemistry* 37:14471-6.

Errede, B. & Kamen, M. D. (1978) Comparative kinetic studies of cytochromes *c* reactions with mitochondrial cytochrome *c* oxidase and reductase. *Biochemistry* 17:1015-1027.

Ferguson-Miller, S. & Babcock, G. (1996) Heme/copper terminal oxidases. *Chem. Rev.* 96:2889-2907.

Ferguson-Miller, S., Brautigan, D. L. & Margoliash, E. (1978) Definition of cytochrome *c* binding domains by chemical modification. *J. Biol. Chem.* 253:149-159.

Ferguson-Miller, S., Brautigan, D. & Margoliash, E. (1976) Correlation of the kinetics of electron transfer activity of various eukaryotic cytochrome *c* with binding to mitochondrial cytochrome *c* oxidase. *J. Biol. Chem.* 251:1104-1115.

Fetter, J.R., Qian, J., Shapleigh, J., Thomas, J.W., García-Horsman, J.A., Schmidt, E., Hosler, J., Babcock, G.T., Gennis, R.B. & Ferguson-Miller, S. (1995) Possible Proton Relay Pathways in Cytochrome *c* Oxidase. *Proc. Natl. Acad. Sci. U.S.A.* 92:1604-8.

Fishel, L. A., Villafrance, J. E., Mauro, J. M. & Kraut, J. (1987) Yeast cytochrome *c* peroxidase: Mutagenesis and expression in *Escherichia coli* show tryptophan-51 is not the radical site in compound I. *Biochemistry* 26:351-60.

Flöck, D., & Helms, V. (2002) Protein-Protein Docking of Electron Transfer Complexes: Cytochrome *c* Oxidase and Cytochrome *c*. *Proteins: Structure, Function, and Genetics.* 47:75-85.

Florens, L., Hoganson, C., McCracken, J., Fetter, J.R., Mills, D. A., Babcock, G. T. & Ferguson-Miller, S. (1998) The Role of Magnesium and Its Associated Water Channel in Activity and Regulation of Cytochrome c Oxidase in *The Phototropic Prokaryotes* Preschek, G., Eds. (Kluwer Academic/Plenum Publishers N.Y.), pp. 329-339

Flory, J. E. & Donohue, T. J. (1995) Organization and expression of the *Rhodobacter sphaeroides* cycFG operon. *J. Bateriol.* 177:4311-4320.

García-Horsman, J., Barquera, B., Rumbley, J., Ma, J. & Gennis, R. B. (1994a) The superfamily of heme-copper respiratory oxidases. *J. Bacteriol.* 176:5587-5600.

García-Horsman, J. A., Berry, E., Shapleigh, J. P., Alben, J. O. & Gennis, R. B. (1994b) A novel cytochrome *c* oxidase from *Rhodobacter sphaeroides* that lacks Cu_A. *Biochemistry* 33:3113-3119.

Geren, L., Hahm, S., Durham, B., Millett, F. (1991) Photoinduced electron transfer between cytochrome c peroxidase and yeast cytochrome c labeled at Cys 102 with (4-bromomethyl-4'-methylbipyridine)[bis(bipyridine)]ruthenium2+. *Biochemistry* 30:9450.

Gregory, L. C., & Ferguson-Miller, S. (1988) (1) Effect of subunit III removal on control of cytochrome c oxidase activity by pH. *Biochemistry.* 27:6307-14.

Gregory, L. C., & Ferguson-Miller, S. (1988) (2) in *Advances in Membrane Biochemistry and Bioenergetics* (Kim, C.H., Tedeschi, H., Diwan, J. J., & Salerno, J. C., eds.) pp 301-309, Plenum Publishing.

Hahm, S., Durham, B., Millett, F. (1992) Photoinduced electron transfer between cytochrome c peroxidase and horse cytochrome c labeled at specific lysines with (dicarboxybipyridine)(bisbipyridine)ruthenium(II) *Biochemistry* 31:3472.

Haltia, T., Saraste, M., & Wikstrom, M. (1991) Subunit III of cytochrome c oxidase is not involved in proton translocation: a site-directed mutagenesis study. *EMBO J.* 10:2015-21.

Haltia, T., Finel, M., Harms, N., Nakari, T., Raitio, M., Wikstrom, M., & Saraste, M. (1989) Deletion of the gene for subunit III leads to defective assembly of bacterial cytochrome oxidase. *EMBO J.* 8:3571-9.

Hállen, S. & Nilsson, T. (1992) Proton transfer during the reaction between fully reduced cytochrom oxidase and dioxygen: pH and deuterium isotope effects. *Biochemistry* 31:11853-11859.

Harrenga, A., Reincke, B., Rüterjans, H., Ludwig, B. & Michel, H. (2000) Structure of the Soluble Domain of Cytochrome c_{552} from *Paracoccus denitrificans* in the Oxidized and Reduced States. *J. Mol. Biol.* 295:667-678.

Hatefi, Y. (1985) The mitochondrial electron transport and oxidative phosphorylation system. *Annu. Rev. Biochem.* 54:1015-1069.

Hill, B. C. (1991) The reaction of the electrostatic cytochrome *c*-cytochrome oxidase complex with oxygen. *J. Biol. Chem.* 266:2219-2226.

Hiser, C., Mills, D. A., Schall, M., & Ferguson-Miller, S. (2001) C-terminal truncation and histidine-tagging of cytochrome c oxidase subunit II reveals the native processing site, shows involvement of the C-terminus in cytochrome c binding, and improves the assay for proton pumping. *Biochemistry*. 40(6):1606-15.

Ho, S. N., Hunt, H. D., Horton, R. M., Pullen, J. K. & Pease, L. R. (1989) Site-directed mutagenesis by overlap extension using the polymerase chain reacton. *Gene* 77: 51-59.

Hosler, J.P., Espe, M.P., Zhen, Y., Babcock, G.T. & Ferguson-Miller, S. (1995) Analysis of site-directed mutants locates a non-redox-active metal near the active site of cytochrome *c* oxidase of *Rhodobacter sphaeroides*. *Biochemistry* 34:7586-92.

Hosler, J.P., Ferguson-Miller, S., Calhoun, M.W., Thomas, J.W., Hill, J., Lemieux, L. Ma, J.X., Georgiou, C., Fetter, J., Shapleigh, J., Techlenburg, M.M.J., Babcock, G.T., Gennis, R.B. (1993) Insight into the active-site structure and function of cytochrome-oxidase by analysis of site-directed mutants of bacterial cytochrome – aa3 and cychrome-bo. *J. Bioenergetics and Biomembranes* 25:121-136.

Hosler, J. P., Fetter, J., Teckkenburg, M. M. J., Espe, M., Lerma, C. & Ferguson-Miller, S. (1992) Cytochrome aa_3 of *Rhodobacter sphaeroides* as a model for mitochondrial cytochrome *c* oxidase. *J. Biol. Chem.* 267:24264-24272.

Hunte, C., Solmaz, S. & Lange C. (2002) Electron transfer between yeast cytochrome bc_1 complex and cytochrome *c*: a structural analysis. *Biochim. Biophys. Acta*. 1555:21-8.

Iwata, S., Ostermeier, C., Ludwig, B. & Michel, H. (1995) Structure at 2.8 Å resolution of cytochrome *c* oxidase from *Paracoccus denitrificans*. *Nature* 376:660-669.

Jenney Jr., F. E. & Daldal, F. (1993) A novel membrane-associated *c*-type cytochrome cyt c_Y, can mediate the photosynthetic growth of *Rhodobacter capsulatus* and *Rhodobacter sphaeroides*. *EMBO J.* 12:1283-1292.

Junemann, D., Meunier, B., Fisher, N. & Rich, P.R. (1999) Effects of mutation of the conserved glutamic acid – 286 in subunit I of cytochrome *c* oxidase from *Rhodobacter sphaeroides*. *Biochemistry*. 38:5248-55.

Kang, C. H., Brautigan, D. L., Osheroff, N. & Margoliash, E. (1978) Definition of cytochrome *c* binding domains by chemical modification. Reaction of carboxydinitrophenyl- and trinitrophenyl-cytochromes *c* with baker's yeast cytochrome *c* peroxidase. *J. Biol. Chem.* 253:6502-10.

Kang, C.H., Ferguson-Miller, S., Margoliash, E. (1977) Steady state kinetics and binding of eukaryotic cytochromes c with yeast cytochrome c peroxidase. *J Biol Chem.* 252:919-26.

Karpefors, M., Adelroth, P., Zhen, Y., Ferguson-Miller, S. & Brzezinski, P. (1998) Proton uptake controls electron transfer in cytochrome c oxidase. *Proc. Natl. Acad. Sci. USA* 95(23):13606-11.

Kituchi, G., Sairo, Y. & Motokawa, Y. (1965) On cytochrome oxidase as the terminal oxidase of dark respiration of non-sulfur purple bacteria. *Biochem. Biophys. Acta* 94:1-14.

Konstantinov, A. A., Siletsky, A., Mitchell, D., Kaulen, A., & Gennis R. B.. (1997) The roles of the two proton input channels in cytochrome *c* oxidase from *Rhodobacter sphaeroides* probed by the effects of site-directed mutations on time-resolved electrogenic intraprotein proton transfer. *Proc. Natl. Acad. Sci. USA* 94:9085-90.

Konvicka K., Guarnieri F., Ballesteros J. A., & Weinstein, H. (1998) A proposed structure for transmembrane segment 7 of G protein-coupled receptors incorporating an Asn-Pro/Asp-Pro motif. *Biophys. J.* 75(2):601-11.

Lange, C. & Hunte, C. (2002) Crystal structure of the yeast cytochrome bc_1 complex with its bound substrate cytochrome *c*. *Proc. Natl. Acad. Sci.* USA 99: 2800-2805.

Lappalainen, P., Watmough, N. J., Greenwood, C. & Saraste, M. (1995) Electron transfer between cytochrome *c* and the isolated CuA domain: identification of substrate-binding residues in cytochrome *c* oxidase. *Biochemistry* 34: 5824-5830.

Long, J. E., Durham, B., Okamura, M. & Millett, F. (1989) Role of specific lysine residues in binding cytochrome c_2 to the *Rhodobacter sphaeroides* reaction center in optimal orientation for rapid electron transfer. *Biochemistry* 28:6970-6974.

Luo, X., Zhang, D. & Weinstein H. (1994) Ligand-induced domain motion in the activation mechanism of a G-portein-coupled receptor. *Protein Eng.* 7:1441-1448.

Malatesta, F., Nicoletti, F., Zickermann, V., Ludwig, B., & Brunori, M. (1998) Electron entry in a CuA mutant of cytochrome c oxidase from Paracoccus denitrificans. Conclusive evidence on the initial electron entry metal center. *FEBS Lett.* 434, 322-324.

Margoliashi, E. & Schejterm A. in *Cytochrome c:A multidisplinary approach* Acott, R. A. & Mauk, A. G., Eds. (University Science Book, Sausalito, California, 1996)

Margoliash, E. & Schejter, A. (1966) Cytochrome *c*. *Adv. Protein Chem.* 21:113-286.

Mather, M., Springer, P., Hensel, S., Buse, G. & Fee, J. A. (1993) Cytochrome oxidase genes from *Thermus thermophilus*: nucleotide sequence of the fused gene and analysis of the deduced primary structures for subunits I and III of cytochrome caa_3. *J. Biol. Chem.* 268:5395-5408.

Meyer, T. E. & Cusanovich, M. A. (1985) Soluble cytochrome composition of the purple phototrophic bacterium *Rhodopseudomonas sphaeroides* ATCC 17023. *Biochim. Biophys. Acta* 807:308-391.

Meyer, T.E. & Kamen, M.D. in *Advances in protein chemistry* (Academic Press, Inc., 1982), vol.25, pp. 105-212

Michel, H. (1999) Cytochrome *c* oxidase: catalytic cycle and mechanisms of proton pumping – a discussion. *Biochemistry* 38: 15129-40.

Miller, M. A., Geren, L., Han, G. W., Saunders, A., Beasley, J., Pielak, G. J., Durham, B., Millett, F. & Kraut, J. (1996) Identifying the physiological electron transfer site of cytochrome *c* peroxidase by structure-based engineering. *Biochemistry* 35:667-73.

Miller, M. A., Liu, R. Q., Hahm, S., Geren, L., Hibdon, S., Kraut, J., Durham, B. & Millett, F. (1994) Interaction domain for the reaction of cytochrome *c* with the radical and the oxyferryl heme in cytochrome *c* peroxidase compound I. *Biochemistry* 33:8686-93.

Millett, F. & Durham, B. in *Metal Ions in Biological Systems* Sigel, H. & Siegel, A., Eds. (Marcel Dekker, Inc., Basel, Switzerland, 1991), vol. 27, pp. 223-64.

Millett, F., de Jong, C., Paulson, L. & Capaldi, R. A. (1983) Identification of specific carboxylate groups on cytochrome *c* oxidase that are involved in binding cytochrome *c*. *Biochemistry* 22:546-552.

Millett, F., Darley-Usmar, V. & Capaldi, R. A. (1982) Cytochrome *c* is cross-linked to subunit II of cytochrome *c* oxidase by a water-soluble carbodiimide. *Biochemistry* 21:3857-3862.

Mitchell, P. (1976) Possible Molecular Mechanisms of the Protonmotive Function of Cytochrome Systems. *J. Theor. Biol.* 62:327-367.

Mitchell, P. (1966) Chemiosmotic Coupling in Oxidastive and Photosynthetic Phosphorylation. Glynn Research Ltd, Bodmin.

Mitchell, P. & Moyle, J. (1965) Stoichiometry of proton translocation through the respiratory chain and adenosine triphosphatase systems of rat liver mitochondria. *Nature* 208:147-51.

Mkrtchyan, H., Vygodina, T. & Konstantinov, A. (1990) Na(+)-induced reversal of the Ca2(+)-dependent red-shift of cytochrome a. Is there a hydronium output well in cytochrome c oxidase? *Biochem. Int.* 20:183-9.

Moore, G. R. & Pettigrew, G. W., Eds., *Cytochrome c: evolutionary, structural and physiochemical aspects* (Springer Verlag, Berlin, 1990).

Myllykallio, H., Zannoni, D. & Daldal F. (1999) The membrane-attached electron carrier cytochrome c_y from *Rhodobacter sphaeroides* is functional in respiratory but not in photosynthetic electron transfer. *Proc. Natl. Acad. Sci. USA* 96:4348-4353.

Nicoletti, F., Witt, H., Ludwig, B., Brunori, M. & Malatesta, F. (1998) *Paracoccus denitrificans* cytochrome c oxidase: a kinetic study on the two- and four-subunit complexes. *Biochim. Biophys. Acta* 1365:393-403.

Oliveberg, M., Hallén, S. & Nilsson, T. (1991) Uptake and release of protons during the reaction between cytochrome *c* oxidase and molecular oxygen: A flow-flash investigation. *Biochemistry* 30: 436-440.

Osheroff, N., Brautigan, D. L. & Margoliash, E. (1980) Definition of enzymic interaction domains on cytochrome *c*. Purification and activity of singly substituted carboxydinitrophenyl-lysine 7, 25, 73, 86, and 99 cytochromes *c*. *J. Biol. Chem.* 255:8245-51.

Ostermeier, C., Harrenga, A., Ermler, U. & Michel, H. (1997) Structure at 2.7Å resolution of the *Paracoccus denitrificans* two-subunit cytochrome *c* oxidase complexed with an antibody Fv fragment. *Proc. Natl. Acad. Sci. USA* 94:10547-10553.

Ostermeier, C., Iwata, S., & Michel, H. (1996) Cytochrome *c* oxidase. *Curr. Opin. Struct. Biol.* 6:460-466.

Overfield, R. E., Wraight, C. A. & Devault, D. (1979) Microsecond photooxidation kinetics of cytochrome c_2 from *Rhodopseudomonas sphaeroides*: In vivo and solution studies. *FEBS Lett.* 105:137-142.

Pan, L. P., Hibdon, S., Liu, R.-Q., Durham, B. & Millett, F. (1993) Intracomplex electron transfer between ruthenium-cytochrome *c* derivatives and cytochrome *c* oxidase. *Biochemistry* 32:8492-8498.

Pelletier, H. & Kraut, J. (1992) Crystal structure of a complex between electron transfer partners, cytochrome *c* peroxidase and cytochrome *c*. *Science* 258:1748-1755.

Pettigrew, G. W. & Moore, G. R., Eds., *Cytochrome c: biological aspects* (Springer Verlag, Berlin, 1987)

Pfitzner, U., Kirichenko, A., Konstantinov A.A., Mertens, M., Wittershagen, A., Kolbesen, B.O., Steffens, G.C., Harrenga, A., Michel, H. & Ludwig, B. (1999) Mutations in the Ca^{2+} binding site of the *Paracoccus denitrificans* cytochrome c oxidase. *FEBS Lett.* 456:365-9.

Poulos, T., Freer, S., Alden, R., Edwards, S., Skogland, U., Takio, K., Eriksson, B., Xuong, N., Yonetani, T. & Kraut, J. (1980) The crystal structure of cytochrome *c* peroxidase. *J. Biol. Chem.* 255(2):575-580.

Proshlyakov, D.A., Pressler, M.A., DeMaso, C., Leykam, J.F., DeWitt, D.L. & Babcock, G.T. (2000) Oxygen activation and reduction in respiration: involvement of redox-active tyrosine 244. *Science* 290:1588-91.

Qian, J., Shi, W., Pressler, M., Hoganson, C., Mills, D., Babcock, G.T. & Ferguson-Miller S. (1997) Aspartate-407 in *Rhodobacter sphaeroides* cytochrome *c* oxidase is not required for proton pumping or Mn binding. *Biochemistry* 36:2539-43.

Rieder, R. & Bosshard, H. R. (1980) Comparison of the binding sites on cytochrome *c* for cytochrome *c* oxidase, cytochrome bc_1, and cytochrome c_1. *J. Biol. Chem.* 255:4732-4739.

Rott, M. A. & Donohue, T. J. (1990) *Rhodobacter sphaeroides spd* mutations allow cytochrome c_2-independent photosynthetic growth. *J. Bacteriol.* 172:1954-1961.

Reincke, B., Thöny-Meyer, L., Dannehl, C., Odenwald, A., Aidim, M., Witt, H., Rüterjans, H. & Ludwig,, B. (1999). Heterologous expression of soluble fragments of cytochrome c_{552} acting as electron donor to the *Paracoccus denitrificans* cytochrome c oxidase. *Biochim. Biophys. Acta* 1411:114-120.

Rich, P. R. (1995) Toward understanding the chemistry of oxygen reduction and proton translocation in iron-iron respiratory oxidases. *Aust. J. Plant Physiol.* 22:479-484.

Riistama, S., Laakkonen, L., Wikström, M., Verkhovsky, M.I., & Puustinen, A. (1999) The Calcium Binding Site in Cytochrome aa_3 from *Paracoccus denitrificans*. *Biochemistry* 38: 10670-10677.

Riistama, S., Puustinen, A., Garcia-Horsman, A., Iwata, S., Michel, H. & Wikström, M. (1996) Channeling of dioxygen into the respiratory enzyme. *Biochim. Biophys. Acta* 1275:1-4.

Roberts, V. A. & Pique, M. E. (1999) Definition of the interaction domain for cytochrome *c* on cytochrome *c* oxidase. III. Prediction of the docked complex by a complete, systematic search. *J. Biol. Chem.* 274:38051-38060.

Saari, H., Penttila, T. & Wikstrom, M. (1980) Interactions of Ca^{2+} and H^+ with heme A in cytochrome oxidase. *J Bioenerg Biomembr.* 12:325-38.

Saraste, M. (1990) Structural features of cytochrome oxidase. *Q. Rev. Biophys.* 23:331-366.

Scott, R. A. & Mauk, A. G., Eds., *Cytochrome c: A multidisciplinary approach* (University Science Books, Sausalito, California, 1996).

Shapleigh, J. P. & Gennis, R. B. (1992) Cloning, sequencing, and deletion from the chromosome of the gene encoding subunit I of the aa_3-type cytochrome *c* oxidase of *Rhodobacter sphaeroides. Mol. Microbiol.* 6:635-642.

Shapleigh, J.P., Hosler, J.P., Techlenburg, M.M.J., Kim, Y.Y., Babcock, G.T., Gennis, R.B. & Ferguson-Miller, S. (1992) Definition of the Catalytic Site of Cytochrome-c-Oxidase-Specific Ligands of Heme-*a* and the Heme-a_3-Cu_B Center. *Proc. Natl. Acad. Sci. USA*. 89:4786-90.

Sigurdson, H., Brändén, M., Namslauer, A., & Brzezinski, P. (2002) Ligand binding reveals protonation events as the active site of cytochrome *c* oxidase; is the K-pathway used for the transfer of H^+ or OH^-? *J. Inorganic Biochem.* 88:335-42.

Smith, H. T., Ahmed, A. J. & Millett, F. (1981) Electrostatic interaction of cytochrome *c* with cytochrome c_1 and cytochrome oxidase. *J. Biol. Chem.* 256:4984-90.

Smith, H. T., Staudenmayer, N. & Millett, F. (1977) Use of specific lysine modifications to locate the reaction site of cytochrome *c* with cytochrome oxidase. *Biochemistry* 16:4971-4974.

Smith, L. & Davies, H. C. (1991) The reactions of the oxidase and reductase of *Paracoccus denitrificans* with cytochromes *c*. *J. Bioenerget. Biomemb.* 23:303-319.

Smith, M. B. & Millett, F. (1980) A 19F nuclear magnetic resonance study of the interaction between cytochrome *c* and cytochrome *c* peroxidase. *Biochim. Biophys. Acta* 626:64-72.

Solioz, M., Carafoli, E., & Ludwig, B. (1982) The cytochrome c oxidase of *Paracoccus denitrificans* pumps protons in a reconstituted system. *J. Biol. Chem.* 257:1579-1582.

Speck, S.H., Ferguson-Miller, S., Osheroff, N., & Margoliash, E. (1979) Definition of cytochrome c binding domains by chemical modification: kinetics of reaction with beef mitochondrial reductase and functional organization of the respiratory chain. *Proc. Natl. Acad. Sci. USA* 76(1):155-9.

Speck, S.H. & Margoliash, E. (1984) Characterization of the interaction of cytochrome *c* and mitochondrial ubiquinol-cytochrome *c* reductase. *J. Biol. Chem.* 259: 1064-72.

Staudenmayer, N., Smith, M. B., Smith, H. T., Spies, F. K., Jr. & Millett, F. (1976) An enzyme kinetics and 19F nuclear magnetic resonance study of selectively trifluoroacetylated cytochrome *c* derivatives. *Biochemistry* 15:3198-205.

Steinrücke, P., Gerhus, E., Jetzek, M., Turba, A. & Ludwig, B. (1991) The cytochrome *c* reductase/oxidase respiratory pathway of *Paracoccus denitrificans*: Genetic and functional studies. *J. Bioenerget. Biomemb.* 23:227-239.

Svensson-Ek, M., Abramson, J., Larsson, G., Törnroth, S., Brzezinski, P. & Iwata, S. (2002) The X-ray crystal structure of wild-type and EQ(I-286) mutant cytochrome *c* oxidases from *Rhodobacter sphaeroides*. *J. Mol. Biol.* 321:329-339.

Taha, T. S. M. &Ferguson-Miller, S. (1992) Interaction of cytochrome *c* with cytochrome *c* oxidase studied by monoclonal antibodies and a protein modifying reagent. *Biochemistry* 31:9090-9097.

Thompson, D.A., Gregory, L., & Ferguson-Miller, S. (1985) Cytochrome c oxidase depleted of subunit III: proton-pumping, respiratory control, and pH dependence of the midpoint potential of cytochrome a. *J. Inorg. Biochem.* 23:357-364.

Trumpower, B. L. & Gennis, R. B. (1994) Energy transduction by cytochrome complexes in mitochondrial and bacterial respiration: the enzymology of coupling electron transfer reactions to transmembrane proton transloction. *Annu. Rev. Biochem.* 63: 675-716.

Trumpower, B. L. (1990) The protonmotive Q cycle. *J. Biol. Chem.* 265:11409-11412.

Tsukihara, T., Aoyama, H., Yamashita, E., Tomizaki, T., Yamaguchi, H., Shinzawaitoh, K., Nakashima, R., Yaono, R. & Yoshikawa, S. (1996) The whole structure of the 13-subunit oxidized cytochrome *c* oxidase at 2.8 Å. *Science* 272:1136-1144.

Tsukihara, T., Aoyama, H., Yamashita, E., Tomizaki, T., Yamaguchi, H., Shinzawaitoh, K., Nakashima, R., Yaono, R. & Yoshikawa, S. (1995) Structure of metal sites of oxidized bovine heart cytochrome *c* oxidase at 2.8 Å. *Science* 269:1069-1074.

Turba, A., Jetzek, M. & Ludwig, B. (1995) Purification of *Paracoccus denitrificans* cytochrome c_{552} and sequences analysis of the gene. *Eur. J. Biochem.* 231:259-265.

Van Rhee, A. M. & Jacobson, K. A. (1996) Molecular architecture of G protein-coupled receptors. *Drug Dev. Res.* 37:1-38.

Wang, K., Zhen, Y., Sadoski, R., Grinnell, S., Geren, L., Ferguson-Miller, S., Durham, B. & Millett, F. (1999) Definition of the interaction domain for cytochrome *c* on cytochrome *c* oxidase. II. Rapid kinetic analysis of electron transfer from cytochrome *c* to *Rhodobacter sphaeroides* cytochrome oxidase surface mutants. *J. Biol. Chem.* 274:38042-38050.

Wess, J., Nanavati, S., Vogel, Z., & Maggio, R. (1993) Functional role of proline and tryptophan residues highly conserved among G protein-coupled recptors studied by mutational analysis of the m3 muscarinic receptor. *EMBO J.* 12:331-338.

Wikström, M. (1977) Proton Pump Coupled to Cytochrome c Oxidase in Mitochondria. *Nature(London)* 266:271-273.

Wilmanns, M., Lappalainen, P., Kelley, M., Sauer-Eriksson, E. & Saraste, M. (1995) Crystal structure of the membrane exposed domain from a respiratory quinol oxidase complex with an engineered dinuclear copper center. *Proc. Natl. Acad. Sci.* (USA) 92:11955-11959.

Witt, H., Malatesta, F., Nicoletti, F., Brunori, M. & Ludwig, B. (1998) Cytochrome-*c*-binding site on cytochrome oxidase in *Paracoccus denitrificans. Eur. J. Biochem.* 251:367-73.

Witt, H. & Ludwig, B. (1997) Isolation, analysis, and deletion of the gene coding for subunit IV of cytochrome *c* oxidase in *Paracoccus denitrificans. J. Biol. Chem.* 272:5514-7.

Witt, H., Zichermann, V. & Ludwig, B. (1995) Site-directed mutagenesis of cytochrome *c* oxidase reveals two acidic residues involved in the binding of cytochrome *c*. *Biochim. Biophys. Acta* 1230: 74-6.

Yoshikawa, S., Tera, T., Takahashi, Y., Tsukihara, T. & Caughey, W. S. (1998) Crystalline cytochrome *c* oxidase of bovine heart mitochondrial membrane: Composition and x-ray diffraction studies. *Proc. Natl. Acad. Sci. USA* 85:1354-1358.

Yoshikawa, S., Shinzawa-Itoh, K. Nakashima, R., Yaono, R. Yamashita, E., Inoue, N. Yao, M., Fei, M. J., Libeu, C. P., Mizushima, T., Yamaguchi, H., Tomizaki, T. & Taukihara, T.. (1998) Redox-Coupled Crystal Structural Changes in Bovine Heart Cytochrome c Oxidase. *Science* (280): 1723-9.

Yoshikawa, S., Mochizuki, M., Zhao, X.J. & Caughey, W.S. (1995) Effects of Overal Oxidation State on Infrared Spectra of Heme *a*3 Cyanide in Bovine Heart Cytochrome *c* Oxidase – Evidence of Novel Mechanistic Roles for Cu_B. *J. Biol. Chem.* 270:4270-79.

Yu, C.A., Yu, L. & King, T.E. (1973) Kinetics of electron transfer between cardiac cytochrome c 1 and c. *J. Biol. Chem.* 248(2):528-33.

Yu, L., Dong, J.-H. & Yu, C.-A. (1986) Characterization of purified cytochrome c_1 from *Rhodobacter sphaeroides* R-26. *Biochim. Biophys. Acta* 852: 203-211.

Yun, C.-H., Barquera, B., Iba, K., Takamiya, K.-I, Shapleigh, J., Crofts, A. R. & Gennis, R. B. (1994) Deletion of the gene encoding cytochrome b_{562} from *Rhodobacter sphaeroides. FEMS Microbio. Letts.* 120:105-110.

Zhang, D. & Ewinstein, H. (1993) Signal transduction by a 5-HT2 receptor: a mechanistic hypothesis from molecular dynamics simulations of the three-dimensional model of the receptor complexed to ligands. *J. Med. Chem.* 36:934-938.

Zhen, Y., Schmidt, B., Kang, U.G., Antholine, W.,& Ferguson-Miller, S. (2002) Mutants of the CuA Site in Cytochrome *c* Oxidase of *Rhodobacter sphaeroides*: I. Spectral and Functional Properties. *Biochemistry* 41:2288-97.

Zhen, Y., Hoganson, C. W., Babcock, G. T. & Ferguson-Miller, S. (1999) Definition of the interaction domain for cytochrome *c* on cytochrome *c* oxidase. I. Biochemical, spectral, and kinetic characterization of surface mutants in subunit II of *Rhodobacter sphaeroides* cytochrome aa_3. *J. Biol. Chem.* 274:38032-41.

Zhen, Yuejun (1998) The role of subunit II in cytochrome *c* oxidase in cytochrome *c* binding and electron transfer. *Ph.D. Dissertation.*